



National Library
of Canada

Bibliothèque nationale
du Canada

Canadian Theses Service

Services des thèses canadiennes

Ottawa, Canada
K1A 0N4

CANADIAN THESES

THÈSES CANADIENNES

NOTICE

The quality of this microfiche is heavily dependent upon the quality of the original thesis submitted for microfilming. Every effort has been made to ensure the highest quality of reproduction possible.

If pages are missing, contact the university which granted the degree.

Some pages may have indistinct print especially if the original pages were typed with a poor typewriter ribbon or if the university sent us an inferior photocopy.

Previously copyrighted materials (journal articles, published tests, etc.) are not filmed.

Reproduction in full or in part of this film is governed by the Canadian Copyright Act, R.S.C. 1970, c. C-30.

**THIS DISSERTATION
HAS BEEN MICROFILMED
EXACTLY AS RECEIVED**

AVIS

La qualité de cette microfiche dépend grandement de la qualité de la thèse soumise au microfilmage. Nous avons tout fait pour assurer une qualité supérieure de reproduction.

S'il manque des pages, veuillez communiquer avec l'université qui a conféré le grade.

La qualité d'impression de certaines pages peut laisser à désirer, surtout si les pages originales ont été dactylographiées à l'aide d'un ruban usé ou si l'université nous a fait parvenir une photocopie de qualité inférieure.

Les documents qui font déjà l'objet d'un droit d'auteur (articles de revue, examens publiés, etc.) ne sont pas microfilmés.

La reproduction, même partielle, de ce microfilm est soumise à la Loi canadienne sur le droit d'auteur, SRC 1970, c. C-30.

**LA THÈSE A ÉTÉ
MICROFILMÉE TELLE QUE
NOUS L'AVONS REÇUE**

**Reversible Ring-opening of Thiamine
and Related Thiazolium Cations**

Georgia Karamitsoglou-Spiropoulos

**A Thesis
in
The Department
of
Chemistry**

**Presented in Partial Fulfillment of the Requirements
for the Degree of Master of Science at
Concordia University
Montréal, Québec, Canada**

September 1986

© Georgia Karamitsoglou-Spiropoulos, 1986

Permission has been granted to the National Library of Canada to microfilm this thesis and to lend or sell copies of the film.

The author (copyright owner) has reserved other publication rights, and neither the thesis nor extensive extracts from it may be printed or otherwise reproduced without his/her written permission.

L'autorisation a été accordée à la Bibliothèque nationale du Canada de microfilmer cette thèse et de prêter ou de vendre des exemplaires du film.

L'auteur (titulaire du droit d'auteur) se réserve les autres droits de publication; ni la thèse ni de longs extraits de celle-ci ne doivent être imprimés ou autrement reproduits sans son autorisation écrite.

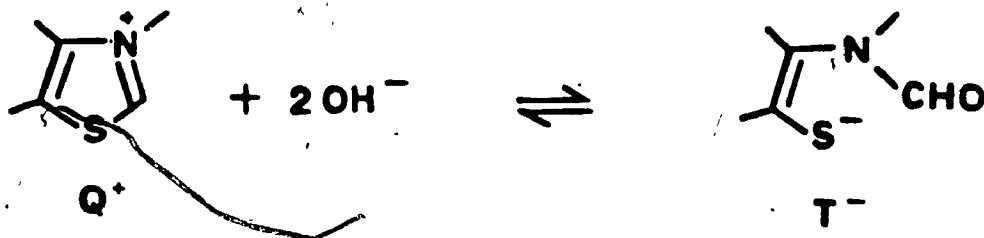
ISBN 0-315-35561-1

ABSTRACT

Reversible ring-opening of thiamine and related thiazolium cations

Georgia Karamitsoglou-Spiropoulos

Quaternary thiazolium ions (Q^+) open reversibly in aqueous solution to give amido enethiolates (T^-):



Following an earlier study of the N-methylbenzothiazolium ion (BT^+), the kinetics of the ring-opening and ring-closing of 3,4-dimethyl-5-(2-hydroxyethyl)thiazolium (HET^+) and thiamine (B_1^+ , Vitamin B_1) ions, were studied in aqueous solution at pH 0-14, at 25 °C and $I = 1.0$ M, using stopped-flow UV spectrophotometry. Various static NMR experiments were also carried out.

Ring-opening of BT^+ and HET^+ simply involves rate-limiting attack by hydroxide ion, whereas that of thiamine is more complex, due to the prior formation of the "yellow form".

We found that reclosure of the enethiolates of BT^+ , HET^+ , and B_1^+ show one kinetic phase at intermediate pHs but at low pHs, two distinct phases are observable. This biphasic behaviour is ascribed to the formation of an amino thiol ester by an N-S acyl transfer, preceding the

reconstitution of the thiazolium ring. The mechanism of the acyl transfer involves a change in the rate-limiting step as is shown from the observed curved buffer plots near the break on the pH-rate profile of this process. The results are rationalized in terms of the pH dependence of the formation and breakdown of the tetrahedral intermediate, T° .

5

*To my mother,
for her endless help and encouragement.*

ACKNOWLEDGEMENTS

The author wishes to express her sincere thanks to her supervisor, Dr. O.S. Tee, for his assistance and guidance, as well as for his encouragement and valuable advice during the course of this study and writing of this thesis.

Grateful acknowledgement is made to:

- Dr. L.D. Colebrook for his help to conduct NMR experiments;
- Dr. R.S. McDonald and his co-workers for their collaboration in the kinetic studies.
- Miss Suzanne Miscevic for her great help in typing this text.

Thanks are also due to the Department of Chemistry for financial support, to the Graduate Studies Office for the awarding of a teaching fellowship, and to Funds F.C.A.C. for a research fellowship.

TABLE OF CONTENTS

	Page
<u>INTRODUCTION</u>	
General Introduction.	1
The Thiamine Function.	4
Ring-opening of Thiamine - Earlier work.	9
Tetrahedral Intermediates - Pseudobases.	15
General Acid-Base Catalysis. Buffer Catalysis.	20
<u>EXPERIMENTAL</u>	
Materials.	29
Kinetic Solutions.	30
Stopped-flow Technique.	32
Apparatus and Kinetic Procedure.	34
Mathematical Treatment of Kinetic Data.	41
NMR.	44
<u>RESULTS AND DISCUSSION</u>	
NMR Studies.	46
Kinetic Studies.	61
. Reversible ring-opening of BT ⁺ .	61
. Reversible ring-opening of HET ⁺ .	86
- Ring-closing of ETH ⁻ .	74
. Thiamine B ₁ ⁺ .	86
- Ring-opening of B ₁ ⁺ .	86
- Formation of the YF ⁻ .	90
- Decay of the "yellow form". Formation of the ring-opened form.	96

	viii
- Ring-closing of Bi^+ .	99
- 1-Methylthiaminium Dication (N_1MeBi^+).	104
Activation Parameters.	108
Concluding Remarks.	110
REFERENCES	114
APPENDIX	120

LIST OF FIGURES

<u>Number</u>		<u>Page</u>
1	Structures of BT ⁺ , HET ⁺ , and B ₁ ⁺ .	3
2	Stopped-flow acquisition system.	37
3	Proton NMR spectrum of HET ⁺ in D ₂ O.	47
4	¹ H NMR spectrum of the ring-opened thiol of HET ⁺ in NaOD / D ₂ O.	49
5	¹ H NMR spectrum of HET ⁺ in D ₂ O / DCl taken 12 seconds after the acidification of the ring-opened thiol sample.	51
6	¹ H NMR spectrum of Thiamine chloride hydrochloride in D ₂ O.	53
7	¹ H NMR spectrum of the ring-opened form of thiamine in NaOD / D ₂ O.	54
8	Proton NMR spectrum of N-methylated thiamine (N ₁ MeB ₁ ⁺) in D ₂ O.	57
9	¹ H NMR spectrum of the ring-opened form of N ₁ MeB ₁ ⁺ , in NaOD / D ₂ O.	58
10	The pH - rate profile for the reversible opening of BT ⁺ .	62
11	pH dependence of the first order rate constants for the reversible opening HET ⁺ .	67

		x
12	Static UV spectra of HET ⁺ and ETh ⁻ in aqueous solution.	69
13	Plot of k_{obs} vs [OH ⁻] for the ring-opening reaction of HET ⁺ .	73
14	Buffer catalysis plots for process (b) and process (a) of HET ⁺ .	79
15	UV scans of the ring-closing of HET ⁺ of process (c).	82
16	pH-rate profile of the formation of the "yellow form" (YF ⁻) and the ring-opened form (Th ⁻) of thiamine (B1 ⁺).	87
17	pH-rate profile for the kinetics of the ring-closing reaction of thiamine B1 ⁺ .	88
18	Kinetic spectra of the decay of the yellow form of thiamine.	93
19	pH dependence of the first order rate constants for the ring closing of 1'-methylthiaminium ion (N1 MeB1 ⁺).	106

LIST OF SCHEMES

<u>Number</u>		<u>Page</u>
1	Cleavage of thiazolium ions in aqueous basic solution.	2
2	Cleavage of thiamine molecule by sulfite ion.	6
3	Decarboxylation of pyruvate catalyzed by thiamine.	8
4	Reclosure of thiazolium ions.	13
5	Mechanism of the hydrolysis of 2-methyl Δ^2 -thiazoline.	14
6	General acid catalysis.	22
7	General base catalysis.	22
8	Specific acid catalysis.	24
9	Specific base catalysis.	25
10	Specific acid/general base case.	28
11	Overall scheme of the ring-opening and ring-closing of N-methyl-benzothiazolium cation.	64
12	Ring-opening of HET ⁺ .	70
13	Species involved in the ring-opening and reclosure of thiazolium cations (Q ⁺).	85

		xii
14	Reaction scheme for thiamine thiazolium ring-opening.	89
15	Suggested mechanism for the generation of the yellow form of thiamine.	91
16	Possible modes of cleavage of the tetrahedral intermediate T ^o .	104

LIST OF TABLES

<u>Number</u>		<u>Page</u>
1	The NMR assignments for HET ⁺ and its ring-opened thiol form in D ₂ O.	50
2	Proton chemical shifts assignments, in ppm, of the thiamine spectra in Figures 6 and 7.	55
3	Proton chemical shifts assignments, in ppm, of the spectra on Figures 8 and 9.	59
4	Summary of results.	109
5	Rate constants for ring-opening of HET ⁺ .	119
6	Rate constants for ring-closing of HET ⁺ (fast process).	120
7	Rate constants for ring-closing of HET ⁺ (slow process).	121
8	Buffer catalysis rate constants for process (b) of HET ⁺ .	122
9	Rate constants for the formation of the "yellow form" of B ₁ ⁺ .	123
10	Rate constants for ring-opening of B ₁ ⁺ .	124
11	Rate constants for ring-closing of B ₁ ⁺ (fast process).	125

- 12 Rate constants for ring-closing of B_1^+ 126
 (slow process).
- 13 Rate constants for ring-closing of 127
 $N_1 MeB_1^+$.

I N T R O D U C T I O N

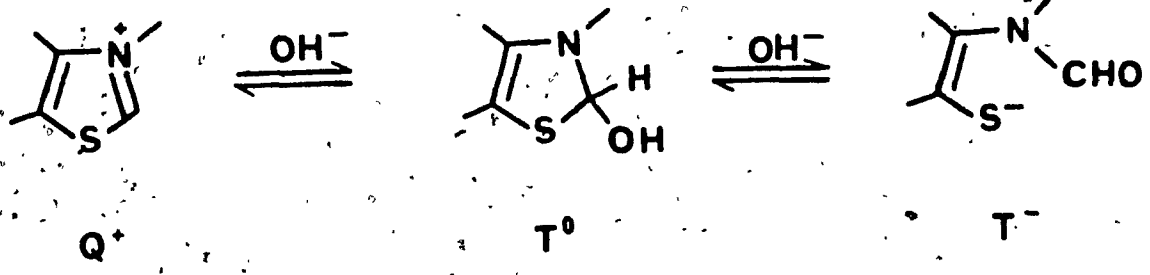
GENERAL INTRODUCTION

Thiamine, the anti-beriberi vitamin (vitamin B₁), is a fundamental compound in many biochemical processes. As a consequence, much research on various aspects of the chemistry of thiamine are under study¹.

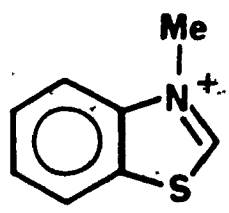
Although hydrolytic cleavage of thiamine represents the major mode of anaerobic degradation of the vitamin, the kinetic dependency of this reaction on pH has not been completely explored²⁻⁴. This is surprising since, at physiological pH, there is a dynamic conversion between the ring-opened and ring-closed forms of thiamine²⁻⁴. This interconversion may be important in thiamine transport across cell membranes⁴.

As is shown in Scheme 1, quaternary thiazolium ions (Q⁺) ring-open in basic aqueous solutions, presumably through a tetrahedral intermediate (T^o), producing amidoenethiolates (T⁻), which reclose upon acidification².

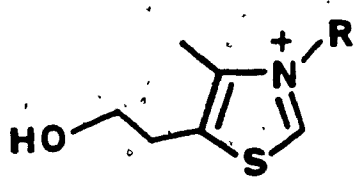
The object of the work in this thesis was to study the kinetics, and investigate the mechanism of the ring-opening reaction of thiamine (eq. 2) in aqueous base (pH 7-14), and of the ring-closing of the corresponding thiol form under acidic conditions (pH 0-7). As an approach to this investigation, the reversible ring-opening reaction of some simpler thiamine analogs (Figure 1), such as the N-methylbenzothiazolium ion (BT⁺), the 3,4-dimethyl-5-(2-hydroxyethyl)-thiazolium ion (HET⁺), over the whole pH range (0-14)



Scheme 1. Cleavage of thiazolium ions in aqueous basic solution.



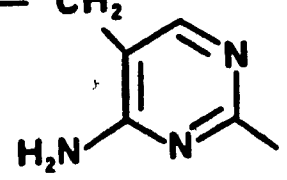
BT⁺



R = Me

HET⁺

R = CH₂



B₁⁺

Figure 1. Structures of the N-methyl-benzothiazolium ion (BT⁺), the 3,4-dimethyl-5-(2-hydroxyethyl)thiazolium ion (HET⁺) and thiamine (B₁⁺).

4
were studied as well.

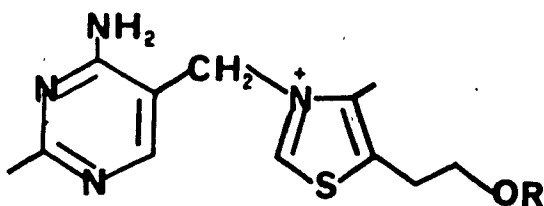
In our study, stopped-flow and conventional UV-visible spectrophotometry were used for all kinetic measurements. Dynamic and static NMR experiments were also carried out in order to clarify the products of the reactions under study and also to confirm the identity of synthesized quaternary salts.

It is hoped that the results of the present work will be of help in further understanding the chemistry of thiamine. Moreover, as will be discussed later, this study is relevant to the chemistry of tetrahedral intermediates, which are of great importance for many organic reactions.

THE THIAMINE FUNCTION

Thiamine, Vitamin B₁, (1), is an extremely important component in cellular metabolism¹⁰⁻¹². Its pyrophosphate derivative (2), cocarboxylase, is the coenzyme for such biochemical reactions as the decarboxylation of pyruvate, the synthesis of α -acetolactate, the transketolase and the phosphoketolase reactions¹².

Thiamine is composed of two organic heterocycles, a substituted pyrimidine ring and a substituted thiazolium ring connected by a CH₂ bridge (see below).



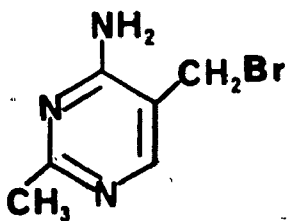
1 R = H

2 R = P₂O₆⁻²

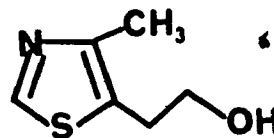
In general, thiazole ring systems are quite common in natural products because they can be produced by the cyclization of cysteine residues in peptides. Also, of course, pyrimidine rings are major components of RNA and DNA.

Investigations of thiamine were impeded by the difficulty of obtaining sufficient quantities of the material, which had been first isolated and crystallized by Jansen and Donath in 1926⁵. In 1934, Williams and his colleagues⁶ improved the yield by modifying the method of isolation and, in 1935, he successfully established the chemical structure as (1). The elucidation of the structure of thiamine was greatly assisted by Williams' discovery⁷ that thiamine is quantitatively split by sulphite in weakly acidic solutions into the pyrimidine and the thiazole halves (Scheme 2).

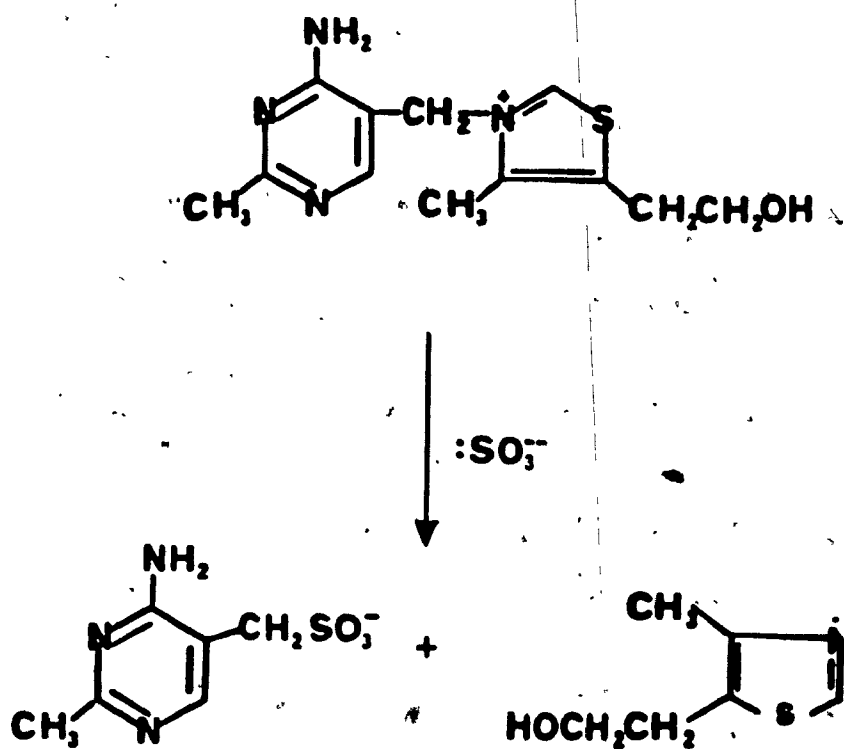
Soon afterwards, the above mentioned investigator reported⁸ the total synthesis of thiamine from 2-methyl-5-bromomethyl-4-aminopyridine (3) and 4-methyl-5- β -hydroxyethylthiazole (4).



3

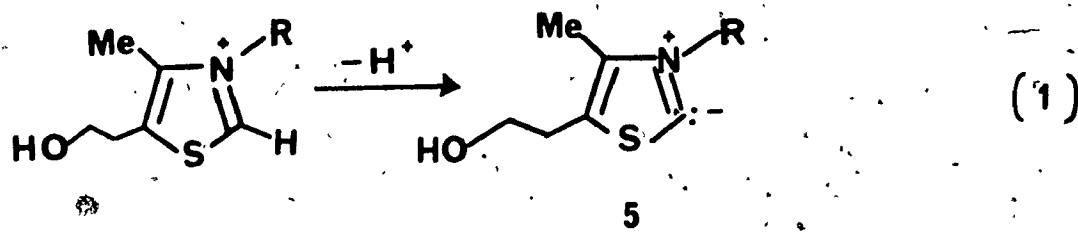


4



Scheme 2. Cleavage of thiamine molecule by sulfite ion.

The mechanism of the thiamine action was unclear until Breslow demonstrated⁹ from NMR studies that the thiazolium ion is acidic and that the hydrogen at the C-2 position can be exchanged with deuterium in basic heavy water under mild conditions.

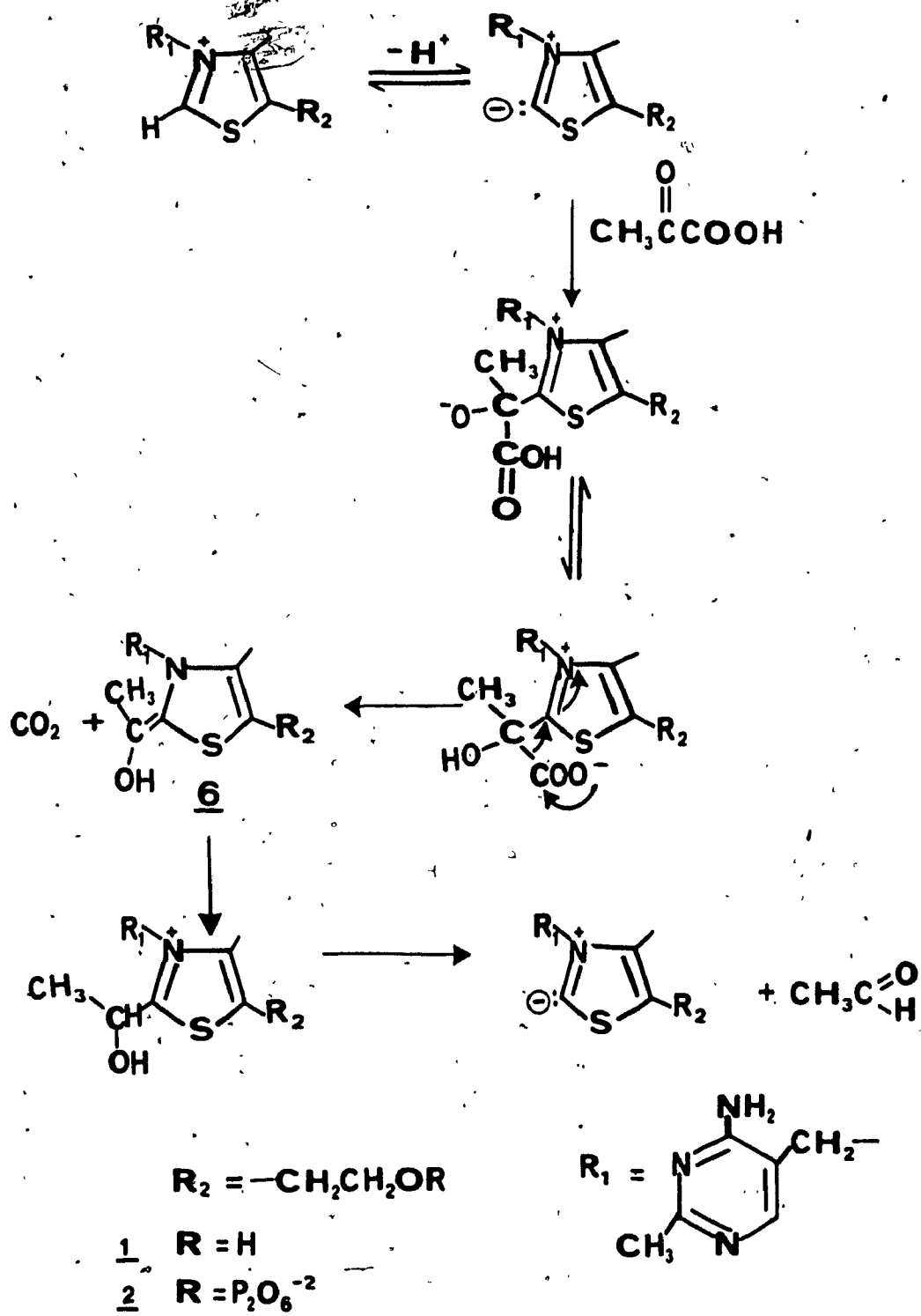


Breslow further proposed that the zwitterion (5), the thiazolium ylide, is the reactive species in a cocarboxylase function.

An example of cocarboxylase catalysis is the decarboxylation of pyruvate, which involves thiamine diphosphate (2) as the required cofactor⁸ or thiamine itself (1) for the case of the nonenzymic decarboxylation. Scheme 3 presents the commonly accepted^{7,9} pathway of the biochemical reaction.

The nucleophilic enolic intermediate (6), the hydroxyethyl-thiamine or the "active aldehyde" as it can be called in biochemical terms, is a form in which much of the coenzyme is formed in vivo. The significance of the "active aldehyde" in many biochemical reactions^{1,2} makes thiamine an important part of the cellular metabolism.

Another area of continuing interest in the chemistry of thiamine is the reversible ring opening of the



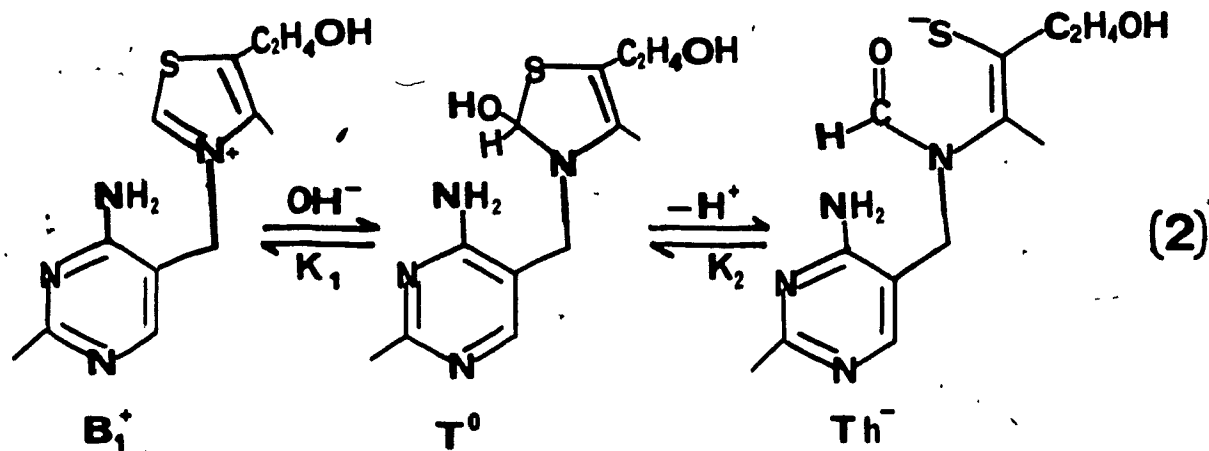
Scheme 3. Decarboxylation of pyruvate catalyzed by thiamine.

thiazolium ring in aqueous solution and its possible role in the transport of this vitamin across cell walls⁴. Earlier work on this reaction of thiamine and thiamine analogs will be discussed in the following section.

RING OPENING OF THIAMINE. EARLIER WORK

It is well known that in aqueous base thiazolium salts are in equilibrium with a ring-opened form, an enethiolate, T^- (Scheme 1)².

Williams and Ruelle^{1,3} were the earliest investigators who studied the attack of hydroxide ion on the thiazole moiety of thiamine. They found titrimetrically, that two equivalents of base were required to fully titrate one equivalent of thiamine (eq. 2).

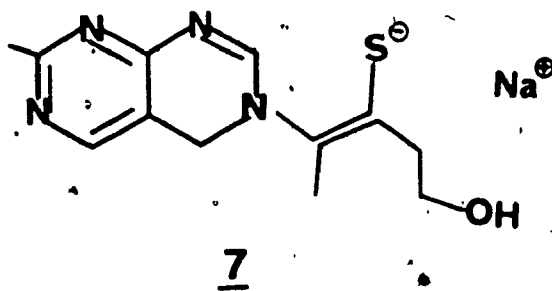


$$K_{av}^2 = \frac{(Th^-)_e (H^+)^2}{(B_1^+)_e}$$

They estimated the apparent pK_a (average of the apparent pK_a 's for the two steps) as 9.0, which is very close to the pK_a of 9.33 at 25 °C reported later by Watanabe and Asahi and obtained by polarographic and potentiometric methods¹⁴.

Maier and Metzler¹⁵ estimated pK_a spectrophotometrically as 9.3 for thiamine and 10.3 for the simpler 3,4-dimethyl-5-(2-hydroxyethyl)- and 3-benzyl-4-methyl-5-(2-hydroxyethyl)-thiazolium ions. Zima and Williams¹⁶ also proposed the pseudobase (T^*) as the primary addition intermediate formed when a thiazolium species is treated with aqueous base.

In addition, it has been known for a long time that thiamine develops a transient yellow colour in alkaline solutions^{14, 15}. Indeed, when Zima and Williams treated thiamine with ethoxide instead of hydroxide, they isolated a yellow sodium salt of thiamine, which they proposed to be the bicyclic species (7).



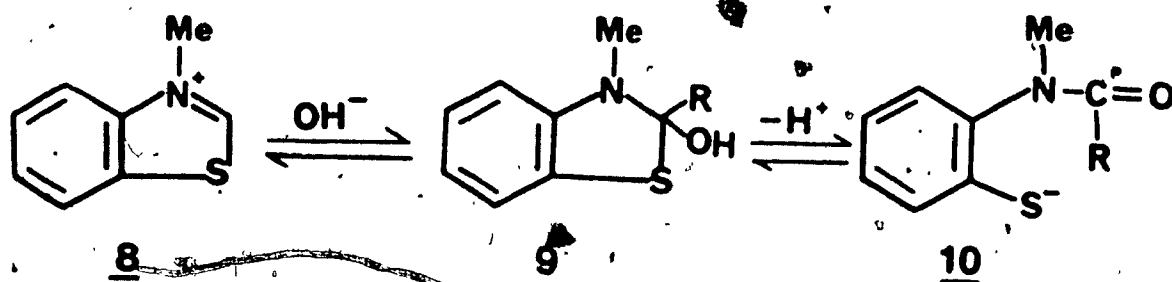
Maier and Metzler¹⁵ also investigated the "yellow form" of thiamine and they found that this form of thiamine does not exist to an appreciable extent below pH 10.6. Thus, they reasoned that the "yellow form" was in rapid

equilibrium with the thiamine itself and that the fading of the yellow colour was due to the slower process of the ring opening. On the basis of rapid-reaction studies, Höpmann and Brugnoni¹⁷ have recently postulated that the "yellow form" of thiamine can be directly transformed by an acid catalyzed reaction into the opened form thiolate.

A number of studies have also appeared on the pH dependence of the kinetics of the reversible ring opening of some substituted thiazolium and benzothiazolium cations.

Haake and Duclos⁴ investigated the opening of simpler thiazolium ions such as the 3,4-dimethylthiazolium ion and reported that the thiolate is the product of the ring-opening process. Further, they presented evidence based on their kinetic studies that the pseudobase is the intermediate on the reaction path leading to the ring-opening thiolate anion⁴.

Vorsanger¹⁸ has investigated the kinetics of the interconversion of the N-methyl benzothiazolium cations (8), eq. 3) and the corresponding ring opened thiophenolate ions (10) over the range pH 5-10.



BT⁺, R=H
MeBT⁺, R=Me

(3)

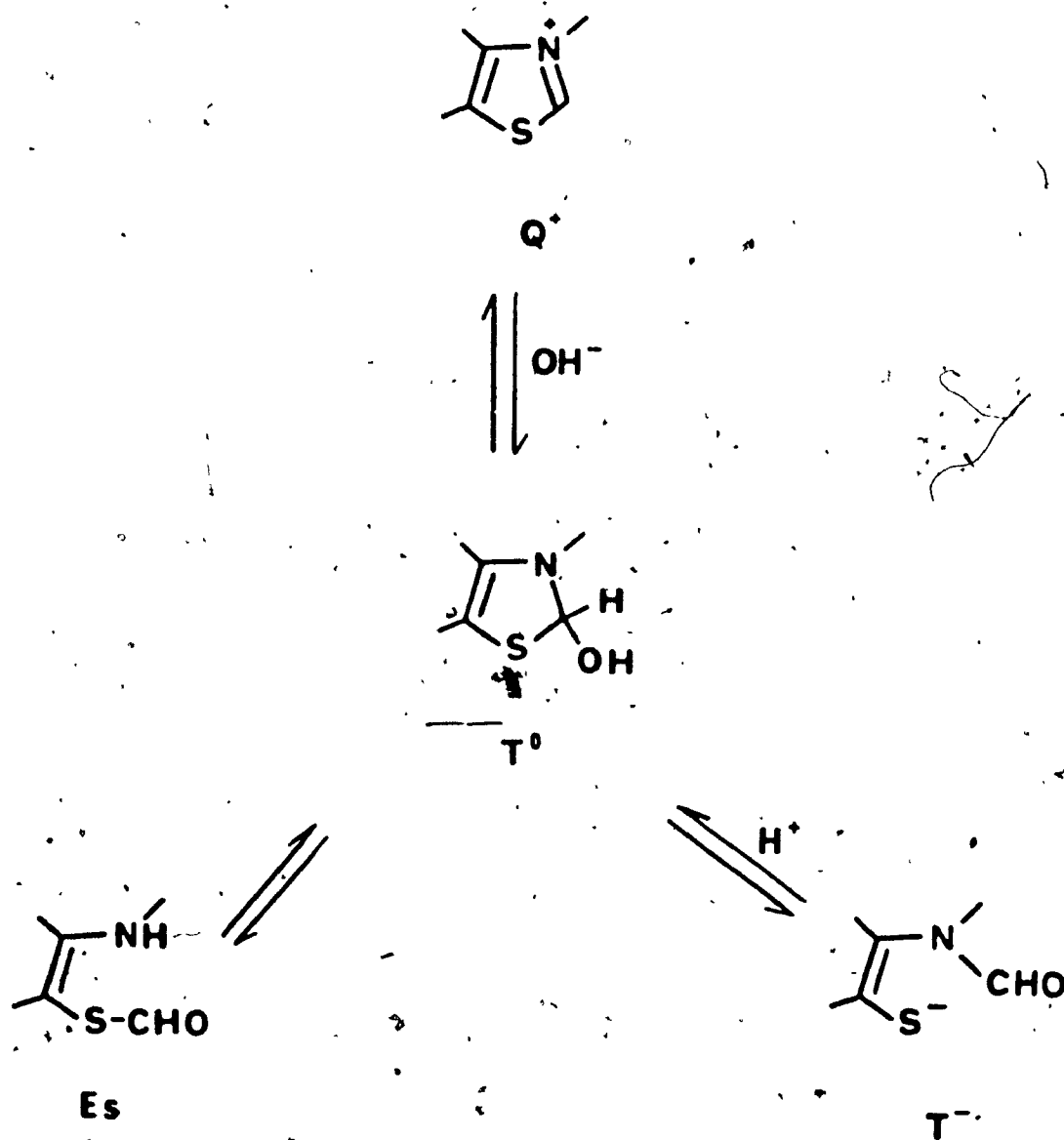
Our data for these compounds (BT^+ and MeBT^+)^{19a} meet with those of Vorsanger's with no significant discontinuities.

However, studies^{19a} on the cyclization of BT^+ showed two distinct processes between $\text{pH} = 0$ and 4. Likewise, two processes were also observed later for HET^+ at low pH ^{19b}. It is believed that the faster of the two processes leads to the formation of thiol ester, Es (Scheme 4), while the slower process is the cyclization of the thiolester to the thiazolium cation.

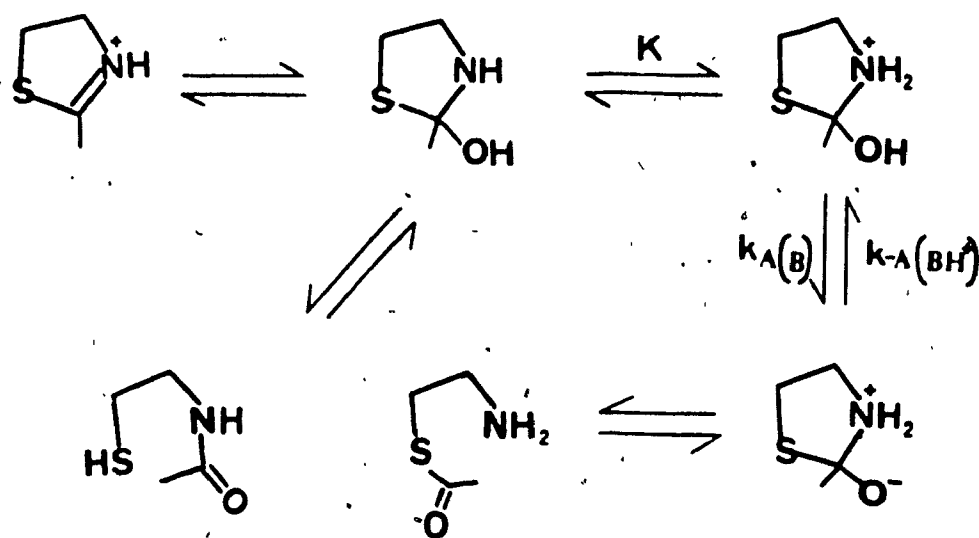
In earlier work, two processes were observed by Martin et al²⁰, in the hydrolytic ring opening of 2-methyl- Δ^2 -thiazoline below $\text{pH} = 3.0$ (Scheme 5). In this case too, the fast process was assigned to S-N acyl transfer ($\text{Es} \longrightarrow \text{T}$). To account for the thiazoline hydrolysis, a more complete mechanism was proposed later by Jencks and Barnett²¹.

The kinetics and the thermodynamics of the structural transformations of thiamine in neutral and basic media were also studied by Dubois and Chahine^{2c} using a pH jump technique. These researchers also claim to observe two kinetic phases when a basic thiamine solution is neutralized but their study was limited to a very small pH range ($\text{pH} = 6.5-7.5$).

Another study related to our work is the hydrolytic cleavage of the thiazolium ion ring of the 1'-methylthiaminium ion (11) carried out by Zoltezcic and Uray^{2a} using

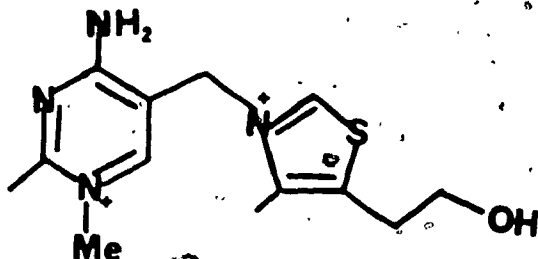


Scheme 4. Reclosure of thiazolium ions.



Scheme 5. Mechanism of the hydrolysis of 2-methyl- Δ^2 -thiazoline as it was proposed by Barnett and Jencks.

a pH stat method. They studied both the ring opening and ring closing process, but over a limited pH range near $\text{pH} = \text{pK}_{\text{a}}$. They estimated that the tetrahedral intermediate, pseudobase, cannot have a half-life greater than 20 seconds^{2a}.

11

Our study also includes some work on the 1-methylthiazolium ion but only one process was observed on the ring closing pathway to this ion.

Since the majority of the past investigations have concentrated on the ring opening reaction and the ring closing reaction over a limited pH range, we have studied the behaviour of thiamine and simpler analogues over the whole pH range 0-14.

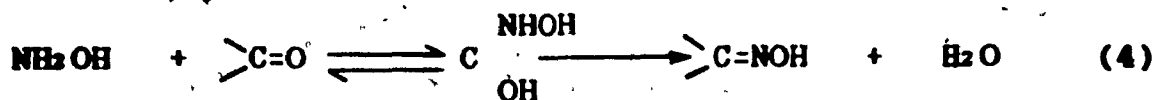
TETRAHEDRAL INTERMEDIATES - PSEUDOBASES

As was discussed in the previous section, thiamine and other thiazolium ions are well known to react with hydroxide ions to give a form in which the thiazolium ring is opened. The mechanism of this reaction is presumed to involve initial addition of hydroxide ion to C2 of the thiazolium ring forming a tetrahedral intermediate, the so-called pseudobase, followed by a base-catalyzed ring opened form (Scheme 1).

The formation of such tetrahedral intermediates, formed by the covalent addition of hydroxide ion to other unsaturated heterocyclic cations, is also well documented². Thus, many of the early structural investigations of some quaternary alkaloids, such as berberine and cotarnine, included attempts to differentiate between the pseudobase and the ring-opened amino-carbonyl tautomer as the major structure of the alkaloids in solutions.

Similarly, tetrahedral intermediates of many carbonyl compounds (e.g. ketones, aldehydes, carboxylic acids, esters, amides, amidines and anhydrides) are very well known to be important in many chemical and biochemical processes^{22, 23}. For example, tetrahedral intermediates are involved in many acyl-group transfer reactions^{22, 23}. The usual problem of mechanistic studies of such reactions is the direct detection of the intermediate and the determination of whether the rate-determining step of the reaction involves the formation or the breakdown of this intermediate.

As an example, the reaction of hydroxylamine with an aldehyde (eq. 4) is a simple carbonyl-group reaction in which the tetrahedral intermediate has been directly observed²⁴.

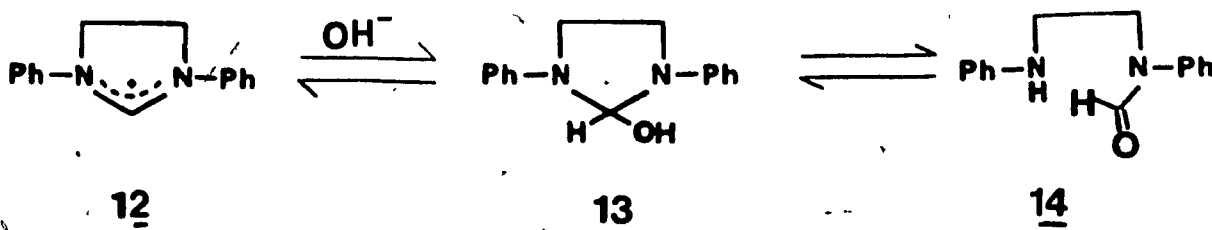


tetrahedral
intermediate

At neutral pH, hydroxylamine adds to the carbonyl compound in a fast reaction and the loss of water from the addition intermediate is the rate-determining step of the reaction. The formation of the tetrahedral intermediate in this reaction can be directly observed, at high concentrations of hydroxylamine, by the disappearance of the ultraviolet and infrared absorptions of the carbonyl group. The equilibrium constant for the formation of the intermediate may also be calculated by measuring the amount of the decrease in carbonyl-group absorption at different concentrations of hydroxylamine.

The formation of pseudobases as the intermediates in the hydrolysis of heterocyclic compounds was first observed by Decker²⁵ and Hantzsch²⁶ in 1890 for acridinium and quinolinium cations.

Another study that involves a pseudobase as an intermediate is the hydrolysis of 1,3-diphenylimidazolinium chloride (12, eq. 5) a system similar to the thiazolium heterocycle, initially studied by Jencks and Robinson²⁷.

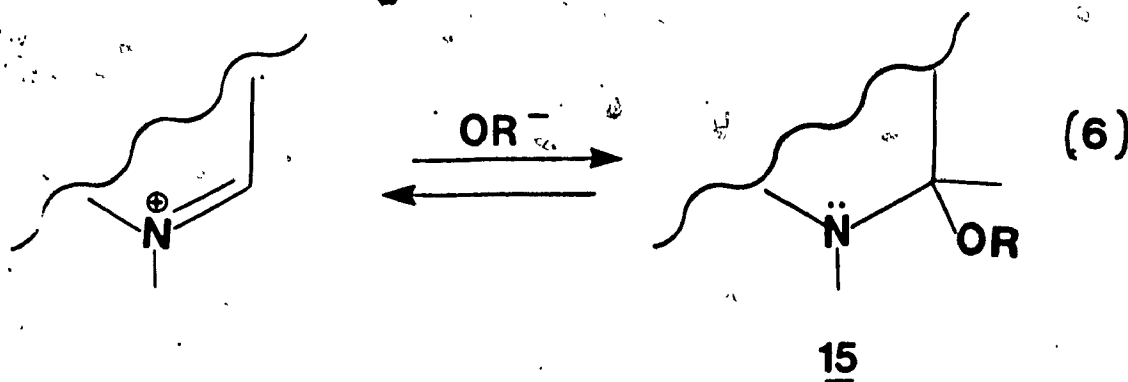


(5)

The rate and equilibrium constants of this reaction were measured by the use of stopped-flow methods. Although UV spectra indicated the build up of the suggested tetrahedral intermediate, Capon and coworkers²⁸ were unable to observe (13) by NMR studies under slightly different conditions.

More recently, in our laboratory, pseudobases have been observed during the hydrolysis of some quinazolium and pyrimidinium cations using both NMR and UV methods²⁹.

The formation of pseudobases from heterocyclic cations can often be detected spectroscopically². A pH-dependent electronic spectrum for a heteroatomic cation, which contains no readily ionizable protons, is usually attributable to pseudobase formation. Generally speaking, significant spectral changes occur upon pseudobase formation, since nucleophilic addition of hydroxide ion to an unsaturated carbon atom leads to a major change in the electronic conjugation of the molecule, (eq. 6), particularly when an aromatic ring is disrupted.

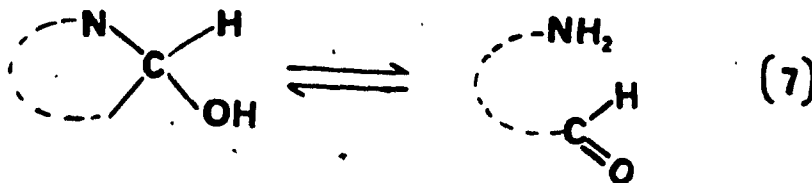


(R = H or alkyl)

Likewise, NMR spectra can also be used as a tool for studying pseudobase formation³⁰. The saturation of an unsaturated carbon atom, when pseudobase is formed, results in an upfield chemical shift of approximately 4 ppm for the signal of a hydrogen atom attached to that carbon atom. Upfield shifts of the signals from other nearby protons in the molecule may also be observed. NMR spectral data can also be used in order to distinguish between pseudobase and the anhydrobase or ylid, formed by deprotonation in mild basic solutions as it was suggested by Breslow⁶.

Pseudobase formation is a reversible pH-dependent process. Therefore, the parent quaternary ion is obtained upon acidification of the solution of the pseudobase. The reversibility of the reaction can be proved by both UV and NMR studies.

However, it is more difficult to distinguish between pseudobases (carbinolamines) and their ring opened amino-carbonyl tautomers (eq. 7) as the predominant species in basic solutions.



For this reason, much of the early work on alkaloidal heterocyclic cations was devoted to attempts to distinguish between the pseudobase and its ring-opened tautomer on the

basis of chemical reactivity³¹. But, in most cases, experiments designed for this reason did not provide enough information regarding the major component of this tautomeric mixture. Nowadays, spectroscopic techniques, which do not influence the position of the equilibrium, can be used to ascertain the composition of the equilibrium tautomeric mixture with more certainty. For example, a method proposed by Bunting³² allows the presence of other than minor amounts of the ring-opened tautomer to be ruled out.

By using basic methanol as solvent, the methoxide adduct of the heterocyclic cation (15, eq. 6), which is incapable of ring opening, is formed. Thus, if the UV spectra in aqueous base and the spectrum of the methoxide adduct in methanol show only minor differences due to solvents effects, then the pseudobase is the major tautomer in basic aqueous solution. On the other hand, major differences in the spectra of the cation dissolved in aqueous base and in basic methanol indicates that the ring opened tautomer is the major form existing in aqueous solutions. Experiments based on this method were also carried out in our research.

GENERAL ACID-BASE CATALYSIS. BUFFER CATALYSIS

Many biochemical and chemical reactions involve at least one proton transfer^{23, 23}. The most common mechanism of catalysis of these reactions, by enzymes or in the

laboratory, involves some sort of facilitation of this proton transfer. This type of catalysis is referred to as acid-base catalysis and is subdivided into general or specific catalysis:

General acid or base catalysis refers to contributions from all the acidic or basic species present in the solution; each individual acid or base present in the system can act as a proton donor or acceptor in the rate-limiting step and thus, the overall rate equation includes terms representing each of this species.

Scheme 6 is a simple example of a reaction that involves a proton transfer in the rate-limiting step and therefore, is subject to general acid catalysis.

Similarly, Scheme 7 shows a reaction that involves a slow ionization of the substrate followed by a rapid reaction of the anion to give the products and therefore, this reaction is subject to general base catalysis; i.e. bases in addition to hydroxide ion accelerate the reaction.

General acid/base catalysis has been encountered in many chemical and enzymatic reactions. Some typical examples are: enolization of ketones, aldol condensation of acetaldehyde, hydrolysis of ethylorthoacetate and addition of hydrazine and hydroxylamine to aldehydes and ketones.

On the other hand, specific catalysis usually does not involve any proton transfer in the rate-limiting step.



$$\text{Rate} = k_1 [S][HX_1] + k_2 [S][HX_2] + k_3 [S][HX_3] + \dots$$

where HX_1 , HX_2 , HX_3 , etc., are the acids present in the solution;

$$\text{or, Rate} = [S] \sum k_i [HX_i]$$

Scheme 6. General acid catalysis.



$$\text{Rate} = [HS] \sum k_i [B_i]$$

Scheme 7. General base catalysis.

Thus, Scheme 8 illustrates a reaction that follows specific acid catalysis. The acid present in the solution catalyzes the reaction by forming the conjugate acid of the substrate, S, in a rapid equilibrium preceeding a slower step. Under these circumstances, the reaction rate depends only on the H^+ concentration. In the case where other acids are present in the solution, they contribute to the reaction rate only through their contribution for the determination of pH of the solution.

By analogy, in specific base catalysis, the catalysis is caused only by the hydroxide ion. Reactions of this kind either involve hydroxide ion directly as a reactant or involve the formation of the conjugate base of the substrate in a rapid equilibrium step before the rate-limiting step (Scheme 9).

Some reactions that are subject to specific catalysis are: aldol condensation, inversion of sucrose, the decomposition of diazoacetic ester and the hydrolysis of orthoformate esters.

An experimental distinction between the general and specific catalysis can be made by measuring the reaction rate with various concentrations of the general acids or bases at constant concentration of H^+ . Since the pH depends only on the ratio of the undissociated acid to its conjugate base, and not on their absolute concentrations, this experiment can be carried out by the use of buffer



$$\text{Rate} = k[SH^+]$$

$$K = \frac{[SH^+][A^-]}{[S][HA]}$$

$$K_{HA} = \frac{[H^+][A^-]}{[HA]}$$

$$\frac{K}{K_{HA}} = \frac{[SH^+]}{[H^+][S]} = \frac{1}{K_{SH^+}}$$

$$\begin{aligned} \text{and so Rate} &= \frac{k}{K_{SH^+}} [H^+][S] \\ &= k_{H^+} [H^+][S] \end{aligned}$$

$$\text{where } k_{H^+} = \frac{k}{K_{SH^+}}$$

Scheme 8. Specific acid catalysis.



$$\text{Rate} = k[\text{S}^-] \text{ and } K = \frac{[\text{S}^-][\text{BH}^+]}{[\text{SH}][\text{B}]}$$

and so

$$\text{Rate} = \frac{kK[\text{SH}][\text{B}]}{[\text{BH}^+]}$$

$$\text{but, } K_a = \frac{[\text{BH}^+][\text{OH}^-]}{[\text{B}]}$$

$$\text{therefore, Rate} = \frac{kK[\text{SH}][\text{OH}^-]}{K_a}$$

Scheme 9. Specific base catalysis.

solutions. As the concentration of the undissociated acid is increased, the rate of a reaction subject to general acid catalysis will rise, whereas the reaction subject to specific acid catalysis will be unaffected. Similarly, a reaction that is general base catalyzed will increase in rate with increasing buffer concentration at constant pH and ionic strength and will show a larger increase with the buffer which contains a larger amount of the basic components.

In these experiments, the slope of the plot of the observed rate constants vs. the buffer concentrations gives the apparent second order rate constant of the buffer catalyzed reaction. In addition, the way in which the slope changes as the composition of the buffer changes shows whether the basic, the acidic or both component of the buffer are the active species of catalysis. The intercept of the plot at zero buffer concentration is the rate constant due to H^+ or OH^- catalysis and any catalysis by the solvent.

Buffer catalysis experiments has been widely used in the investigation of the mechanism of many organic reactions, such as hydration of alkenes, hydrolysis of esters and amides and nucleophilic addition to carbonyl compounds²³.

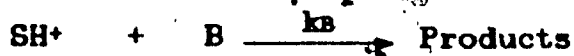
In our research work, general acid catalysis has been observed for the recyclization process of ring-opened

thiamine. In some cases, curved buffer plots were obtained which were rationalized due to change in the rate-determining step with increasing concentration of buffer. Similar interpretations for the same type of curves have been given in previous studies for other reactions involving tetrahedral intermediates^{21, 24, 25}.

It should also be pointed out that, in another pH region (around pH 4), apparent general base catalysis was observed due to actual specific base/general acid catalysis. This is a case of two kinetically indistinguishable processes. Similarly, apparent general acid catalysis can be due to simultaneous general base and specific acid catalysis²³.

Consider a general base catalyzed reaction of the protonated form of a substrate, S. As shown in Scheme 10, the form of the rate equation is such that the reaction appears to be a general acid catalyzed reaction of the substrate S. Thus, the reaction of SH^+ with B is kinetically indistinguishable from the reaction of S with BH^+ .

An example of reaction which follows Scheme 10 is the general acid catalyzed enolization of ketones²³.



$$\text{Rate} = k_b [SH^+] [B]$$

$$\text{but, } K_{SH^+} = \frac{[S][H^+]}{[SH^+]}$$

$$\text{thus, Rate} = \frac{k_b [S][H^+][B]}{K_{SH^+}}$$

$$\text{however, } K_{BH^+} = \frac{[B][H^+]}{[BH^+]}$$

and so

$$\text{Rate} = \frac{k_b K_{BH^+}}{K_{SH^+}} [S][BH^+]$$

Scheme 10. Specific acid/general base case.

EXPERIMENTAL

MATERIALS

Thiamine hydrochloride (B₁) was obtained from Aldrich.

1'-Methylthiaminium perchlorate was prepared following the method in the literature³⁶. The product, white crystals, was collected in good yield (76.5%); m.p. 232-235 °C (dec.).

3,4-Dimethyl-5-(2-hydroxy-ethyl)thiazolium (HET⁺) iodide was initially synthesized by mixing 4-methyl-5-thiazoethanol with a slight excess of methyl iodide in acetone. The reactant mixture was left stirring overnight at room temperature. Tan-coloured crystals were collected the next day. The product was recrystallized from an acetone-methanol (20:1) mixture. Yield: 72%; m.p. 87 - 89 °C. Later on this compound became available from Aldrich. Similar methods of preparation were followed for the synthesis of N-methyl-benzothiazolium and 1,2-dimethyl benzothiazolium salts¹⁶ which were used in studies prior to the current project.

All the synthesized compounds were checked by taking their NMR spectra on a Bruker WP-80 F.T. spectrometer. Melting points were measured on a Gallenkamp melting point apparatus and are uncorrected. All organic and inorganic reagents used were of analytical grade.

All deuterated chemicals used for the NMR experiment were purchased from Merck, Sharp, and Dohme.

KINETIC SOLUTIONS

All substrate solutions used for kinetic runs were prepared in 1 M NaCl, the concentration of substrate being of the order 0.1 mM. For the study of ring closing, the substrate was dissolved in 0.001 M KOH (pH 11), and left for about 10 half-lives prior to kinetic studies, so that all of the substrate was in the ring-opened thiol form. This solution deteriorated with time, probably due to oxidation of the ring opened product to a disulfide derivative¹⁵.

Glass distilled water was used as solvent for all the kinetic solutions. Buffer solutions, of pH between 2 and 11 and $I = 0.01$ M, were made up following Perrin^{27,28}. Buffers of different acids were prepared so that they covered a pH range equal to $pK_a \pm 1$, where pK_a is the pK_a of the acid used²⁹ at $I = 1$ M. The buffers used were chloroacetate ($pK_a = 2.74$), 3-chloropropionate ($pK_a = 3.93$), acetate ($pK_a = 4.65$), succinate ($pK_a = 5.50$), phosphate ($pK_a = 6.55$), borate ($pK_a = 8.90$), and carbonate ($pK_a = 10.20$). The total ionic strength of these solutions was adjusted to 1 M with addition of NaCl. The pH of each buffer solution was measured, after mixing, with equal volume of substrate solution, with a Corning Digital 110 expanded scale pH meter. Standard phosphate buffer (pH = 6.86), borate buffer (pH = 9.18), and phthalate

(pH = 4.01), from Fisher Scientific Company, were used for calibration of the pH meter.

For solutions of pH above 11 or below 2, dilutions of standardized 1 N NaOH and 1 N HCl (A. & C. American Chemicals) were used, respectively. NaCl was again used for these solutions to bring the total ionic strength to 1.0 M.

For buffer catalysis experiments, chloroacetate, acetate, and phosphate buffers were used. First, the most concentrated buffer (0.2 M after mixing in the stopped-flow) was prepared according to the Henderson-Hasselbach equation³⁸:

$$\text{pH} = \text{pK}_a + \log \frac{[\text{A}^-]}{[\text{HA}]} \quad (8)$$

where pK_a is the pK_a of the acid used at $I = 1 \text{ M}$.

Buffers of lower concentration (down to 0.01 M a.m.) were prepared afterwards by dilution of the most concentrated buffer with 1 M NaCl. All buffer solutions were prepared the day previous to the kinetic experiments.

Difficulties were experienced in studying the equilibration of thiamine with its "yellow form". Conversion in the forward direction, thiamine to "yellow form", was easily followed and our results are similar to those of Hopmann^{3b}. However, in the reverse direction, "yellow form" to thiamine, reproducibility was poor and the results are not considered to be very reliable. A solution of the "yellow form" was generated by dissolving thiamine

hydrochloride in 0.2 N NaOH (pH = 13.3). It was mixed with series of boric acid solutions of appropriate concentration to reach a desired pH (calculated by eq. 8). The difficulties noted may be due to various factors or some combination of them: 1) solutions of the "yellow form" are not stable (see later); 2) thiolate to disulphide oxidation may occur¹⁵; 3) the pH may not have been constant during the process monitored.

STOPPED-FLOW TECHNIQUE

For the most part, the reactions studied in this project were quite rapid, and so, the stopped-flow technique was used for all the kinetic measurements. This method, which was first used for reaction in solutions by Chance⁴⁰, allows one to follow reactions with half-lives ranging from few minutes down to few milliseconds.

In this method, two reactant solutions are forced into a mixing chamber, where they are mixed extremely rapidly; from there, the solution passes at once into an observation cell. The flow of the mixed solution into the observation cell is abruptly stopped, after a few milliseconds, and measurements of concentration, as a function of time, are made by following the changes of a suitable property of the solution. Usually, in order to minimize the "dead time", the mixing chamber and the observation cell are one and the

same. (The dead time is the time between mixing and observation.)

It is important, in this method, that the reactant solutions are mixed thoroughly, but in a time which is shorter than the half-life of the reaction under study⁴¹. Also, it is necessary that the flow is stopped abruptly since a gradual decrease in the flow rate may result in incomplete mixing and then a rate lower than the actual rate will be obtained⁴¹.

Most commonly, the progress of the reaction is monitored spectrophotometrically⁴² and the readings are recorded continuously using either a high-speed digital recorder or a storage oscilloscope.

Other techniques, such as e.m.f. measurements⁴³ with a glass electrode, conductivity measurements^{44, 45} and electron-spin resonance⁴⁶, have also been used for the observation system.

The major advantage of the stopped-flow technique over the continuous-flow method is the economical use of reactants. In the stopped-flow method, using spectrophotometry, the volume of the reactant solutions required is very small; this is very important for reactions which include reagents such as enzymes which are difficult or expensive to obtain in large amounts. In addition, by the stopped-flow method a permanent record of the progress of

the reaction, can be obtained and, unlike the continuous-flow method, the results are not affected by the rate and the character of the flow through the observation vessel and they are free from effects of mechanical disturbances⁴⁷, provided the mixing is fast and efficient.

For its advantages, the stopped-flow technique has been widely used in studies of the rates and mechanisms of many biochemical, organic and inorganic reactions^{41, 46, 48}.

APPARATUS AND KINETIC PROCEDURE

All kinetic measurements were carried out with an Aminco-Morrow stopped-flow apparatus attached to an Aminco DW-2 UV-visible spectrophotometer, operating in the dual-wavelength mode.

In this mode, one monochromator is set to a reference wavelength where little or no absorbance change occurs and the other, the sample monochromator, provides a wavelength where a large change in absorbance is observed. The reference and the sample beams alternately pass through a single cuvette, the observation cell of the stopped-flow, by means of an optical chopper, which usually operates at 250 Hz. For very fast reactions, the chopper speed is increased to 1000 Hz.

On the optical unit, the ultraviolet (deuterium) lamp was usually selected as the light source.

In the dual-wavelength mode, both monochromators are illuminated from the same light source and thus, light intensity fluctuations are eliminated. In addition, since the beams from both monochromators pass through the same portion of a single cuvette, the effects of sample settling and scattering are cancelled⁴⁹. Because of these advantages, the dual-wavelength mode is often used for turbid samples and solutions with particles that change size or settle during the recording of the spectra.

Operation of the stopped-flow accessory is as follows⁵⁰: with two 5-ml syringes, the reactant substrate in one syringe and buffer, acid or base solution in the other syringe, in our case, are transferred into two internal drive syringes, each of 2.5 ml capacity, of the stopped-flow apparatus. A drive block, activated with compressed gas of 55-60 p.s.i. pressure, forces a small amount (0.02 ml) of each reactants solution, at high velocity, into a 10 mm long observation cell and finally into a stopping syringe. The piston of the stopping syringe moves upward until it reaches the tip of a micrometer. Just before the piston stops, a switch on the micrometer tip is activated, triggering the recording device. From this point on, the data acquisition begins and the total observed absorbance change is collected as voltage vs. time on a storage oscilloscope or transient recorder. The "dead time" of the system, i.e. the time

required for the reactants to be mixed and reach the observation cell, is 4 msec.

Figure 2 illustrates the stopped-flow and data acquisition system used for this project for relatively fast reactions (half-life less than 20 seconds). From the DW-2 spectrophotometer, a voltage/time trace (2 V = 1 Abs. unit) proportional to the absorbance change of the reaction under study was stored on a Biomation 805 Waveform recorder (8 bit resolution). The stored signal (2048 points) was viewed on a Tektronix 2215, 80 MHz oscilloscope and acceptable traces were transferred serially at 9600-band through a Datas 305 interface, to an Apple II microcomputer for data analysis. Sometimes, the stored trace on the Biomation was plotted out on a Aminco x-y recorder for a record of the absorbance-time curve.

From the 2048 points transferred to the Apple II, the microcomputer displayed every twentieth point, a total of 100 points. An average infinity value was calculated from the last ten points. First order rate constants were calculated from the first 14-40 points, covering approximately 90% of the reaction, using the TR1ST program.

In the case of slower reactions (half-life greater than 20 seconds), an Isaac A/D system (Cyborg 91a), connected directly to the stopped-flow apparatus and to the Apple II microcomputer, was used. This way, the observed signal (200 points) was directly viewed on the monitor.

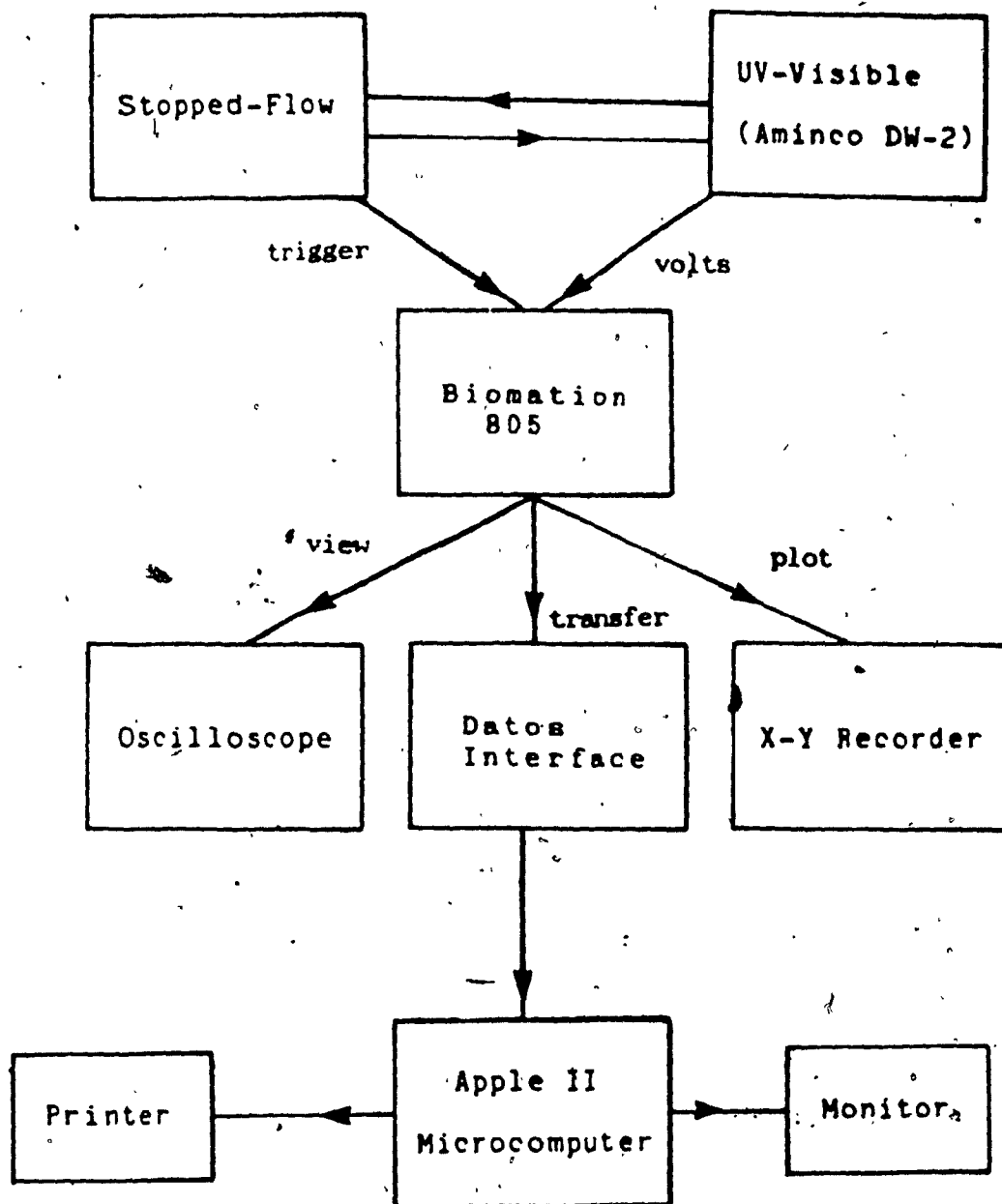


Figure 2. Stopped-flow acquisition system.

Rate constants were calculated the same way as in the case of fast reactions, using the ISAAC program. Both TR1ST and ISAAC programs were written, in BASIC and machine language, by Professor O.S. Tee.

In the cases where the reaction under investigation was too slow to be followed by the stopped-flow apparatus, the experiment was carried out by the conventional UV method. Such experiments were carried out at Mount St-Vincent University, Halifax, Nova Scotia, under the supervision of Dr. R.S. McDonald. It is gratifying to record that the experiments that were done separately in the two laboratories showed good agreement in the region of overlap.

All kinetic experiments, except in the case of temperature dependence studies, were carried out at 25.0 ± 0.1 °C. The temperature of the solutions in the stopped-flow apparatus was maintained with a Lauda-RC 20B constant temperature circulating water bath.

Prior to each kinetic experiment, the stopped-flow accessory was flushed out twice with distilled water and the reactant solutions were left for a while in the stopped-flow apparatus in order to equilibrate at the temperature of the experiment.

All reactions were followed for about ten half-lives (99.9% reaction). For each kinetic experiment, five to six runs were carried out and an average observed rate constant

was calculated from these. A run was considered acceptable if the correlation coefficient of $\ln(A - A_0)$ vs. time was better than 0.998. Most runs had correlation coefficients much better than this. All kinetic experiments were carried out under pseudo-first order conditions since the concentration of the substrate, usually 0.1 mM, was much smaller than the concentration of the base, acid or buffer with which it reacted. Pseudo-first order rate constants were calculated using "Normal", Swinbourne and Guggenheim treatment of the data, as described later.

Temperature dependence studies experiments were carried out in the stopped-flow apparatus by measuring the observed rate constant of the cyclization reaction at low pH (pH = 2) at different temperatures (15 °C, 20 °C, 25 °C, 30 °C, 35 °C). The activation parameters of the reaction under study were calculated by least square analysis of the plot of $\ln(k_{obs}/T)$ vs. $1/T$, where T is the temperature in Kelvin degrees. The least square analysis was done on the Apple II microcomputer, using the LSQPLOT program, written by Professor O.S. Tee.

UV spectra were measured on a Aminco DW-2 spectrophotometer or a Cary 2290 UV-visible spectrophotometer, both operating in the split beam mode. In this mode, a single monochromator is used for scanning and the monochromatic beam is chopped and alternately passes through the reference and sample cuvettes.

UV spectra of each compound studied were recorded in basic (0.1 N NaOH) and acidic (0.5 N HCl) solutions before the kinetic experiments, in order that suitable wavelengths at which to follow each reaction could be determined. Thus, in the case of thiamine, the kinetics of formation of the "yellow form" was followed at 340 nm vs. 380 nm, since the "yellow form" shows an absorption maximum at 340 nm, and there are no other significant absorptions above 320 nm. The ring-opening reaction of thiamine, the formation of the ring-opened thiol, was followed by measuring the rate of disappearance of the "yellow form" at 340 nm or by observing the appearance of the thiol at 250 nm. Both the fast and the slow processes of the ring-closing reaction were conveniently followed at the maximum of thiamine at 265 nm. Also, at 250 nm, the ring-closing reaction of the N_1MeB_1^+ was studied. The step of $\text{TH}^+ \rightleftharpoons \text{YF}$ was followed as a decrease in absorbance at 290 nm vs. 340 nm or as an increase in absorbance at 340 nm vs. 380 nm. Similarly, the behaviour of HET^+ was followed at 242 nm vs. 320 nm for the ring-opening process, and at 256 nm vs. 320 nm for the ring-closing process below pH 8. In both these cases, the rate of the appearance of the product of the reaction (increase in absorbance) was measured.

The kinetics of the ring-closing reaction at pH > 8 were followed as a decrease in absorbance at 240 nm vs. 320 nm.

MATHEMATICAL TREATMENT OF KINETIC DATA

As it was remarked early, the observed first order rate constants were calculated on the Apple II microcomputer by "normal", the Kezdy-Swinbourne⁵¹ and the Guggenheim method⁵².

"Normal" Method⁵²

For a first order reaction, the rate law is given by the equation:

$$\text{Rate} = -\frac{dR}{dt} = k[R] \quad (9)$$

where R is the concentration of reactants at time t , and k is the first order rate constant. Integration of eq. 9 gives:

$$[R] = [R]_0 e^{-kt} \quad (10)$$

where $[R]_0$ is the initial concentration. For a reaction that follows the Beer-Lambert law, eq. 10 can be expressed as a change of absorbance with time:

$$(A_t - A_\infty) = (A_0 - A_\infty)e^{-kt} \quad (11)$$

or

$$\ln(A_t - A_\infty) = \ln(A_0 - A_\infty) - kt \quad (12)$$

where A_0 is the absorbance at $t = 0$, A_∞ is the final absorbance, and A_t is the absorbance at time, t .

As is seen from eq. 12, a plot of $\ln(A_t - A_\infty)$ vs. time should give a straight line, of slope equal to $-k$. The value of A_∞ should be known accurately, since a small error in A_∞ can greatly affect the apparent value of k .

Kezdy-Swinbourne Method⁵¹

For this method, two sets of data are required. If $A_1, A_2, A_3, \dots, A_n$ are absorbance changes at time $t_1, t_2', t_3, \dots, t_n$, respectively and $A_{1+t'}, A_{2+t'}, A_{3+t'}, \dots, A_{n+t'}$, at later times $t_{1+t'}, t_{2+t'}, t_{3+t'}, \dots, t_{n+t'}$, where t' is a constant time interval, then eq. 11, for the first set of data and eq. 13, for the second set, can be applied.

$$(A_{t+t'} - A_\infty) = (A_0 - A_\infty)e^{-k(t+t')} \quad (13)$$

where $A_{t+t'}$ is the absorbance change at time $t + t'$.
Dividing eq. 11 by eq. 13 gives:

$$\frac{(A_t - A_\infty)}{(A_{t+t'} - A_\infty)} = e^{kt'} \quad (14)$$

Rearrangement of eq. 14 gives:

$$A_t = A_\infty(1 - e^{kt'}) + A_{t+t'}e^{kt'} \quad (14a)$$

Thus, a plot of A_t vs. $A_{t+t'}$ gives a straight line and the first order rate coefficient, k , may be evaluated from the logarithm of the slope (equal to $e^{kt'}$) of this line. Also, in cases where A_∞ is not stable, due to subsequent reaction, it can be estimated from the intercept ($A_\infty(1 - e^{kt'})$) and slope.

Guggenheim Method⁵¹

An earlier approach, which is related to the Kezdy-Swinbourne plot, is the Guggenheim method of plotting kinetic data, which also does not require a knowledge of the initial A_0 and final A_∞ absorbance values. Again, two series of readings at times t and $t + t'$ are used.

Subtracting eq. 11 from eq. 13 gives:

$$(A_{t+t'} - A_t) = (A_0 - A_\infty)e^{-kt}(e^{-kt'} - 1) \quad (15)$$

or

$$\ln(A_{t+t'} - A_t) = \ln(A_0 - A_\infty)(e^{-kt'} - 1) - kt \quad (15a)$$

For a given kinetic run, A_∞ , A_0 , and t' are constant and therefore

$$\ln(A_{t+t'} - A_t) = \text{constant} - kt \quad (15b)$$

and so, a plot of the left-hand side against time should be a straight line with a slope equal to $-k$. For best results, t' should be of the order of one half-life and the

data should cover at least two half-life periods. The same is true for the Kezdy-Swinbourne method⁵¹.

Rate constants determined by the "Normal" method were used in this project. The A value estimated by the Kezdy-Swinbourne method was utilized when the observed A was not well defined due to interference from other reactions.

NMR

High-resolution nuclear magnetic resonance spectra were recorded on a Bruker WP-80 Fourier transform spectrometer. D₂O was used as solvent with DSS (sodium 2,2-dimethyl-2-silapentane-5-sulfonate) as the internal reference. Static spectra of the substrate (B⁺ or HET⁺) and ring-opened thiol were taken at ambient temperature. The thiol form was generated by adding an excess of sodium deuterioxide (40% solution in D₂O) to a 0.1 M solution of the substrate. After letting the sample stand for some time, to insure completion of the ring opening reaction, the spectrum of the opened form was taken. Addition of deuterium chloride solution (35% w/w in D₂O) to the thiol sample, regenerated the original spectrum of B⁺ or HET⁺.

The same procedure was followed to carry out dynamic NMR experiments at 274 °K. The instrument was left to equilibrate at the new temperature and after acidification of the basic sample of thiol with DCl, spectra of the products of the ring-closing process were run as fast as

possible (~ 9 seconds). Then, consecutive spectra of the sample were taken every 3 seconds. By this method, it was hoped that the spectrum of the product of the fast process at low pH would be obtained. However, because of the heat evolved from the neutralization reaction (strong acid + strong base), the temperature of the sample apparently increased, which obviously increased the rate of the slow process, and so, only the spectrum of the product of the slow process was recorded.

RESULTS AND DISCUSSION

Results of the kinetic studies of the reversible hydrolytic cleavage of HET^+ , B_1^+ , and N_1MeB_1^+ , over the whole pH range, 0-14, are presented and discussed in this section. UV and NMR qualitative spectra of the principal species involved are also included. Some data on the effect of temperature and buffer concentration on the rate of the reaction are also presented.

Finally, reasonable mechanisms, which are consistent with the experimental findings, are proposed for the ring-opening and ring-closing reactions of the compounds under investigation. Where possible, the present results are compared with those in literature.

NMR STUDIES

Herein are reported dynamic proton NMR spectra of the cations HET^+ , B_1^+ , and N_1MeB_1^+ in D_2O . Spectral studies of the ring-opened thiol forms of these compounds in NaOD are also presented. Tables 1-3 contain the assignments of the various resonance signals for both the ring-closed and ring-opened forms.

Figure 3 presents the spectrum of HET^+ in D_2O at 31 °C (the temperature at the probe of the WP-80 spectrophotometer at room temperature). The $\text{C}_2\text{-H}$ proton is not detected from this spectrum due to its well-known⁹ deuterium exchange with the solvent D_2O . However, the spectrum of the same sample run in H_2O in an earlier study^{5a} clearly

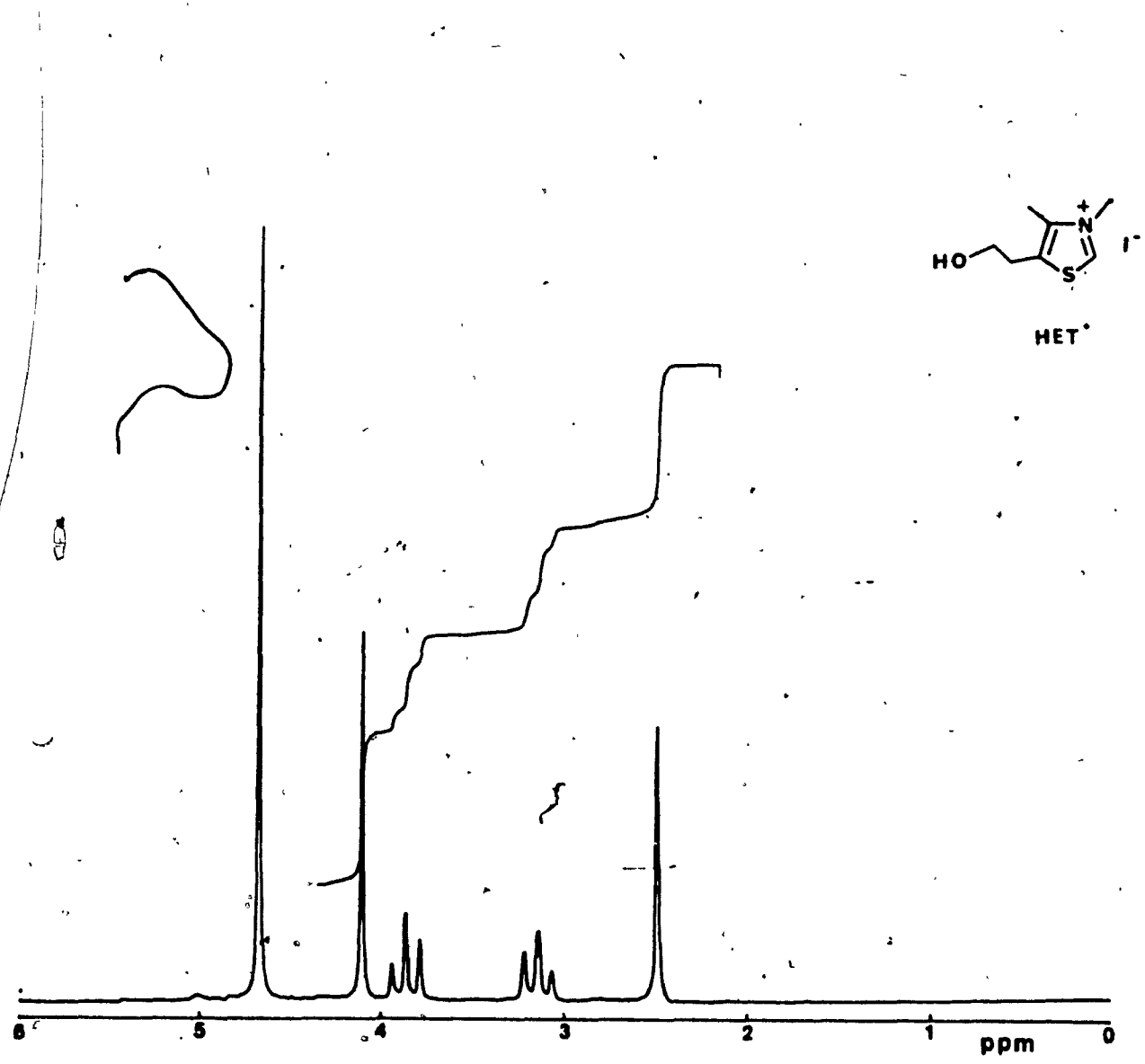


Figure 3. Proton NMR spectrum of 3,4-dimethyl-5-(2-hydroxyethyl) thiazolium iodide in D₂O at 31 °C (Assignments in Table 1).

showed this proton at 9.7 ppm, as expected from equivalent systems^{4, 54, 56, 57}.

Upon addition of an excess of NaOD to the sample of HET⁺ in D₂O (pH of the final solution is equal to 12.5), the spectrum shown in Figure 4 was obtained. This is the spectrum of the ring-opened thiol in its anion form. The spectral assignments, given in Table 1, are in agreement with those made previously⁵³. From a comparison of the spectra in Figures 3 and 4, an upfield shift of all the protons of the thiazolium ring is observed during the ring-opening reaction. The C₂ proton has also been reported⁵² to appear at higher field (8.1 ppm) in the thiol form. These upfield shifts result from the change of the positive quaternary nitrogen in HET⁺ into a neutral tertiary nitrogen atom in the thiol.

In addition, the appearance of the N-methyl protons of the thiol molecule as two sharp singlets, at 2.82 ppm and 3.02 ppm, is due to limited rotation about the amide carbonyl nitrogen bond⁵⁵. For the same reason, two singlets, one at 1.75 ppm and the other at 1.82 ppm, are observed for the C-methyl protons. Such rotational isomerism is common in amides^{29, 55}.

Figure 5 shows the spectrum of HKT⁺, taken 12 seconds after acidification of the ring-opened thiolate, with DCl (pH of the resultant solution is equal to 1.46), at about 0 °C. Although, as was explained in the experimental

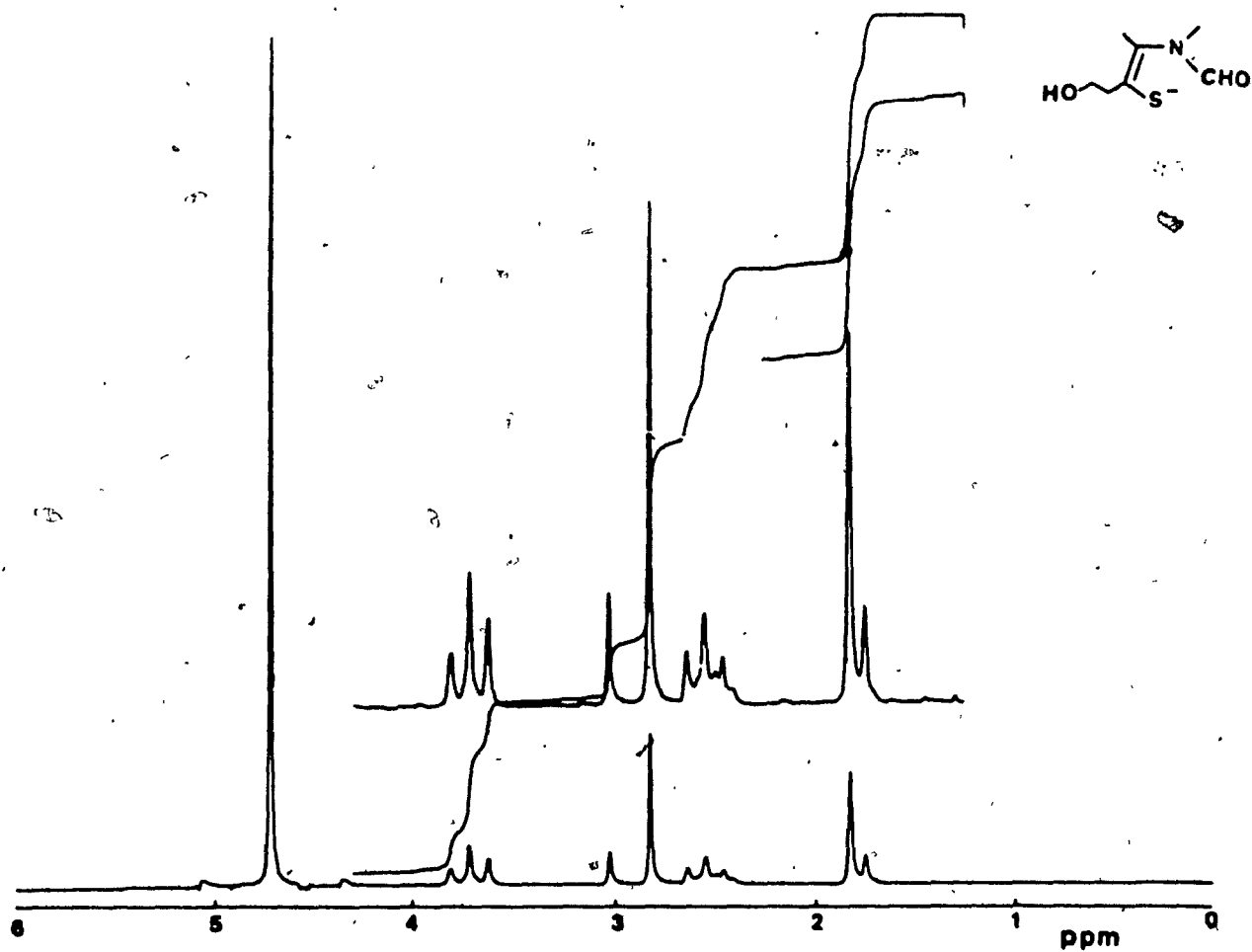
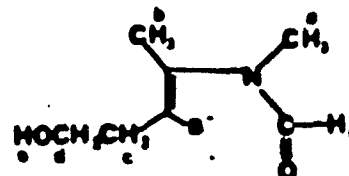
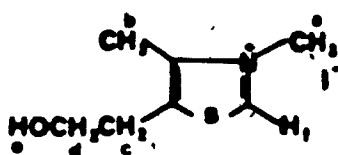


Figure 4. ¹H NMR spectrum of the ring-opened thiol of 3,4-dimethyl-5-(2-hydroxyethyl) thiazolium iodide in NaOD / D₂O (pH = 12.5) at 31 °C (Assignments in Table 1).

Table 1. The NMR assignments for HET⁺ and its ring-opened thiol form in D₂O. Chemical shifts are in ppm.



Assignment

a	4.12 s	2.82 s
b	2.48 s	3.02 s
c	3.16 t	1.82 s
d	3.86 t	2.55 t
e	x	3.71 t
f	x	x

s = singlet t = triplet

x = exchanged with D₂O

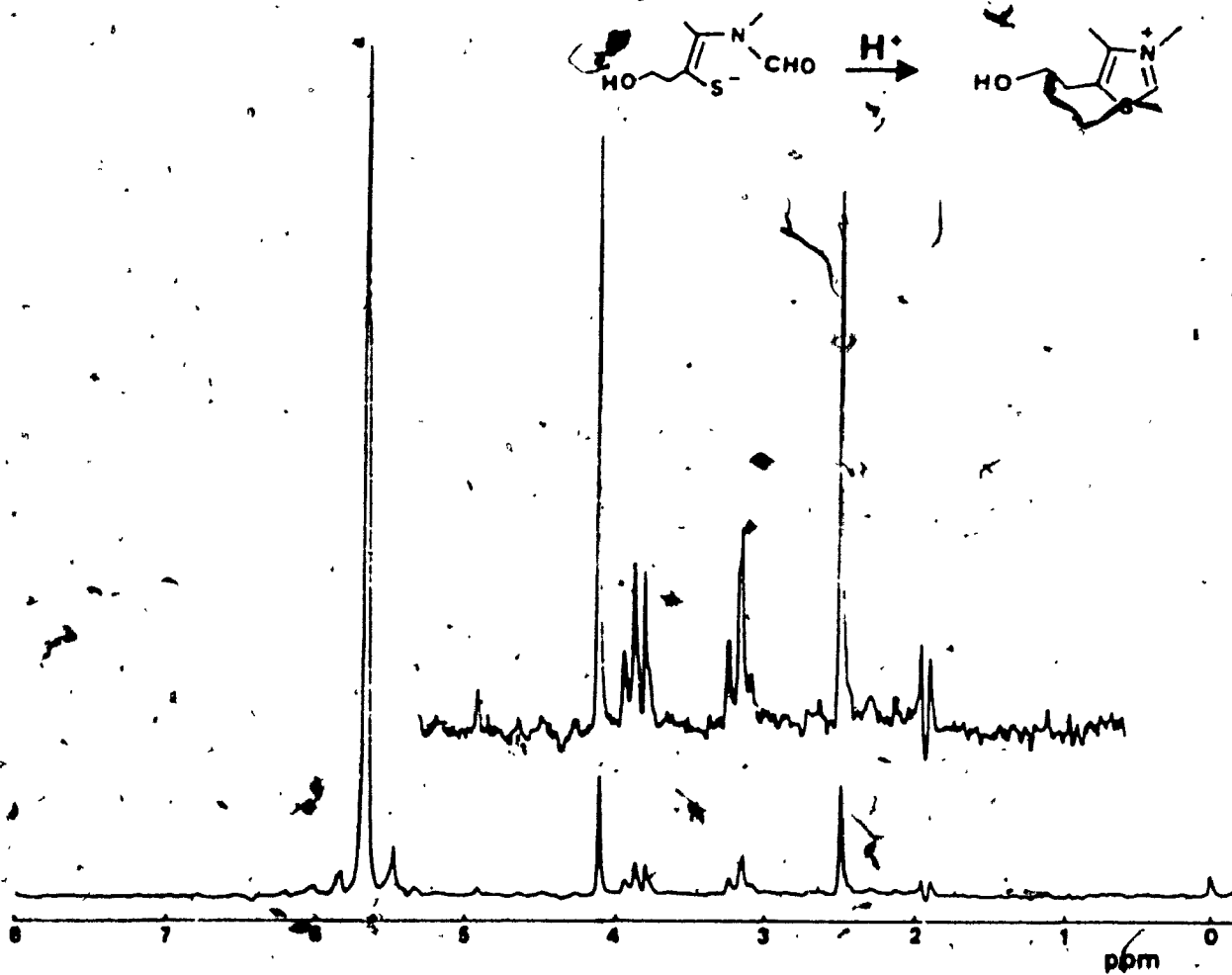


Figure 5. ^1H NMR spectrum of HET $^+$ formed after acidification of the ring-opened thiol sample. Spectrum run in D_2O / DCl (pH = 1.46) at 31 $^\circ\text{C}$, was taken 12 seconds after the acidification of the thiol.

section, this spectrum was initially taken in order to identify the product of the fast process of the cyclization reaction, it proves once again the reversibility of the base-catalyzed ring-opening reaction of the thiazolium cation.

Similarly, spectra of thiamine and its opened-ring thiol form have been observed. Figure 6 illustrates the proton NMR spectrum of thiamine hydrochloride in D_2O at $31^\circ C$. Assignments of the observed peaks and the corresponding chemical shifts are given in Table 2. They are substantially the same as given in References 56 and 57, where $DMSO-d_6$ and H_2O were used as solvent, respectively.

As in the case of HET^+ , the resonance of the C_2-H proton, expected to be seen⁵⁶ at about 9.54 ppm, has not been observed due to deuterium exchange with D_2O . Similarly, exchange of C_4-NH_2 amino protons with the solvent gives C_4-ND_2 , which is not detected.

The spectrum of the ring-opened thiolate form of thiamine, Figure 7, also shows upfield shifts of all the resonances, the shift being greater for the peaks of the protons on the thiazolium ring moiety (~ 1.4 ppm) than the shift (~ 0.5 ppm) of the peaks due to the protons on the pyrimidine ring. Again, two singlets have been observed for the C_5-CH_3 methyl protons because of the hindered rotation about the C-N bond of the amide function. For the same reason, the C_6-H proton of the pyrimidine exhibits two

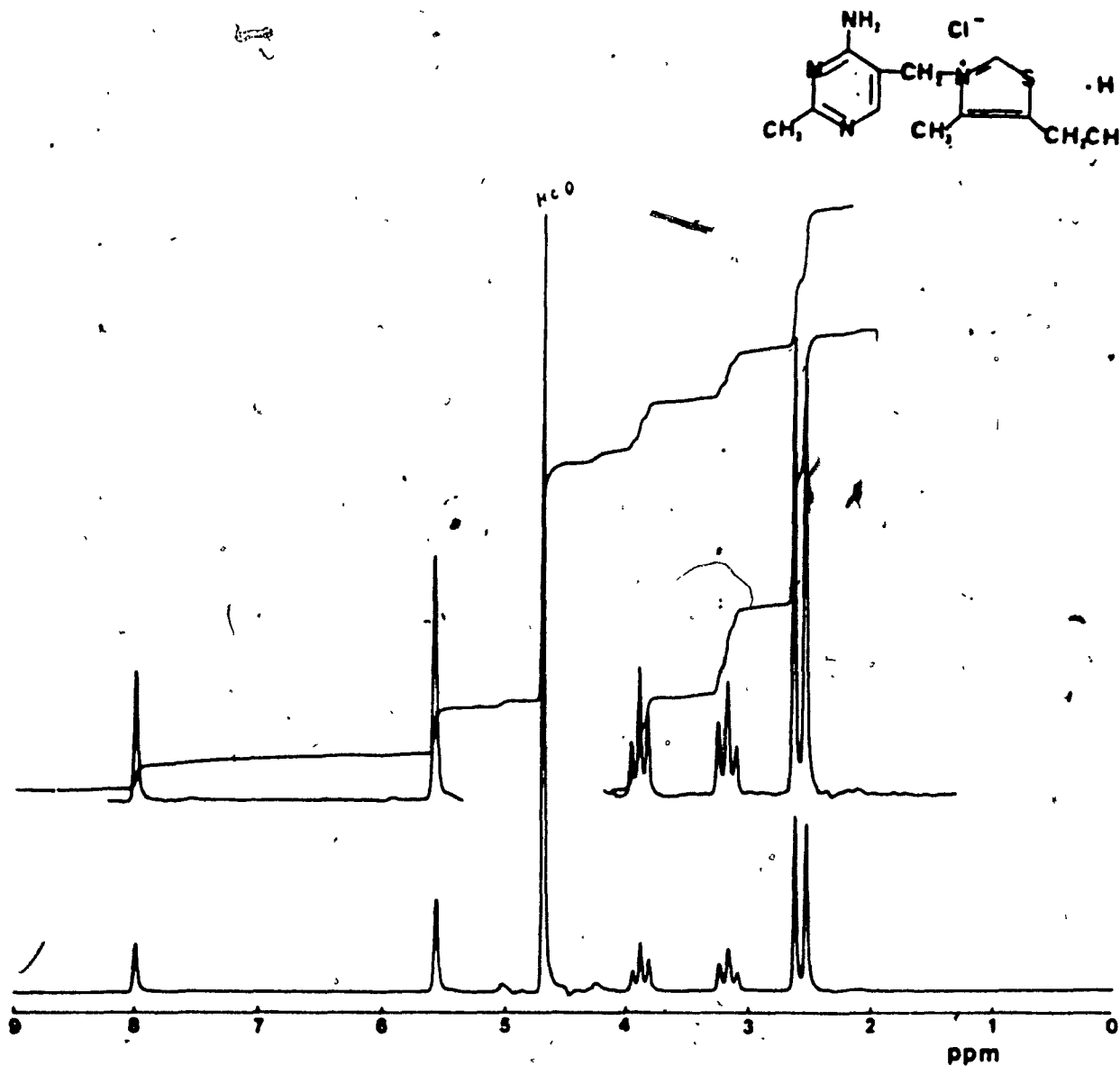


Figure 6. ^1H NMR spectrum of Thiamine chloride hydrochloride in D_2O at 31°C (Assignments in Table 2).

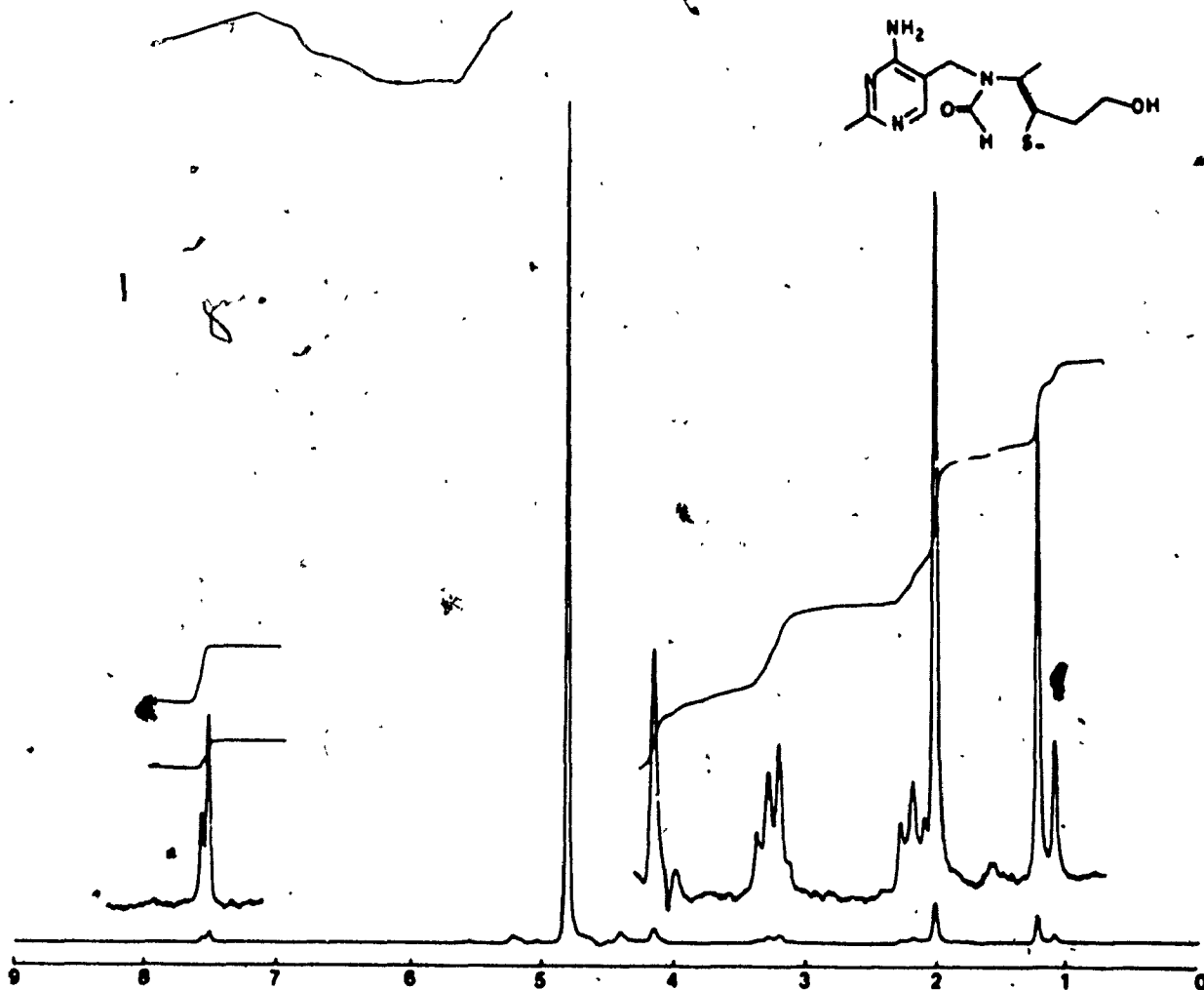
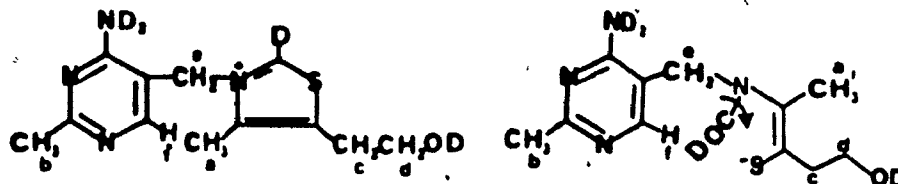


Figure 7. ^1H NMR spectrum of the ring-opened form of thiamine in NaOD / D_2O at 31 °C (Assignments in Table 2).

Table 2. Proton chemical shifts assignments, in ppm, of the thiamine spectra in Figures 6 and 7.



Assignment

a	2.52 s	1.08 s
b	2.61 s	1.21 s
c	3.16 t	2.15 t
d	3.86 t	3.25 t
e	5.55 s	4.14 s
f	7.99 s	7.51 s
		7.56 s

s = singlet

t = triplet

resonance peaks at 7.51 ppm and 7.58 ppm, reflecting two different possible environments.

The proton NMR spectrum of the methylated thiamine derivative ($N_1MeB_1^+$) is shown in Figure 8, and the spectral assignments of the chemical shifts of all detected hydrogen nuclei are reported in Table 3. These are in accord with those given in Reference 56 (spectrum run in DMSO- d_6), despite the use of different solvents. As expected, due to positive charge on N_1 , the spectrum of the $N_1MeB_1^+$ shows a small deshielding of all the pyrimidine protons compared to their analogues in thiamine (Figure 6). Besides the relative position of the two rings in the N_1 methylated and unmethylated states (B_1^+) may be different due to an electrostatic interaction of the positive charge on the pyrimidine ring and the positive charge on the thiazolium ring in $N_1MeB_1^+$.

Similarly, upfield and downfield shift of the resonances due to protons in the pyrimidine and thiazolium ring, respectively, has been observed in the spectrum, Figure 9, of the ring-opened thiolate of the $N_1MeB_1^+$, when compared to the corresponding spectrum of the ring-opened thiamine (Figure 7). This also may be due to difference in conformational differences, because of the possible charge interaction between the positively charged N_1 of the pyrimidine ring and the negatively charged sulfur atom of the thiolate of the methylated thiamine.

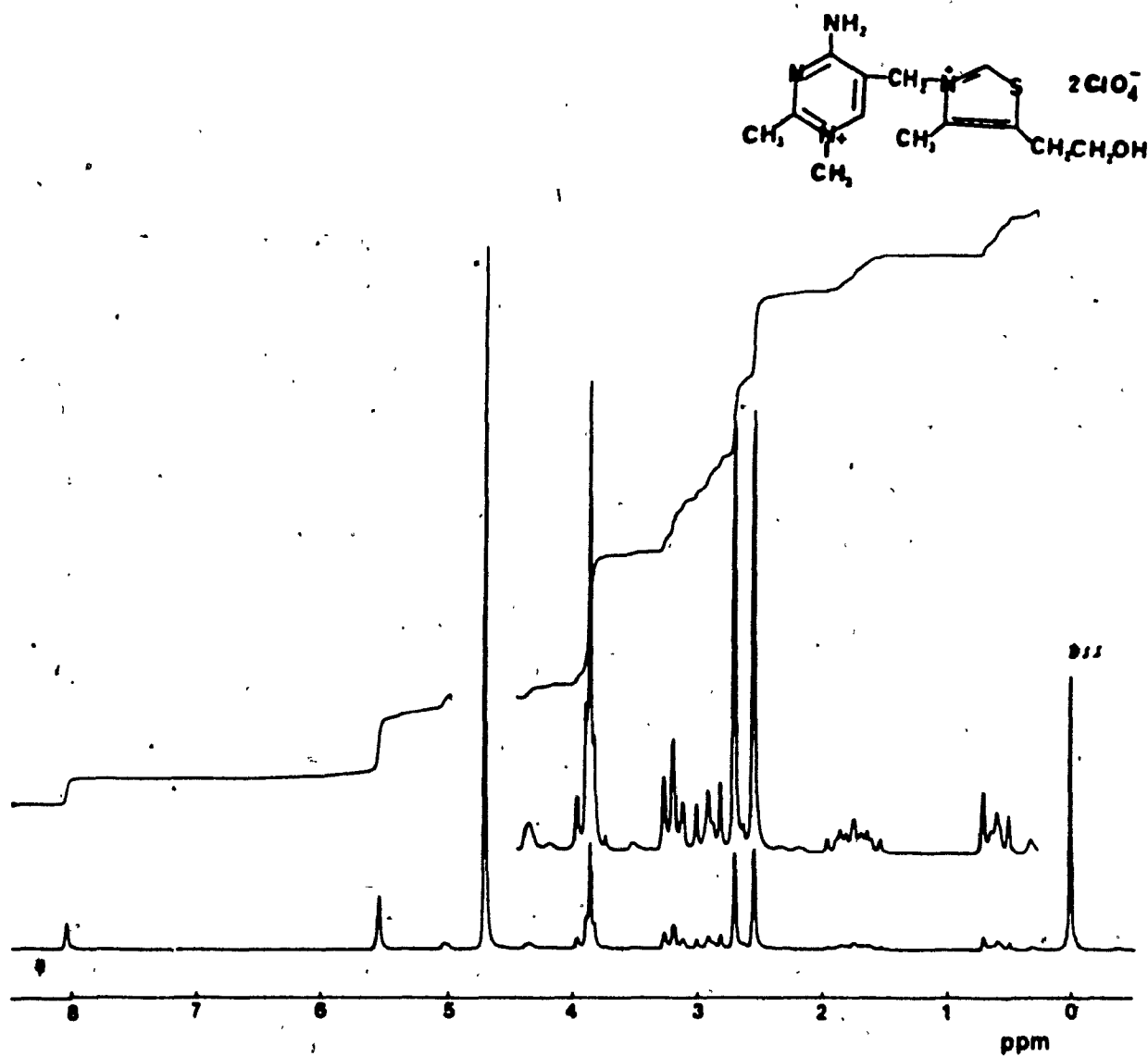


Figure 8. Proton NMR spectrum of N-methylated thiamine (NiMeB1⁺) in D₂O at 31 °C (Assignments in Table 3).

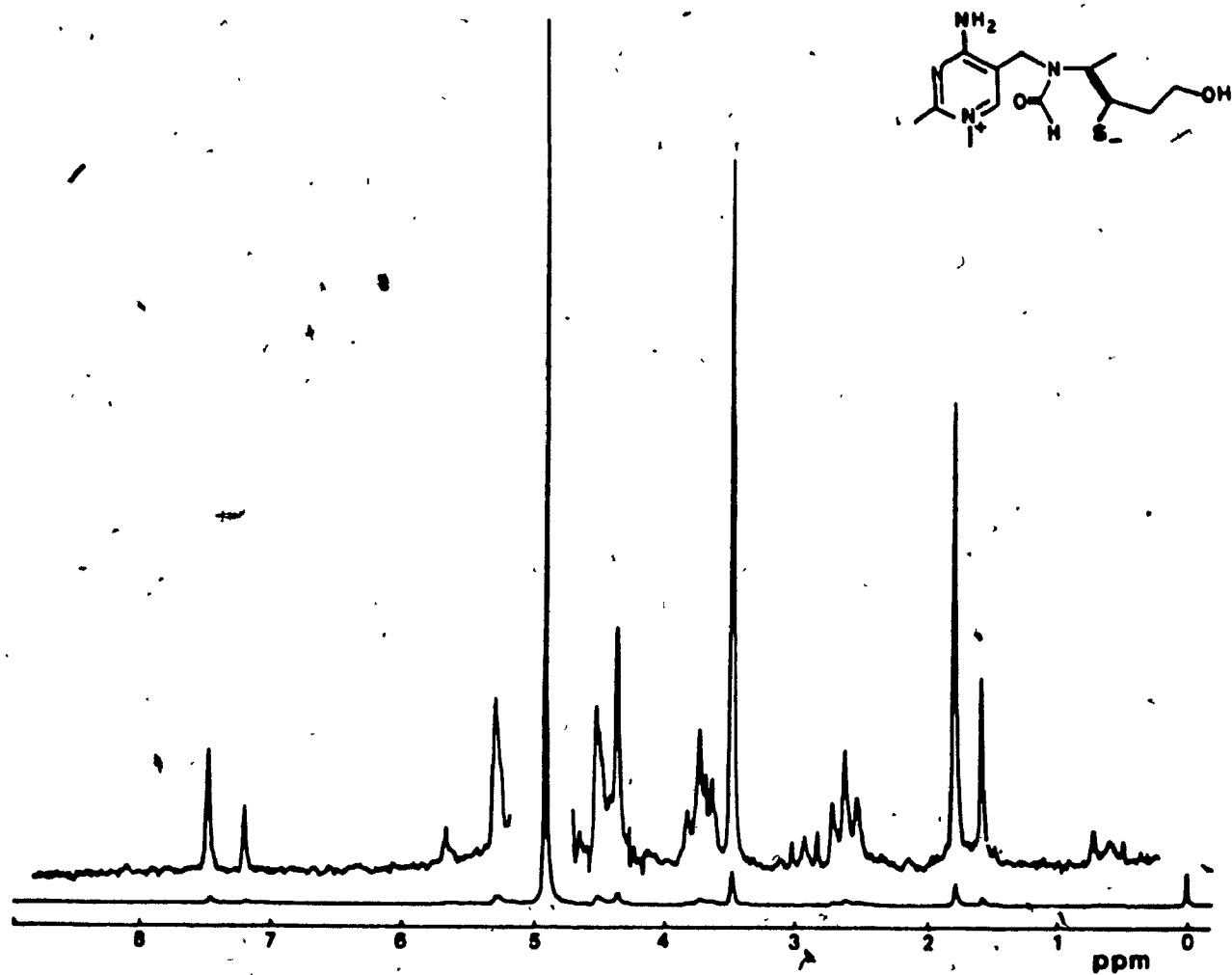
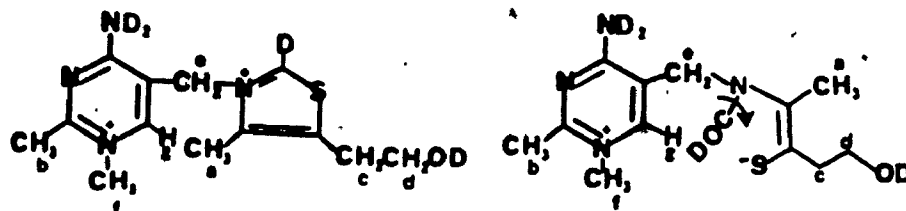


Figure 9. ^1H NMR spectrum of the ring-opened form of NiMeB_1^+ , in $\text{NaOD} / \text{D}_2\text{O}$ at 31°C (Assignments in Table 3).

Table 3. Proton. chemical shifts assignments, in ppm, of the spectra on Figures 8 and 9.



Assignment

a	2.56 s	1.56 s
		1.78 s
b	2.64 s	x
c	3.18 t	2.60 t
d	3.88 t	3.69 t
e	5.55 s	4.37 s
f	3.85 s	3.49 s
		3.60 s
g	8.05 s	7.19 s
		7.45 s

s = singlet t = triplet

x = exchanged with D

Furthermore, it should also be noticed that, in the spectrum of the ring-opened thiolate of $N_1MeB_1^+$ (Figure 9), the C_2-CH_3 protons of the pyrimidine ring are absent though they would be expected to appear around 2.0 ppm. This is due to base-catalyzed deuterium exchange of these protons with the solvent. Such an exchange, which becomes rapid in the presence of strong base, is well-known in pyrimidine systems⁵⁸.

In conclusion, the present NMR studies confirm and extend those of earlier workers^{4, 56, 57}. They reaffirm that the base-catalyzed ring-opening of thiazolium ions is reversible, even in the more complex thiamine system and its N-methylated derivative. A primary object of the studies was to observe the initial (kinetic) product of the "fast process" observed by UV (see later). Unfortunately, all that was observed was the final (thermodynamic) product with the reconstituted thiazolium ring. The problem is almost certainly due to the heat generated under conditions of recyclization. Firstly, an excess of strong base is necessary to ensure complete ring-opening of the thiazolium ion. Then, an excess of mineral acid is required to neutralize this amount of base and to force the pH to less than 3. It seems that so much heat is generated during this latter step that the local temperature in the sample rises so as to speed up the "slow process", and so preclude observation of the initial (kinetic) product). This

problem does not occur with the reactions monitored by UV spectrophotometry, as the concentrations employed are much lower.

KINETIC STUDIES

The kinetics of the reversible ring-opening of the 3,4-dimethyl-5-(2-hydroxyethyl)thiazolium ion (HET^+), thiamine (B_1^+), and N-methylthiaminium ion (N_1MeB_1^+), were studied in basic and acidic aqueous solutions using the stopped-flow and conventional UV spectrophotometry. Before presenting this work, we outline an earlier project^{19a}, in which we investigated the ring-opening of the N-methylbenzothiazolium ion and related derivatives. A summary of this work will be presented as an introduction and to aid a comparison of the kinetic behaviour of this compound with HET^+ , B_1^+ , and N_1MeB_1^+ .

All of the kinetic data are presented in the form of pH-rate profiles, which, for the purposes of a more convenient and comprehensive discussion, will be divided in three main regions: ring-opening and reclosure (fast and slow).

Reversible ring-opening of BT^+ ^{19a}

Figure 10 show the pH-rate profile of the opening ($\text{pH} > 6.5$) and reclosure ($\text{pH} < 6.5$) of the N-methylbenzothiazolium ion, BT^+ , in aqueous solution at 25 °C. This

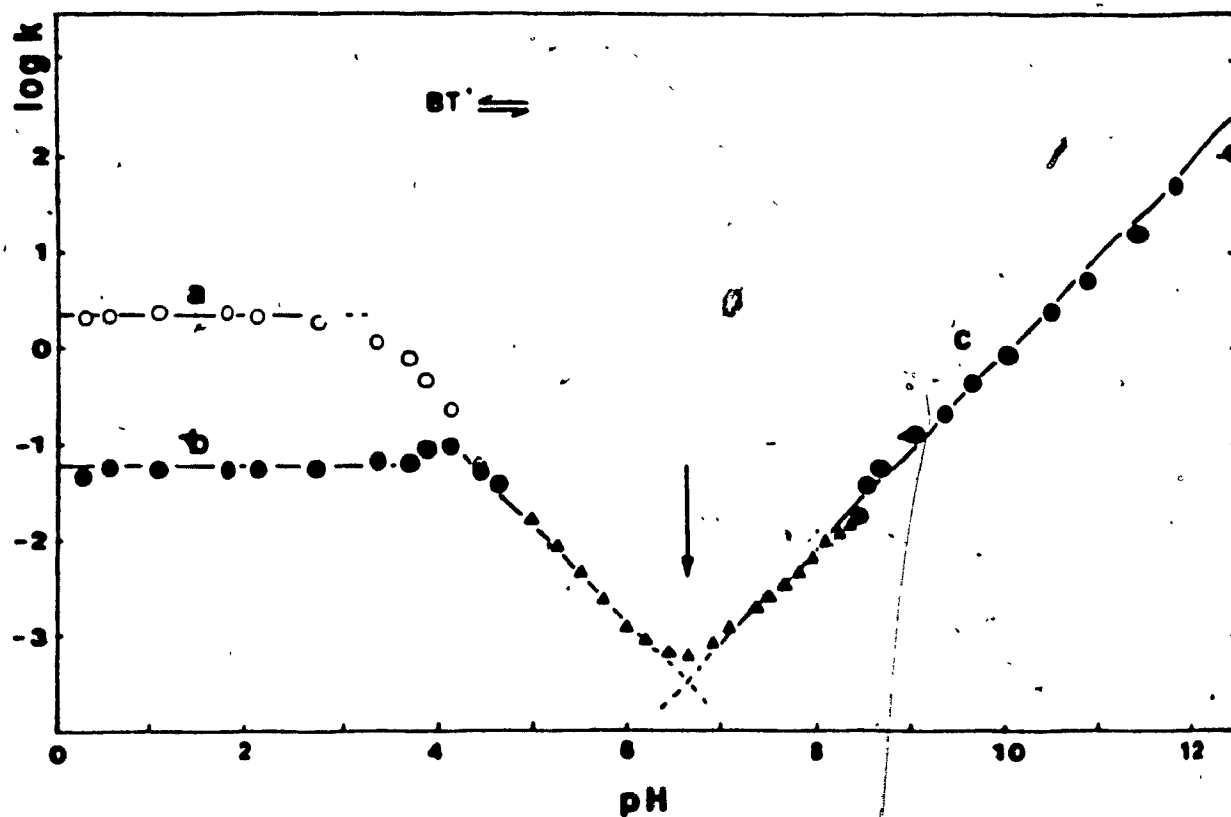


Figure 10. The pH-rate profile for the reversible opening of the N-methyl-benzothiazolium cation (BT^+) in water (at 25 °C, $I = 0.1$ M (NaCl)). The minimum at $pH = 6.57$ corresponds to pK_{av} , i.e. where 50% of BT^+ is ring-opened¹⁰.

●,○ unpublished work from this laboratory^{10a}

▲ data from Vorsanger¹⁰

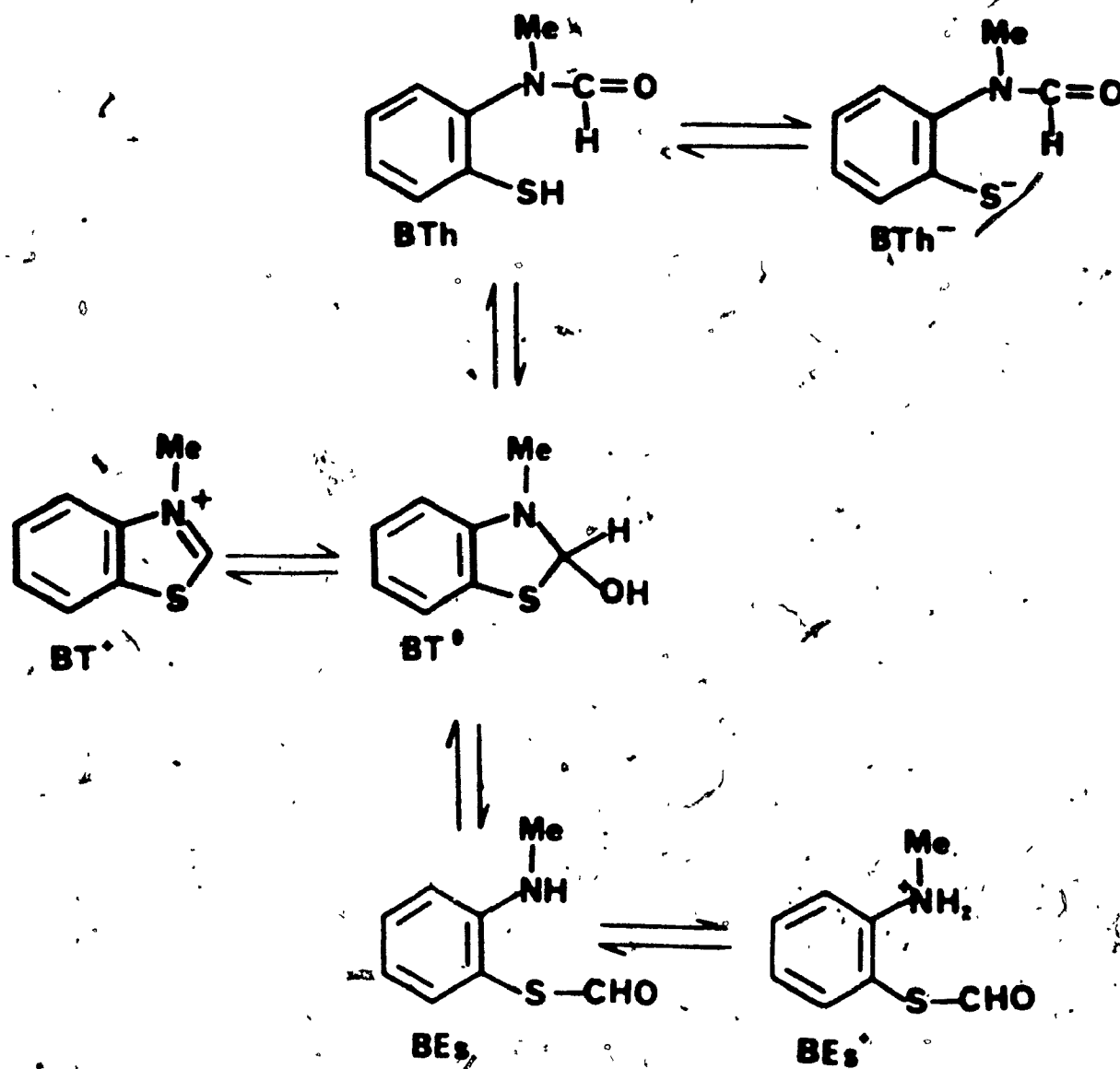
work covers the full pH range, and thereby extends Vorsanger's study¹⁰ who investigated this system (eq. 3) in the limited pH range of 5.0-8.5, near the equilibrium pH of 6.57. As can be seen from Figure 10, our data fit very well with those of Vorsanger.

The results can be rationalized in terms of the pH dependence of the formation and breakdown of the tetrahedral intermediate BT^{\ominus} , (Scheme 11), which is the pseudobase² of the benzothiazolium ion, BT^{\oplus} . As expected for a thiazolium ion²⁻⁴, the ring opening of BT^{\oplus} (process (c), Figure 10) shows a linear dependence on pH with a slope of 1. Thus, the ring-opening is first order in $[OH^-]$. This can be interpreted as the formation of the tetrahedral intermediate (BT^{\ominus}) being the rate limiting step, followed by a fast deprotonation and ring-opening to the o-(N-methylformamido)-benzene thiolate BTh^- (eq. 16).



Analogous behaviour has been found for other thiazolium ions²⁻⁴.

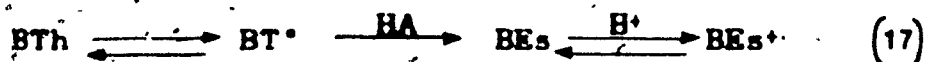
Reclosure of the thiolate to BT^{\oplus} , studied in acidic media, shows one phase at intermediate pHs (4.5-6.5), but at lower pHs, two distinct phases are observed (processes (a) and (b), Figure 10). What is more interesting is that this biphasic behaviour, not previously documented for any



Scheme 11. Overall scheme of the ring-opening and ring-closing of N-methyl-benzothiazolium cation.

thiazolium system, has also been observed for the reclosure of the thiolates of HET⁺ and B⁺.

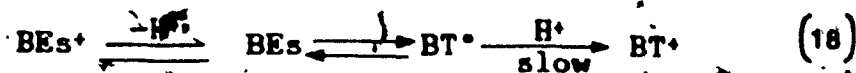
Spectral studies indicate that process (b) involves the formation of BT⁺. However, at pH < 4.5, this step is preceded by a faster process, (a), which is attributed to an intramolecular N to S acyl transfer, forming an α -methylaminobenzenethiol formate ester (BEs) (eq. 17).



Furthermore, the break in the profile (a) around pH 3.5 is ascribed to a change in rate-limiting step, since buffer catalysis studies showed curved buffer plots above the break, but no catalysis is observed below it. Such a change indicates the presence of an intermediate²³. Therefore, the plateau of profile (a) probably corresponds to the formation of the tetrahedral intermediate BT⁺ being the slow step, whereas above pH 3, the acid-catalyzed breakdown of BT⁺ to the amino ester BEs, becomes the rate-limiting step. Support for this interpretation comes from other studies^{20, 21, 24, 25} with similar observations on various reactions, which also involve tetrahedral intermediates.

Thus, profile (a) is seen as the fast formation of the amino ester BEs (kinetic control), whereas, profile (b) is the slower formation (from BEs) of the more stable BT⁺.

(thermodynamic control). At the pHs involved, BEs should be mainly protonated and so the process (b) may be represented as follows:

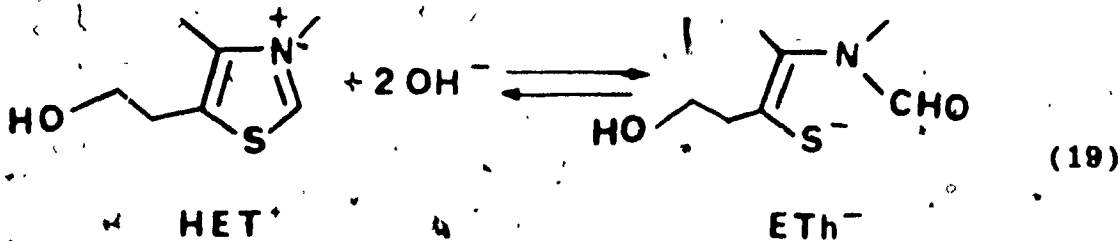


Over most of the range of process (b), there is no pH dependence, because the loss of H^+ from BEs^+ cancels with the proton catalyzing the conversion of BT^+ to BT .

The possible origin of the bifurcation of the rate profile (into processes (a) and (b)), which occurs at about pH 4.2, will be discussed later.

Reversible ring-opening of HET⁺

Similar kinetic behavior to that just presented for BT^+ has been observed for the reversible ring-opening reaction of the 3,4-dimethyl-5-(2-hydroxyethyl)thiazolium ion (HET^+) (eq. 19).



The pH dependence of the observed pseudo-first order rate constants over the full pH range (pH 0-14) is illustrated in Figure 11. The data were obtained using stopped-flow (Concordia University) and conventional UV

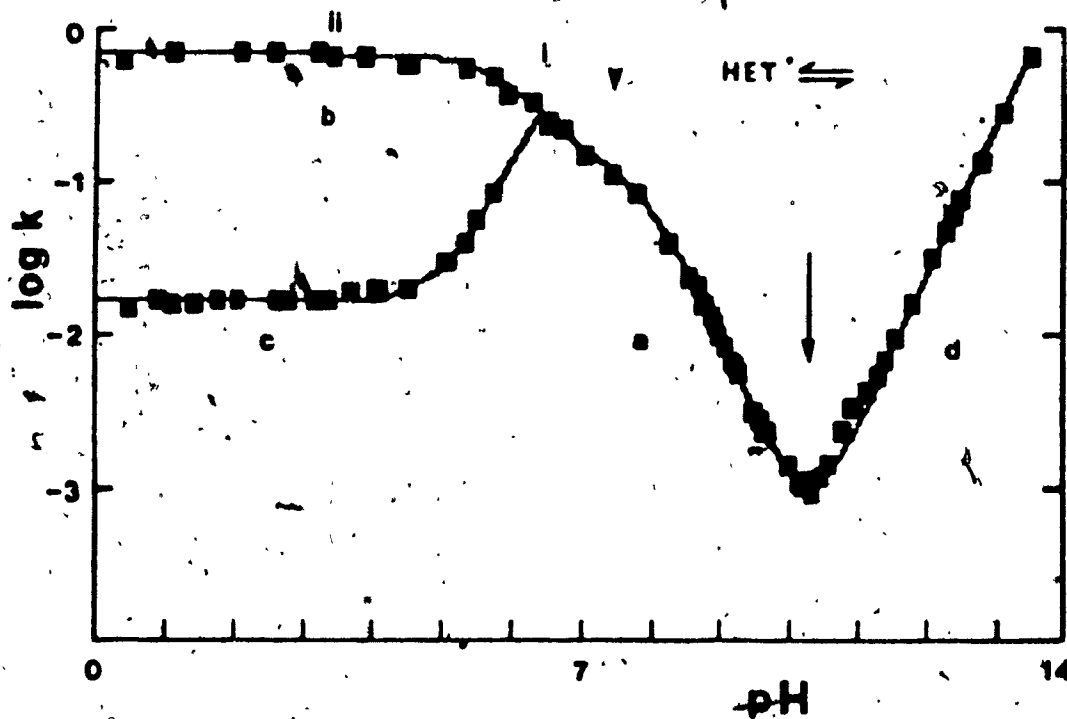
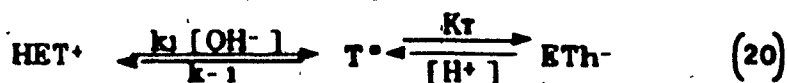


Figure 11. pH dependence of the first order rate constants for the reversible opening of 3,4-dimethyl-5-(2-hydroxyethyl thiazolium ion (HET^+)): The curves are calculated by "computer fitting". The actual data are given in Tables 5, 6, and 7, in the Appendix.

spectrophotometry (Mount St-Vincent University), at 25 °C and $I = 1$ M. They are given in Tables 5, 6, and 7, of the Appendix.

Ring-opening process (d). The rate constants for this process were determined at various pH's above 10.5 from the increase in absorbance at 242 nm, where the UV absorptions of the HET⁺ cation and its ring-opened thiol (ET⁻) have the maximum difference, as is shown by the spectra in Figure 12. During the ring-opening, the spectrum of HET⁺ changes smoothly to that of ET⁻, with no evidence of the accumulation of any intermediate. Likewise, if a solution of ET⁻ is acidified to ca. pH 8, the spectrum of HET⁺ is gradually regenerated. These observations are consistent with the dynamic NMR experiments discussed earlier.

As with BT⁺, the ring-opening of HET⁺ is believed to involve rate-limiting nucleophilic attack by hydroxide ion on the thiazolium cation to form the tetrahedral intermediate, T[°] (Scheme 12). This is followed by a fast deprotonation and ring-opening to yield the amido enethiolate, ET⁻ (eq. 20).



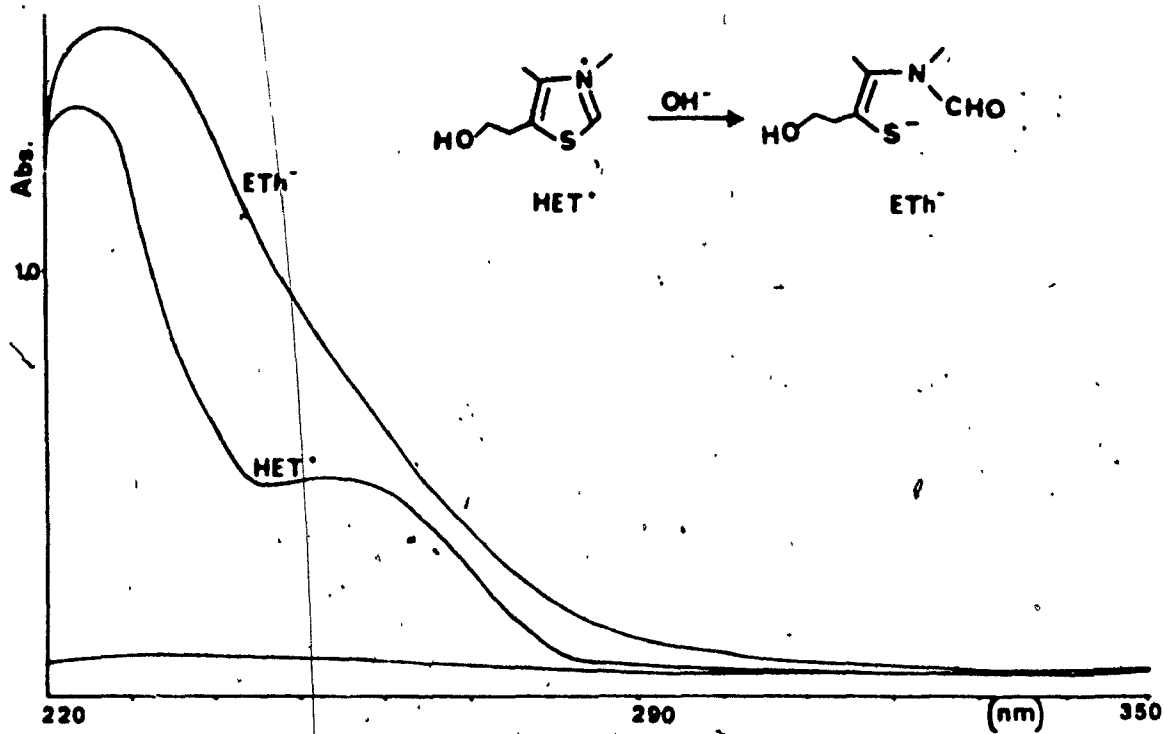
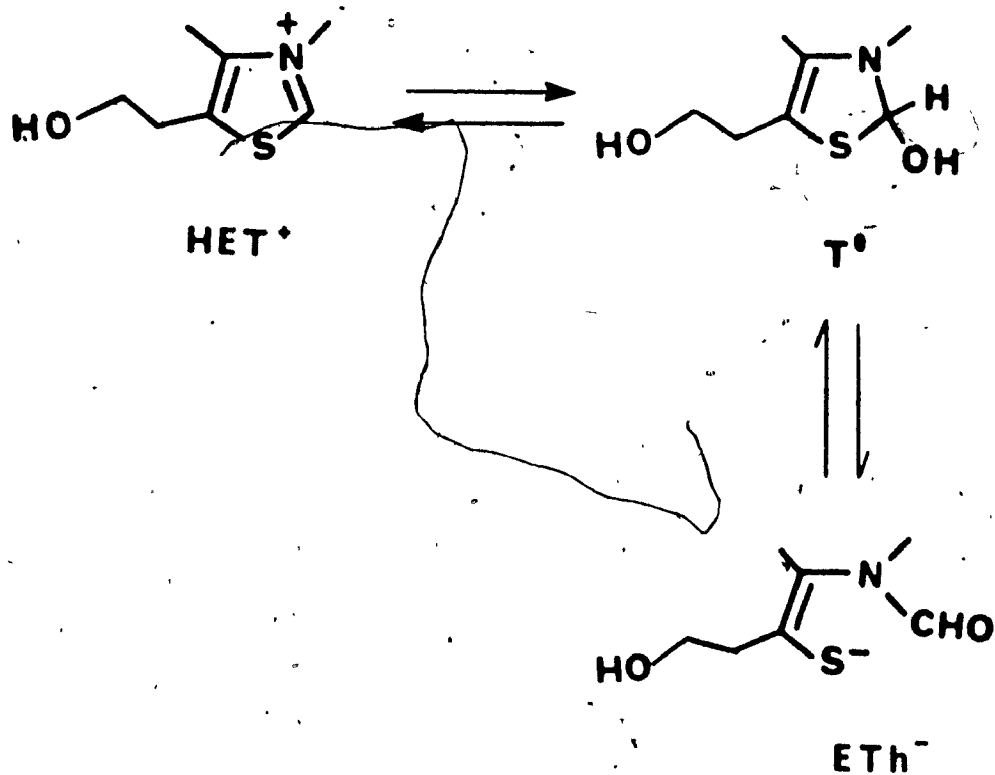


Figure 12. Static UV spectra of HET⁺ (pH = 2) and ETh⁻ (pH = 13.7) in aqueous solution.



Scheme 12. Ring-opening of HET⁺.

Thus, while 2OH^- are consumed for the overall conversion of HET^+ to ETh^- , kinetically, only one OH^- is important and so the rate of the reaction is first-order in both $[\text{HET}^+]$ and $[\text{OH}^-]$. For the overall reaction shown in eq. 20, an average equilibrium constant for the two steps involved can be defined as:

$$K_{av}^2 = \frac{[\text{ETh}^-][\text{H}^+]^2}{[\text{HET}^+]} \quad (21)$$

such that $\text{p}K_{av}$ (equal to 10.33 in this case) is the pH at which the cation HET^+ and its ring-opened form ETh^- are present in equal amounts. In the pH-rate profile (Figure 11), $\text{p}K_{av}$ corresponds to the minimum value of k_{obs} , which is the point of intersection of pH-rate profiles of the forward (ring-opening) and reverse (ring-closing) reactions.

In general, k_{obs} for an equilibration such as for eq. 20, is the sum of the individual pseudo-first order rate constants for formation (k_f) of the pseudobase form and decomposition (k_d) of the pseudobase species to the cation².

Thus, $k_{obs} = k_f + k_d \quad (22)$

where $k_f = k_1[\text{OH}^-]$

and

$$k_d = \frac{k_{-1}[\text{H}^+]}{K_r + [\text{H}^+]}$$

and hence ,
$$k_{obs} = k_1 [OH^-] + \frac{k_{-1} [H^+]}{K_T + [H^+]} \quad (23)$$

At pHs much above 10.33, the ring opening is essentially complete and k_1 , the rate constant for ring closure, is insignificant. Therefore,

$$k_{obs} = k_f = k_1 [OH^-] \quad (24)$$

and the second order rate constant, k_1 , for the attack of OH^- on the thiazolium ring, may be obtained from the slope of the plot of k_{obs} vs. $[OH^-]$ (Figure 13) at high pH. From this plot, a value of $k_1 \approx 1.3 \text{ M}^{-1}\text{s}^{-1}$ is obtained, whereas the intercept being close to zero suggests that a reaction with water is not important in this region.

Although the influence of the ionic strength on the rate constant has not been studied in detail, the inverse dependence of k_{obs} on the ionic strength was observed. This is as expected for the reaction of a cation with an anion, viz $HET^+ + OH^-$. For example, at pH = 13, and $I = 0.1 \text{ M}$, $k_{obs} = 0.32 \text{ s}^{-1}$, whereas, at $I = 1.0 \text{ M}$, the $k_{obs} = 0.13 \text{ s}^{-1}$, all other conditions being the same.

Buffer catalysis of the ring-opening reaction was studied by the research team at Mount St-Vincent University. They found weak general base catalysis (eq. 25) by phosphate and carbonate buffers ($\beta \approx 0.5$), but no catalysis was observed for primary and tertiary amine bases.

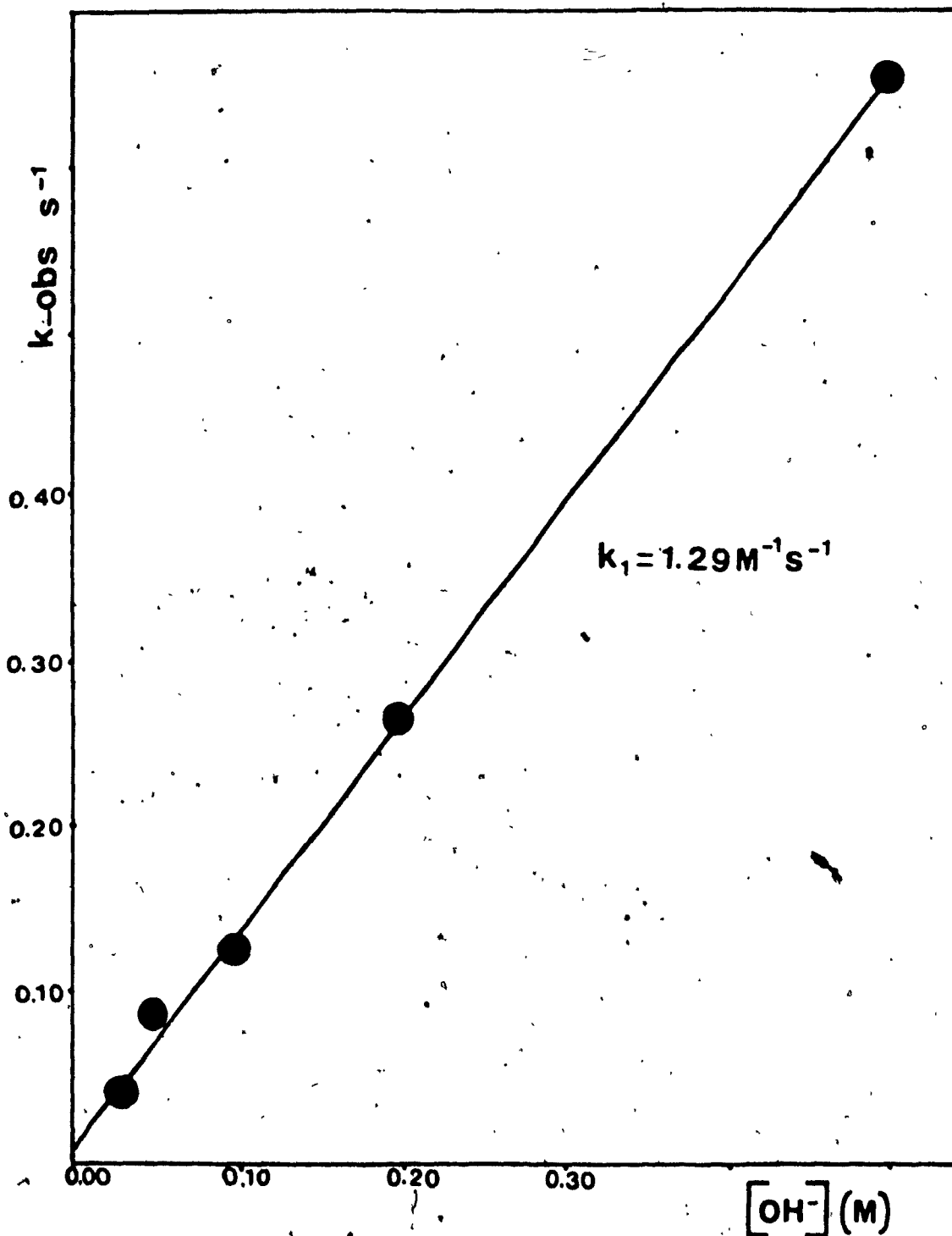
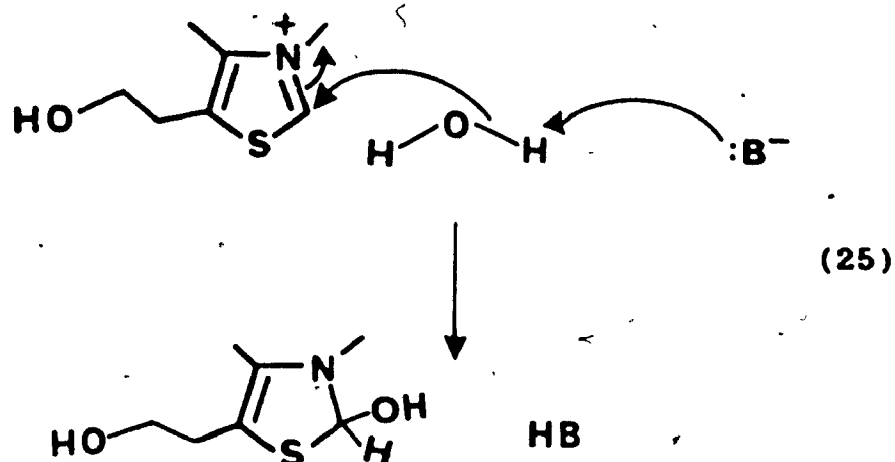


Figure 13. Plot of k_{obs} vs $[\text{OH}^-]$ for the ring-opening reaction of HET^+ at 25 °C and $I = 1 \text{ M}$ (pH 12.5-13.7).



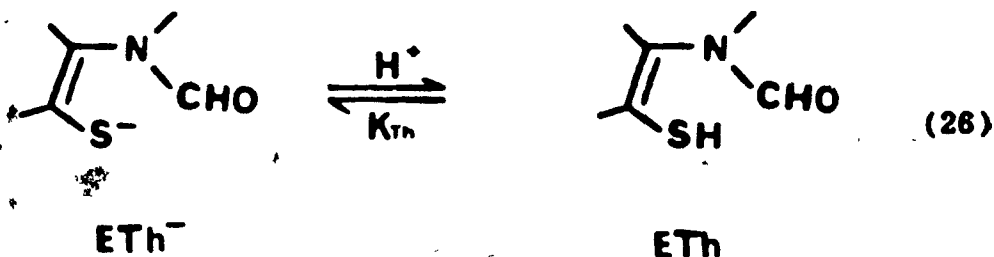
General base catalysis has been found for the reaction of other heterocyclic cations with water².

Ring-closing of ETh^-

The reclosure of the amido enethiolate ETh^- , in aqueous HCl or buffer solutions, was studied at pH 0-10.3. Both UV and NMR spectral studies showed that the final product is HET^+ , but kinetics of this reaction are quite complex.

As seen in the pH-log rate constant profile (Figure 11), between pH 6.5 and 10.3, only one process (labelled (a)) is observed. In contrast, two distinct processes (labelled (b) and (c)) are apparent at pH < 6, as was found with the N-methylbenzothiazolium ion at low pH.

Process (a) (pH 6.5-10.3). For most of this region, the transformation of ETh^- to HET^+ was monitored as a large decrease in absorbance at 240 nm. However, around pH 8, the initial UV spectrum becomes different, indicating a change in the initial species. This is ascribed to protonation of the enethiolate (ETh^-):



where $K_{\text{Th}} = \frac{[\text{ETh}^-][\text{H}^+]}{[\text{ETh}]}$. For this equilibrium, a

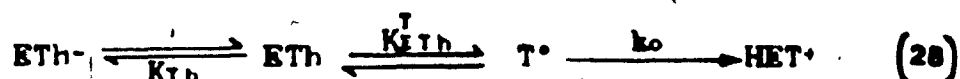
$\text{p}K_{\text{Th}} \approx 8$ is reasonable. Below pH 8, the reaction was followed by the increase at 256 nm. The pH rate profile for process (a) indicates a linear dependence of $\log k_{\text{obs}}$ on pH, with limiting slope -1 at high pH and a tendency to level out below pH 8. This levelling-out, which is more evident in the profile for thiamine (see later), is also compatible with the presence of a $\text{p}K_{\text{a}} \approx 8$. The data can be fitted by the equation:

$$k_{\text{obs}} = \frac{k_p [\text{H}^+]}{(K_{\text{Th}} + [\text{H}^+])} \quad (27)$$

with $k_p = 0.17 \text{ s}^{-1}$ and $K_{\text{Th}} = 1.58 \times 10^{-8} \text{ M}$, i.e. $\text{p}K_{\text{Th}} = 7.8$. This last value is close to the $\text{p}K_{\text{a}}$ s

estimated for similar enethiolates, reported in the literature⁴.

These observations for process (a) can be rationalized by the rate-limiting conversion of the tetrahedral intermediate T° , in equilibrium with ETH^{-} and ETH , into HET° :



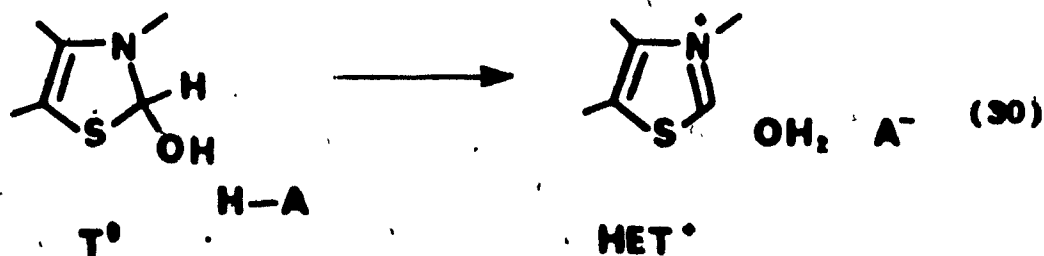
For $K_{ETH}^{\dagger} = \frac{[T^{\circ}]}{[ETH]}$, K_{Th} as previously defined, and assuming

$K_{ETH}^{\dagger} \ll 1$, this mechanism requires that:

$$k_{obs} = \frac{k_o K_{ETH}^{\dagger} [H^+]}{(K_{Th} + [H^+])} \quad (29)$$

This equation is compatible with eq. 27, which fits the data, and so $k_o K_{ETH}^{\dagger} = 0.17s^{-1}$.

McDonald et. al. have carried out extensive buffer catalysis studies in the region of pH 7.5-9.0 for process (a). Their results indicate general acid catalysis, after allowance is made for $pK_{Th} = 7.8$, with a Bronsted $\alpha = 0.7$. Note, however, that catalysis by H^+ is not found in this region. What this means, in terms of the mechanism shown in eq. 28, is that the loss of hydroxyl from T° can be assisted by general acids:



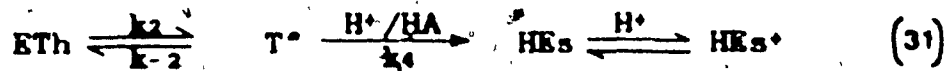
as well as occurring by straight ionization. Such behavior is well known for species like T^* . Moreover, it should be noted that the reaction shown in eq. 30 is the microscopic reverse of a reaction shown to be important in the formation of T^* (see eq. 25).

In summary, process (a) is due to the conversion of the enethiol and its anion (ETH and ETH^-) into HET^+ . The proposed mechanism (Eq 28) involves rate-limiting loss of hydroxyl from the tetrahedral intermediate T^* by straight ionization and by general acid catalysis (eq. 30). This interpretation is compatible with the findings for the reverse reaction (see process (d)), where attack of OH^- and general base catalyzed attack of water (eq. 25) on HET^+ are indicated.

Process (b) (pH 0-6). As shown in Figure 11 (page 67), below pH 6.5, process (a) gives way to two processes (labelled (b) and (c)). The rate of process (b) rises with acidity (i) and then exhibits a plateau from pH 0-4 (ii). General acid catalysis is observed on the rising limb of process (b, i), but not in the plateau region, consistent with a change of rate-limiting step.

Process (b) is ascribed to the conversion of the amido enethiolate ETH^- to thiol ester HEs via an intramolecular N to S acyl transfer. In terms of the formation or breakdown of the tetrahedral intermediate T^* , the kinetic results are

consistent with the proton-catalyzed and general acid-catalyzed breakdown of T^* to give the protonated amino enethiol ester HEs^+ (eq. 31).



The process (b) takes over from process (a), because the rate constant for proton catalysis for T^* to HEs is larger than for the process of formation of HET^+ from T^* . The break in the profile of (b) at pH 4 (Figure 11) is due to a change in the rate-limiting step from the uncatalyzed formation of the T^* (at low pH) to its general acid catalyzed breakdown at higher pH (above pH 4). This interpretation is also consistent with our experimental observation on buffer catalysis experiments, which gave curved buffer plots (Figure 14) in the region of change, whereas, at the plateau of process (b) (b, ii), no buffer catalysis was found.

For the mechanism shown in eq. 31,

$$k_{obs} = \frac{k_2 k_4}{k-2 + k_4} \quad (32)$$

where k_4 is the first order rate constant of the breakdown of the tetrahedral intermediate T^* . However,

$$k_4 = k_{4H} [H^+] + k_{4HA} [HA] \quad (33)$$

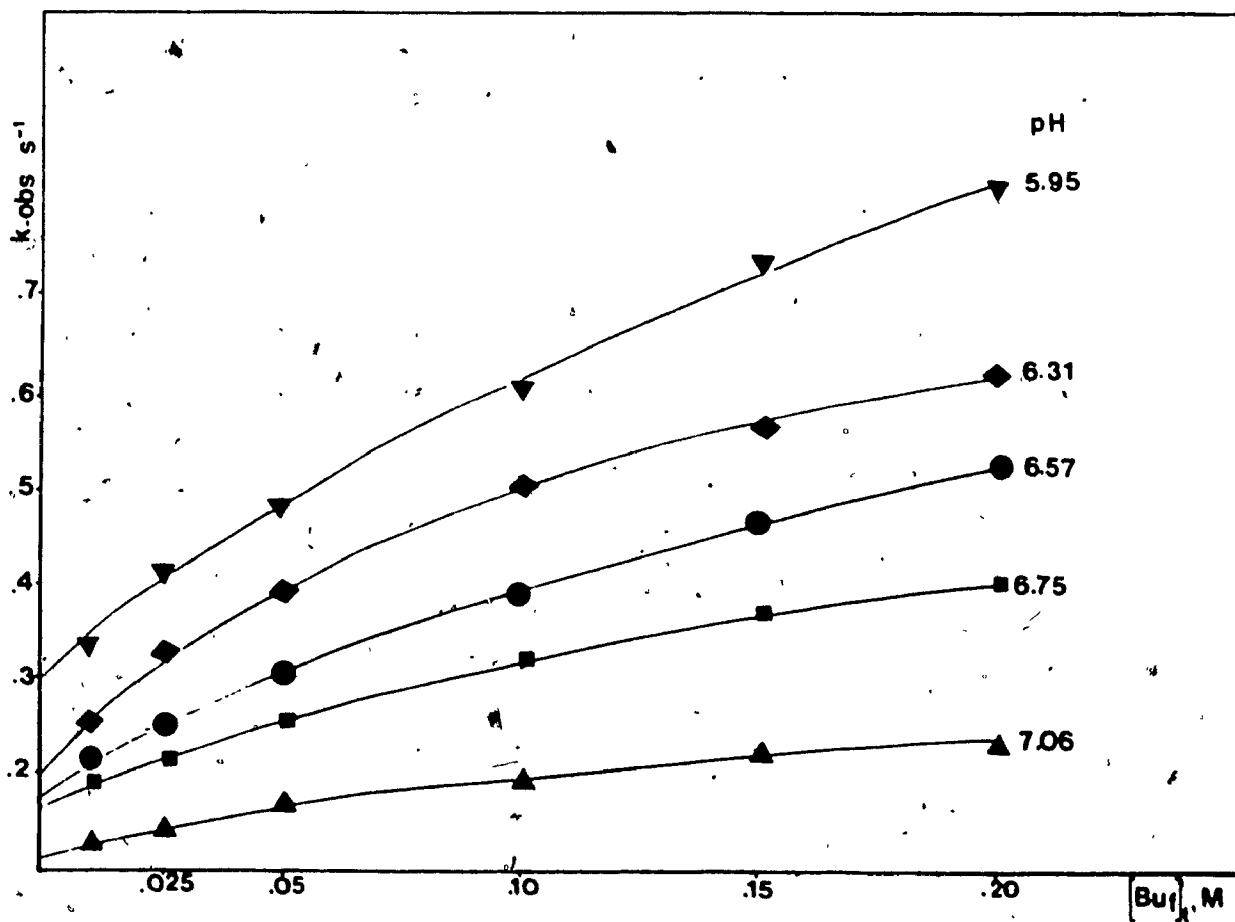


Figure 14. Buffer catalysis plots for process (b) and process (a) of HET^+ . Phosphate buffers. Data are given in Table 8 of the Appendix.

since the buffer plots have non-zero intercepts, which increase with acidity (Figure 14). Therefore, at low pH and/or high [HA] $k_{-2} \ll k_4$, and eq. 32 reduces to

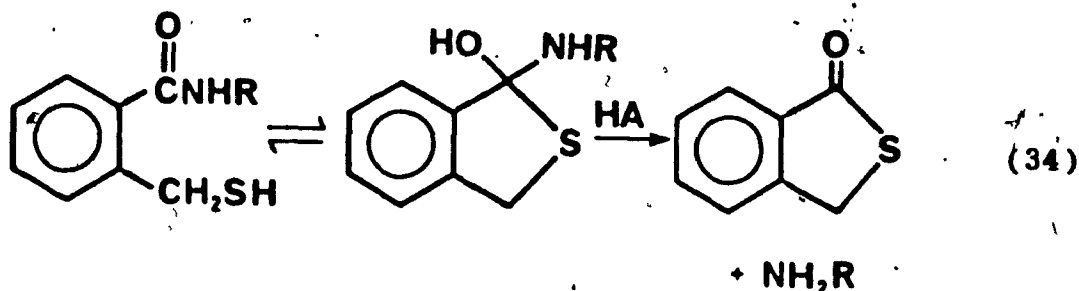
$k_{obs} = k_2$, independent of pH and buffer concentration.

This corresponds to the plateau region (Figure 11, b, i).

From the plateau, the value of k_2 is 0.68 s^{-1} .

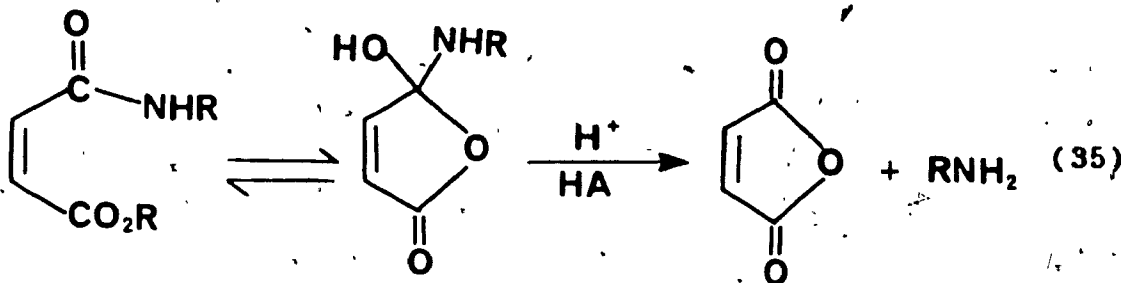
On the other hand, at higher pH ($\text{pH} > 4$), and low [HA], $k_{-2} \gg k_4$, and the general acid breakdown of the tetrahedral intermediate T° becomes the rate-limiting step.

Support for this explanation of our data comes from other studies^{20, 21, 24} that involve intramolecular N to S acyl transfer steps, and where changes of the rate-limiting step have also been detected. For example, work done by McDonald and co-workers³⁴ on the thiolactonization of the N-alkyl-2-mercaptomethylbenzamide (eq. 34), gave a similar pH rate profile.

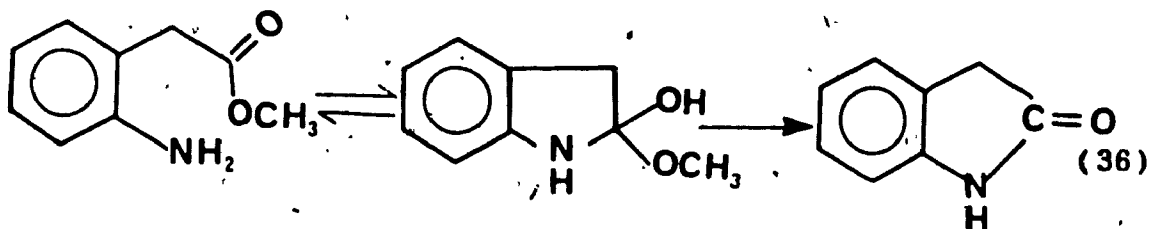


A plateau region was found at acidic pHs and buffer plots were obtained at higher pH, which showed the saturation behavior, consistent with a change in rate-limiting step. The results were interpreted in terms of the formation and breakdown of the N, O, and S tetrahedral intermediate shown

above. Similar kinetic behavior and buffer catalysis have also been observed for the hydrolysis of N-n-propyldiisopropylmaleamic acid⁵⁹ (eq. 35), and the cyclization of the methyl(2-aminophenyl)acetate³⁵ (eq. 36). Both reactions involved tetrahedral intermediates.



and



Process (c). Spectral studies of the slow process, using UV (Figure 15) and NMR (Figure 5) spectroscopy, indicate that the final product is the substrate HET^+ . Therefore, the slower pH-rate profile (Figure 11, process (c)) is attributed to the conversion of the amino thiol ester HEs to the thiazolium ion, HET^+ . This also occurs via the tetrahedral intermediate T^* (eq. 37), the general acid-catalyzed breakdown of the tetrahedral intermediate being the rate-limiting step. The mechanism is depicted as follows:

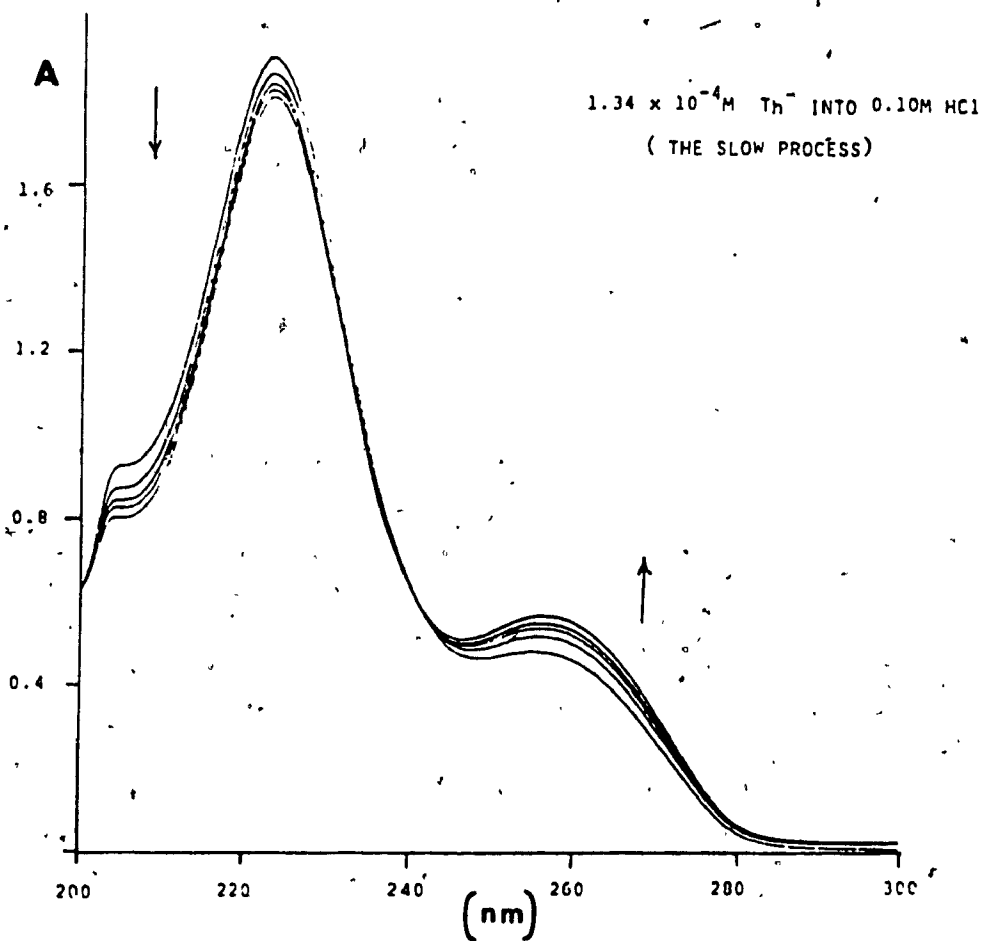
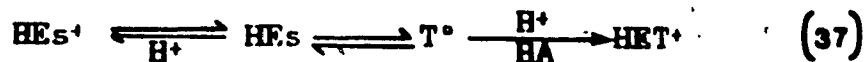


Figure 15. UV scans of the ring-closing of HET^+ of process (c) at pH 1. Spectrum run at Mount St-Vincent University.



At low pHs (pH 0-4.5), where the amino group of ester HEs is largely protonated, the reaction is overall uncatalyzed, and so, the rate profile appears to be flat. Above pH 4.5, the rate profile for process (c) rises as proton catalysis of T[°] to HET⁺ is no longer important relative to simple unassisted ionization. It is this lack of catalysis by H⁺ (relative to H⁺ catalysis of T[°] → HEs) which gives rise to the bifurcation of the rate profiles around pH 6.5. Furthermore, buffer catalysis experiments of this process (c) showed an apparent general base catalysis (Bronsted B = 0.7), due to actual specific base/general acid catalysis.

Assuming the protonated thiol ester HEs⁺ is the dominant form of the reactant, at low pH, a rate expression for eq. 37 can be derived as follows:

From observation,

$$\text{Rate} = k_{\text{obs}} [\text{HEs}^+] \quad (38)$$

For eq. 37, and zero buffer concentration,

$$\text{Rate} = (k_0 + k_{\text{H}} [\text{H}^+]) [\text{T}^\circ] \quad (39)$$

Thus

$$k_{\text{obs}} = \frac{(k_0 + k_{\text{H}} [\text{H}^+]) [\text{T}^\circ]}{[\text{HEs}^+]} \quad (40)$$

Define $K_{\text{HEs}} = \frac{[\text{HEs}]}{[\text{T}^\circ]}$ and $K_{\text{HEs}^+} = \frac{[\text{HEs}][\text{H}^+]}{[\text{HEs}^+]}$

then

$$\frac{[\text{T}^\circ]}{[\text{HEs}^+]} = \frac{K_{\text{HEs}}}{K_{\text{HEs}^+} [\text{H}^+]}$$

and hence
$$k_{obs} = \frac{(k_o + k_H[H^+])K_{HES}}{K_{HES}[H^+]} \quad (41)$$

This equation fits the profile of process (c).

At low pH (0-4.5), $k_H[H^+] \gg k_o$, and, therefore,

$$k_{obs} = \frac{k_H K_{HES}}{K_{ES}} \quad (41a)$$

Thus, k_{obs} is independent of pH and a plateau is seen in the experimental data (Figure 11, c), for this pH region with $k_{obs} = 0.016 \text{ s}^{-1}$.

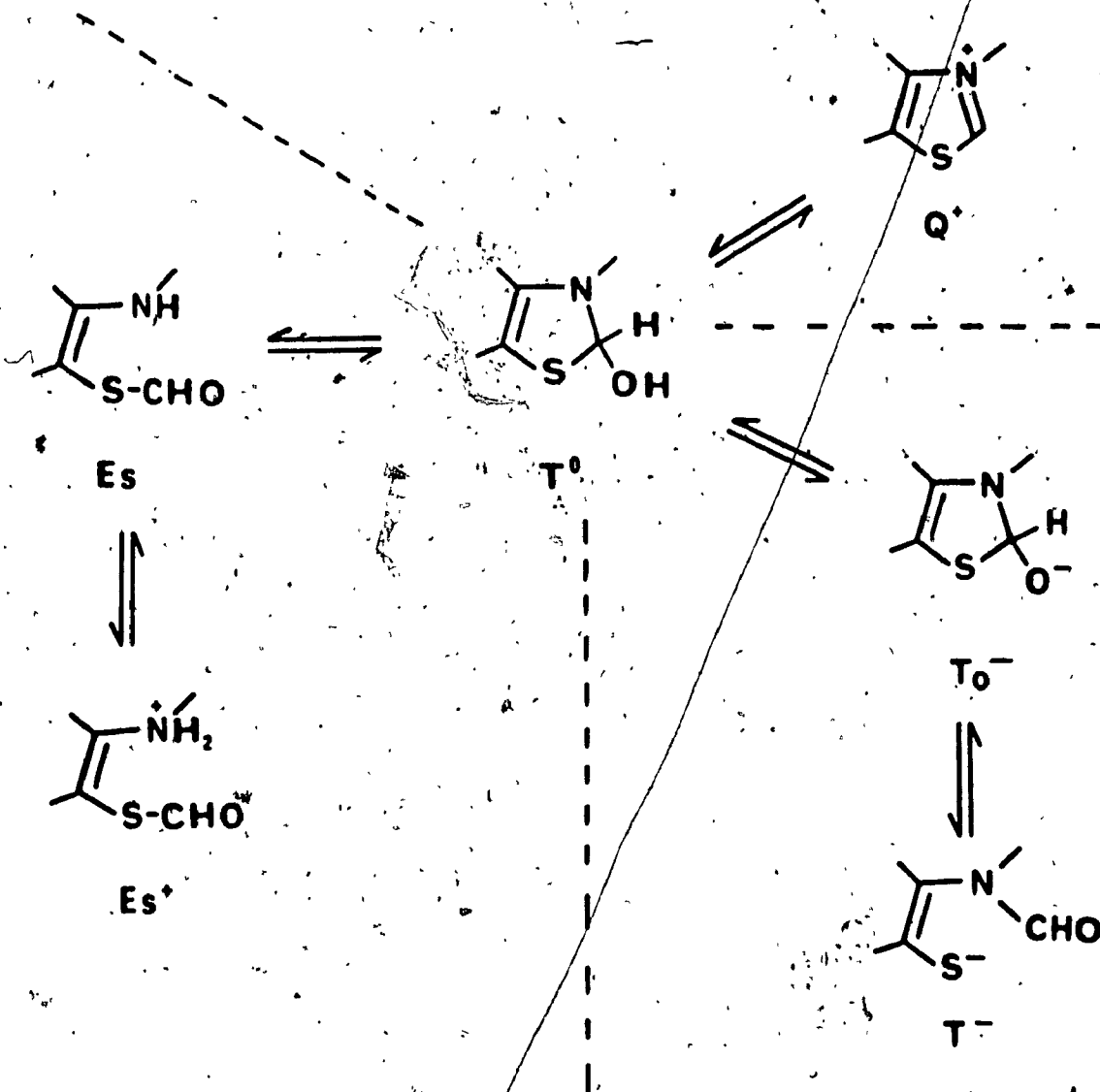
At higher pH (4.5-6.5), $k_o \gg k_H[H^+]$, and eq. 41 simplifies to:

$$k_{obs} = \frac{k_o K_{HES}}{K_{HES}[H^+]} = \frac{1.07 \times 10^{-7}}{[H^+]} \quad (41b)$$

and so the reaction is pH dependent.

Scheme 13 illustrates all the principal structures believed to be involved in the ring-opening / ring-closing reaction of thiazolium ions, such as HET⁺.

All the processes just described for HET⁺ can be rationalized in terms of the tetrahedral intermediate, T^o. In basic solution, C-S bond cleavage of T^o takes place and the enethiolate T⁻ is formed. At acidic pHs, a C-N bond cleavage of T^o gives the amino enethiol ester, whereas, C-O bond cleavage results in the reconstitution of the



Scheme 13. Species involved in the ring-opening and reclosure of thiazolium cations (Q^+).

thiazolium ring. In the case of HET⁺ (and BT⁺), thermodynamic factors favour C-O reformation of the thiazolium ring (cleavage), but kinetic factors favour initial C-N cleavage at low pH.

THIAMINE B₁⁺. The reversible ring-opening and ring-closing reactions of thiamine (B₁⁺) were studied over the pH region 0-14, under the same general conditions as for the BT⁺ and HET⁺. These reactions generally show similar pH dependencies, but the kinetics in basic media (pH > 9.6) are more complicated than for BT⁺ and HET⁺, due to the "yellow form" involved^{15, 20}. Figures 16 and 17 are the pH-rate profiles of the ring-opening and ring-closing of thiamine (B₁⁺), respectively. For simplicity, the kinetics of each of these reactions will be discussed separately.

Ring-opening of B₁⁺

It is well-known that thiamine (B₁⁺) undergoes a reaction, in basic solutions, which leads formally to addition of one oxygen atom and opening of the thiazolium ring, generating the thiolate Th⁻ (Scheme 14). As with the other thiazolium ions already discussed, the formation of the thiolate Th⁻ occurs through the pseudobase T^o (Scheme 14). In addition, it has been known for many years that when thiamine is dissolved in strongly alkaline media, a yellow colour immediately develops, but which slowly fades.

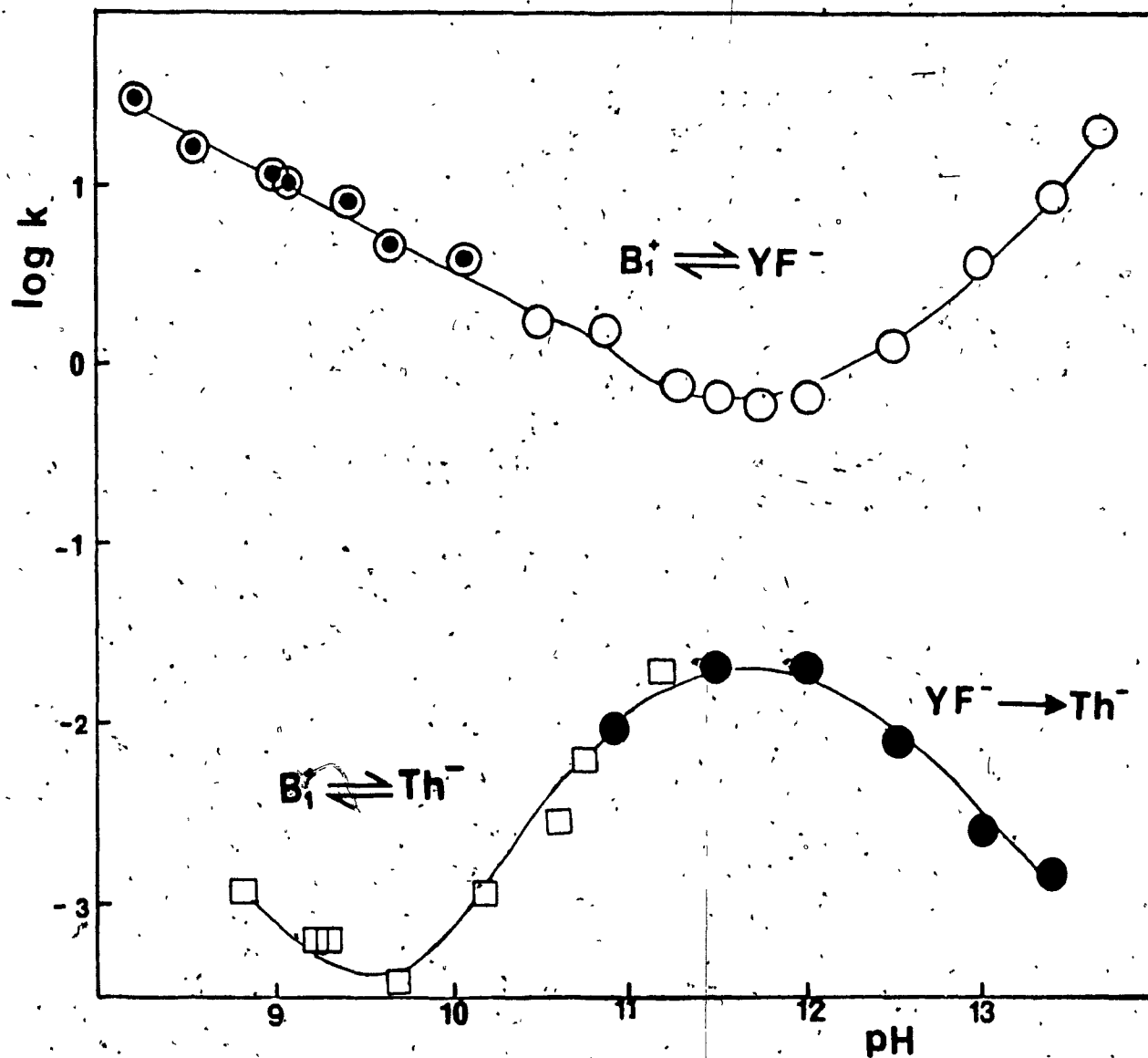


Figure 16. pH-rate profile of the formation of the "yellow form" (YF^-) and the ring-opened form (Th^-) of thiamine (B_1^+), at 25°C and $I = 1.0 \text{ M}$.

- rate constants of the formation of YF^- from B_1^+
- ⊙ rate constants of the formation of B_1^+ from YF^-
- rate constants of the formation of Th^-
- rate constants obtained by conventional UV absorption measurements (Mount St-Vincent University)

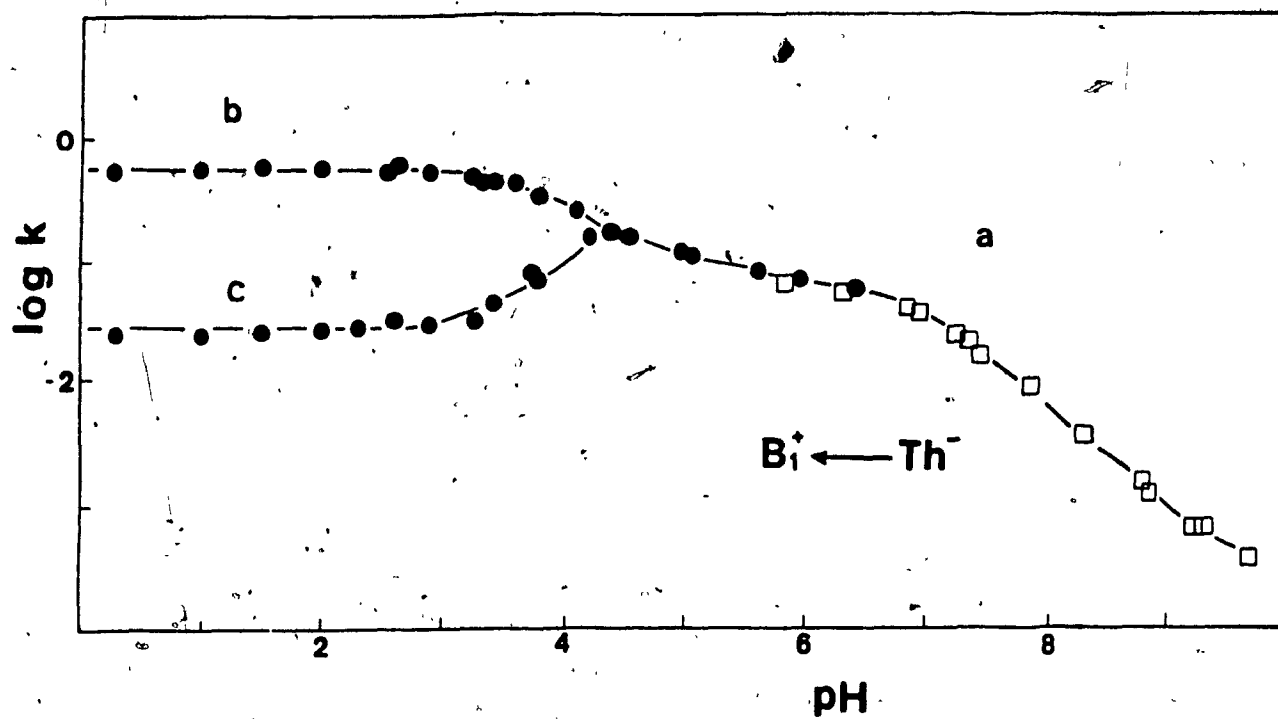
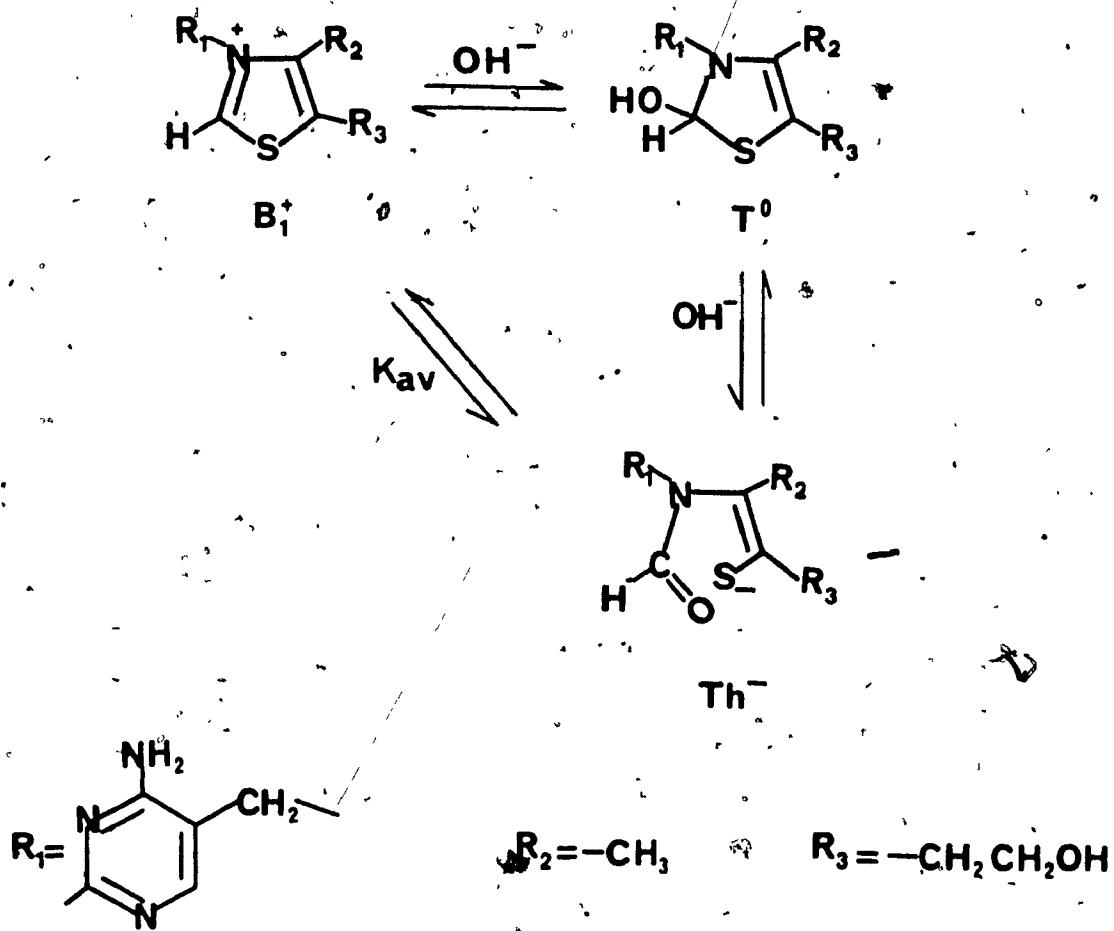


Figure 17. pH-rate profile for the kinetics of the ring-closing reaction of thiamine B_{1+} , at 25 °C and $I = 1.0 M$.

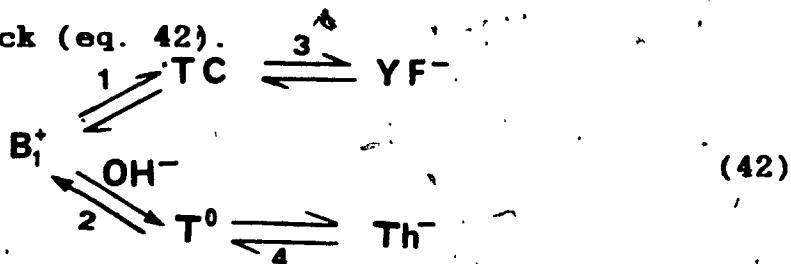
- rate constants (Tables 10 and 11 of the Appendix)
obtained by stopped-flow
- rate constants obtained by conventional UV method
(Mount St-Vincent University)



Scheme 14. Reaction scheme for thiamine thiazolium ring-opening.

This colour is due to the "yellow form" (YF⁻), which has been investigated spectroscopically^{15,57} and kinetically³⁶.

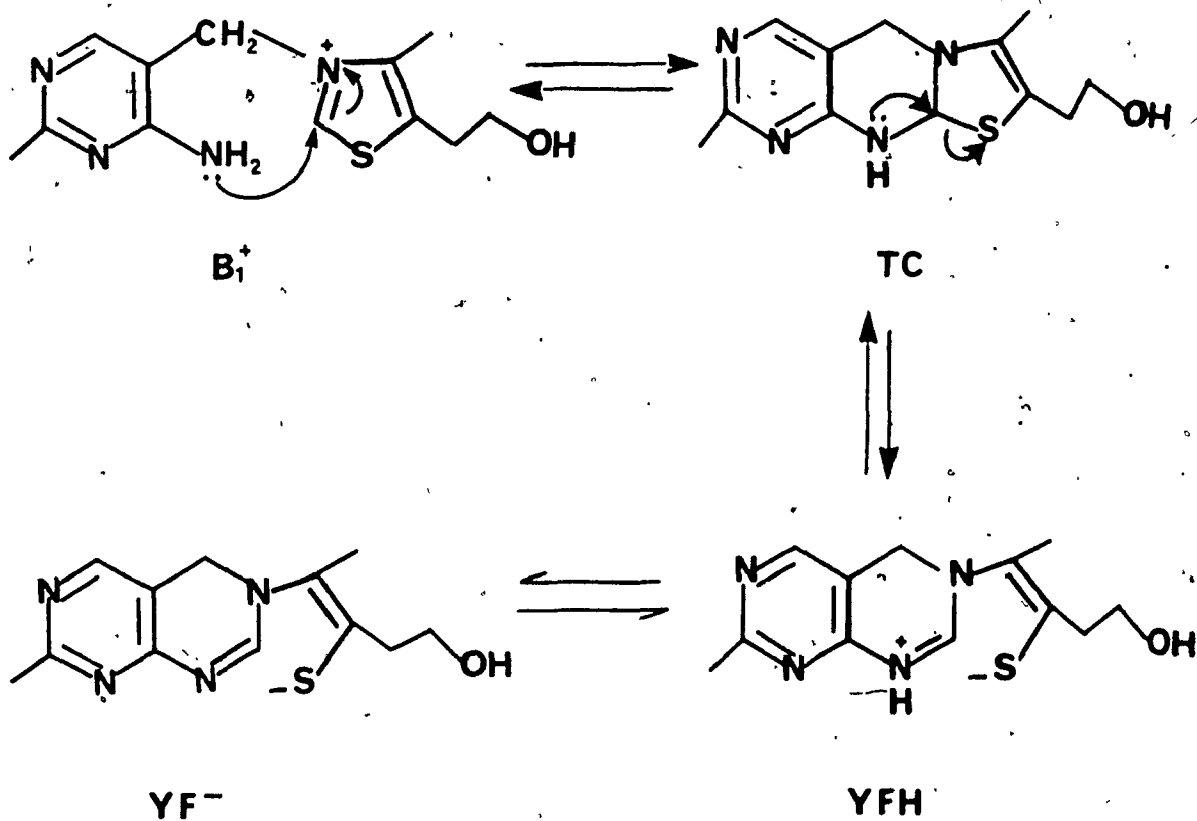
Maier and Metzler¹⁵ have suggested that YF⁻ is in rapid equilibrium with thiamine, which is slowly converted to the open-ring thiol form via the pseudobase T⁰ through a hydroxide ion attack (eq. 42).



Therefore, the pH-rate profile of the ring-opening reaction of thiamine, in high pH's (Figure 16), shows two processes. The fast process (upper phase) corresponds to the formation of the "yellow form" YF⁻ (kinetic control product), whereas the slow process (lower phase) illustrates the pH dependency of the formation of the ring-opened form Th⁻ (thermodynamic control product).

Formation of the YF⁻

The formation and decay of the "yellow form" YF⁻ of thiamine was initially studied by Maier and Metzler¹⁵, who proposed a two-step reaction mechanism (eq. 42) through a tricyclic intermediate (TC) (Scheme 15). According to these researchers, the amino group of thiamine adds, with simultaneous loss of a proton, to the thiazolium ring to yield the intermediate, tricyclic, dihydrothiachromine form TC, in a manner analogous to the addition of a hydroxyl



Scheme 15. Suggested mechanism for the generation of the yellow form of thiamine.

ion, to form the pseudobase, T*. The intermolecular nature of the reaction with the amino group helps to explain its rapidity as compared to the reaction with hydroxide ion (slow process), since in the case of an intramolecular reaction, less desolvation may be required for the interaction of the reactive entities⁶⁰. The ionization of TC, with an opening of the thiazole ring, leads to the "yellow form", YF, which was isolated as the sodium salt^{15,16} and its structure was as proposed by Zima and Williams¹⁵. The yellow colour of this form of thiamine arises from a broad UV absorption band in the blue centered at about 340 nm (Figure 18). It was convenient to use this band for the study of the generation and decay of the "yellow form".

Maier and Metzler¹⁵ estimated spectroscopically the pK_{av} of the two steps of the formation of the "yellow form" (step 1 and 3, eq. 42) to be equal to 11.6 (19 °C, I = 0.2 M). This value is very close to $pK_{av} = 11.75$ (25 °C, I = 1.0 M) from our study, which is derived from the point of inflection of the plot of the $\log k_{obs}$ vs. pH (Figure 16; fast process). A recent study by Hopmann^{3b}, using stopped-flow measurements, obtained $pK_{av} = 11.47$ (20 °C, I = 0.1 M), but his suggested mechanism for YF-formation, which involves the first step as the formation of the ylid of thiamine, seems most unlikely from the present data. According to our results, the mechanism suggested by Maier and Metzler¹⁵ is sufficient with the

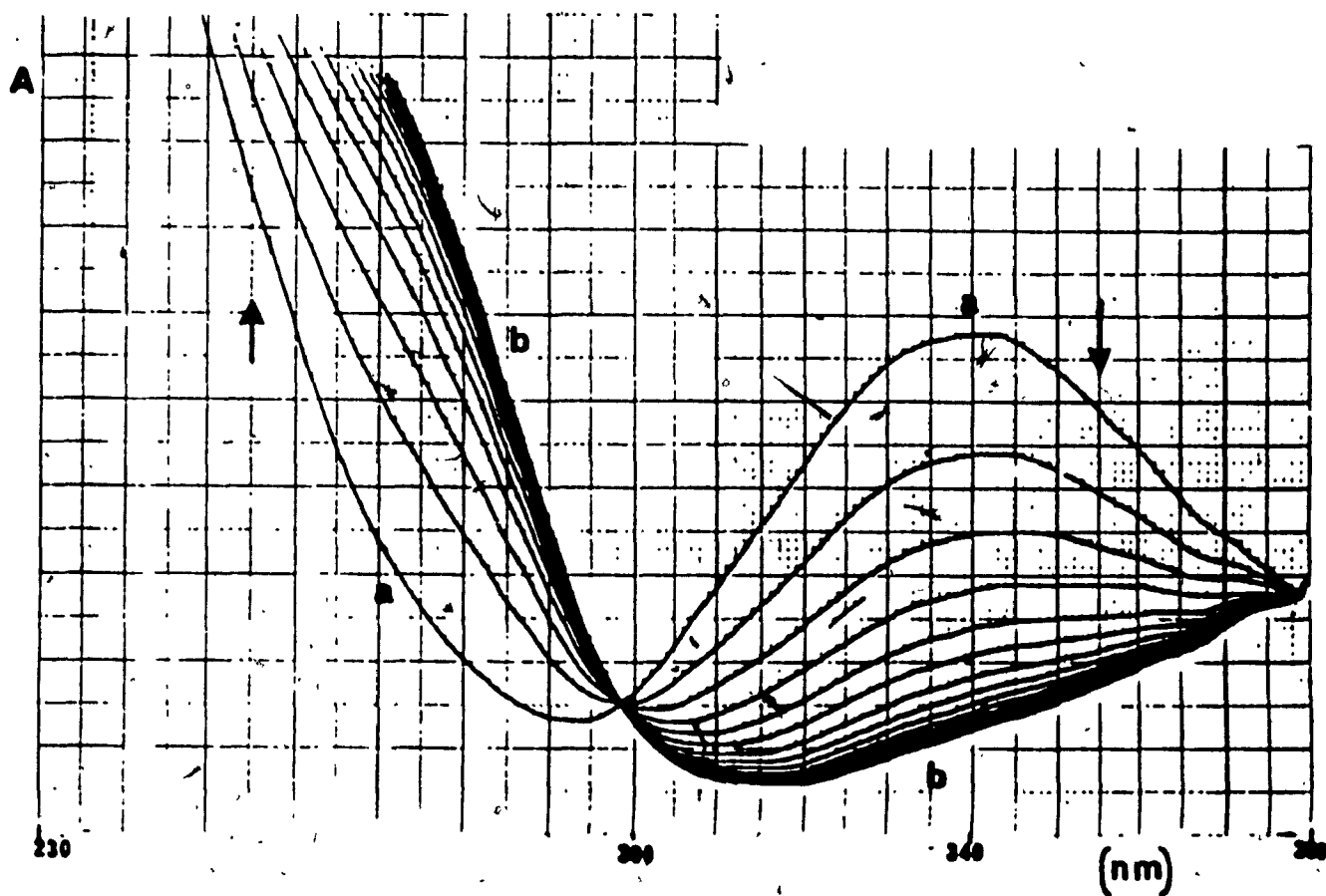


Figure 18. Kinetic spectra of the decay of the yellow form, at pH = 12, scanned in the stopped-flow at 20 nm/sec, every 7.5 seconds (Absorbance scale = 1.0).

a) spectrum of the yellow form, YF-

b) spectrum of the colourless thiolate, Th-

first step, formation of the tricyclic intermediate, being the rate limiting step. One intermediate, which might be considered in this mechanism of the reverse reaction, is the protonated "yellow form", YFH (Scheme 15), to which the apparent $pK_Y = 10.85$, from the break at the ascending side of the plot of the generation of the "yellow form" on Figure 16, can be attributed. This pK_Y is in agreement with the value of 10.55 (20 °C, I = 0.1 M) reported by Hopmann^{3c}. This also can explain the observation made by Maier and Metzler that the "yellow form" does not exist to any appreciable extent below a pH of about 10.6, where the overall equilibrium of Scheme 15 is shifted back to thiamine, B_1^+ .

For the mechanism in eq. 43, which corresponds to the Scheme 14, an expression for k_{obs} for equilibration (eq. 44) can be derived.



$$k_{obs} = k_f + k_d$$

$$= k_{OH}[OH^-] + (k_{-1} + k_2[H^+]) \frac{K_o[H^+]}{K_Y + [H^+]} \quad (44)$$

The first term, $k_{OH}[OH^-] = k_f$, is the rate constant for the formation of YF^- , and the second term is the rate constant for the decomposition of the YF^- ($= k_d$). Around the pH of

equilibration ($pH = 11.75$), both k_f and k_a must be considered, but at higher or lower pHs, one term dominates.

Above pH 11.75, k_a is not significant and eq. 44 is simplified to:

$$k_{obs} = k_{OH}[OH^-] \quad (44b)$$

This explains the dependency of the k_{obs} on pH, the slope of this part of the plot being equal to 1 (Figure 16). From our data (Table 9 of the Appendix), the second order rate constant can be estimated as $k_{OH} = 42.0 \text{ M}^{-1}\text{s}^{-1}$, which is comparable to the value of $108 \text{ M}^{-1}\text{s}^{-1}$ reported by Hopmann^{3b}, taking into consideration the difference in the ionic strength used. However, no break in the rate profile is observed near pH 12.6, which is reported¹⁷ to be the pK_a for ylid formation from the C2-H in thiamine.

In our efforts to extend the earlier study by Hopmann^{3b}, we have also looked at the equilibrium between B_1^+ and YF^- in the reverse direction. Below pH 11.75, only k_a is important, and below pH 10.5, the expression for k_a also simplifies, since $[H^+] \gg K_Y$, and $k_H[H^+] \gg k_{-1}$. Under these conditions, $k_{obs} = k_a = k_H[H^+]K_o$. Unfortunately, our data do not accurately obey this relationship below pH 10.5. This probably reflects experimental difficulties in making the measurements. As explained in the experimental section, a quickly prepared solution of YF^- in strong

base must be quenched with a buffer acid. The resultant values of k_{obs} (and perhaps pH), are not considered reliable.

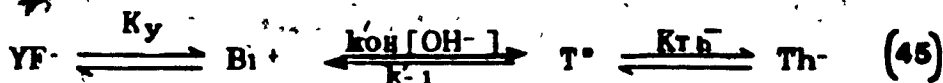
Decay of the "yellow form". Formulation of the ring-opened form

It has been known for years that, when alkaline solutions of thiamine are allowed to stand for a sufficiently long period of time, the final spectra are the same regardless of whether the solutions had been strongly or weakly alkaline. Evidently, the same product must have been formed, which is the ring-opened thiol (Figure 18), and is the thermodynamically stable form of thiamine in alkaline solutions. This was also confirmed by our NMR experiments, discussed earlier.

As previously mentioned, Maier and Metzler¹⁵ presented arguments suggesting that the "yellow form" is the kinetically-controlled product, which decays via thiamine to the ring-opened thiol form, and that all of these transformations are reversible equilibria (eq. 42). In addition, the time dependent UV spectra of the transformation of the "yellow form" to the thiol form (Figure 18), pass through an isosbestic point at 298 nm, indicating that no intermediate is formed in significant amounts. Hopmann's mechanistic suggestions about the direct conversion of the "yellow form" to the thiol form, are rather

unreasonable, since they are not supported by enough experimental evidence.

The kinetics of the decay of the "yellow form" constitutes part of a bell-shaped pH-rate profile, illustrated on Figure 15 (slow process, pH > 10.6). Our rate profile is in agreement with the literature^{15, 3b} and, in fact, extends those already reported^{15, 3b}, since we studied this reaction up to pH 13.4. The points on the curve below pH 10.6 correspond to the rate of the reaction of thiamine with hydroxide ion to form the colourless thiol (steps 2 and 4; eq. 42). Therefore, the top of the pH-rate profile, pH = 11.75, corresponds to the pK_a for the equilibration of the "yellow form" and the thiamine, whereas, the lowest part of this rate profile at pH = 9.6 corresponds to the pK_a of the conversion of thiamine to the ring opened thiol, Th⁻ (eq. 45).



From the pK_a values of 11.75 for the conversion to the "yellow form", and of 9.6 for the conversion to the thiol form, it follows that, at equilibrium, the ratio of the colorless thiol form to the "yellow form" should be 10,000 and the disappearance of the yellow colour essentially complete. Consequently, k_{obs} may be defined as follows:

$$\begin{aligned}
 k_{obs} &= k_f + k_d \\
 &= k'_{OH} [OH^-] \frac{[H^+]^2}{K_y^2 + [H^+]^2} + \frac{k'_{-1} [H^+]}{(K_{Th-} + [H^+])} \quad (46)
 \end{aligned}$$

where $K_y^2 = \frac{[YF^-][H^+]^2}{[B_1^+]}$ = $(10^{-11.75})^2$

and the term $\frac{[H^+]^2}{K_y^2 + [H^+]^2}$ represents the fraction of

thiamine present in equilibrium with the YF^- . Above pH 9.6, the term containing k'_{-1} for the reverse reaction is not important, therefore, eq. 46 is simplified to eq. 47.

$$k_{obs} = \frac{k'_{OH} K_w [H^+]}{K_y^2 + [H^+]^2} \quad (47)$$

It is this equation which accounts for the bell-shaped profile shown in Figure 16 (lower). For $pH < 11.75 = pK_y$, $[H^+] \gg K_y$, and,

$$\text{and} \quad k_{obs} = \frac{k'_{OH} K_w}{[H^+]} = k'_{OH} [OH^-] \quad (48)$$

This explains the positive dependency of the observed rate constant on pH seen as the ascending part of the pH-rate profile. From our data in this pH region, the second order rate constant k'_{OH} has the value of $10.7 \text{ M}^{-1}\text{s}^{-1}$, which is close to previously reported values^{3b, 14b, 15}.

At $pH > 11.75 = pK_y$, $[H^+] \ll K_y$,

therefore
$$k_{obs} = \frac{k_{OH}K_w[H^+]}{K_y} \quad (49)$$

This expression corresponds to the points on the descending part of the lower profile in Figure 15.

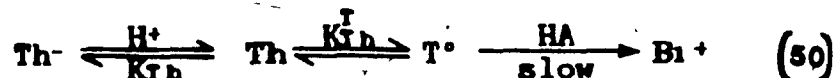
Overall, the data give a good fit to eq. 47, with $k_{OH} = 10.6 \text{ M}^{-1}\text{s}^{-1}$, and $K_y = 1.9 \times 10^{-12} \text{ M}$ ($pK_y = 11.72$). This last value is in excellent agreement with that found from the upper profile in Figure 15 ($pK_y = 11.75$). Thus, the data for the decay of the "yellow form", YF^- , are adequately explained by the mechanism of Maier and Metzler, as is the data for its formation. The additional steps proposed by Hopmann^{17, 2b} do not seem necessary or justifiable.

Ring-closing reaction of B_1^+

When alkaline solutions of thiamine are acidified, ring-closure of the open thiolate takes place through the tetrahedral intermediate and the thiazolium ring of thiamine is rapidly regenerated.

As expected from our previous studies, the BT^+ and HET^+ ions, reclosure of the enethiolate derived from thiamine, shows one kinetic phase (process (a)) at intermediate pHs, but at low pHs ($pH < 4.5$), two distinct phases (processes (b) and (c)) are observable (Figure 17).

Process (a). Similar to the case of HET⁺, process (a) on the pH-rate profile of B₁⁺ represents the regeneration of thiamine from the amido enethiolate Th⁻ or its conjugate acid, Th (eq. 50).



Buffer catalysis experiments for this pH region showed general acid catalysis up to pH 8.5. Beyond this, it was not detectable. These observations, along with the negative dependence of the k_{obs} on the pH, (Figure 17a), can be rationalized by the general acid-catalyzed loss of OH⁻ from the tetrahedral intermediate T[°], being the rate-limiting step. However, this breakdown of T[°] is not significantly catalyzed by H⁺ in this pH region. The apparent break of the pH-rate profile and the plateau, at about pH 6.7, are attributed to the pK_a of the thiol, Th. This value is close to the corresponding pK_a of the thiol of HET⁺ (pK_a = 7.8).

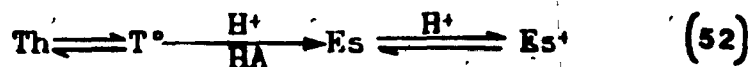
Kinetic analysis, based on eq. 50, requires that

$$k_{\text{obs}} = \frac{k_0 K_{\text{Th}}^{\text{T}} [\text{H}^+]}{(K_{\text{Th}} + [\text{H}^+])} \quad (51)$$

A plot of $1/k_{\text{obs}}$ vs. $1/[\text{H}^+]$ for our data over the pH range 5.8 to 7.8 gives $k_0 K_{\text{Th}}^{\text{T}} = 0.084 \text{ s}^{-1}$ and $K_{\text{Th}} = 1.8 \times 10^{-7} \text{ M}$ (pK_{Th} = 6.7).

In addition, another pK_a that is involved in this pH region is the pK_a of the protonation of the pyrimidine ring at the N_1 position with an estimated value⁶¹ about 5.0. However, this is not conspicuous in the rate profile.

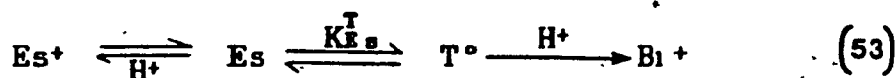
Process (b). As for HET^+ , the bifurcation of the rate profile around pH 4.5 (Figure 17), is ascribed to the onset of the proton-catalyzed (and general acid-catalyzed) breakdown of the tetrahedral intermediate, T° , to give the protonated amino enethiol ester Es^+ (eq. 52). This process corresponds to an acyl transfer from N to S.



As previously, at low pHs (0-3.5), the rate of the reaction is independent of the $[H^+]$ (plateau of process (b)), which can be explained by a change of rate-limiting step: at low pH, the breakdown of T° is sufficiently fast that its formation becomes rate-limiting. The observed pseudo-first order rate constant for the plateau region has been estimated as 0.57 s^{-1} , which is a little lower than that for HET^+ (0.68 s^{-1}).

Hopmann^{2b} reported a k_{obs} for the plateau of 0.25 s^{-1} , but his data are limited at pHs above 3.0, and at 20°C , $I = 0.2 \text{ M}$. Surprisingly, he observed only one process at low pHs.

Process (c). As for HET⁺, NMR and UV spectra of the slow process of the ring-cyclization reaction indicate that thiamine is the final product. Therefore, process (c) (Figure 17) is attributed to the conversion of Es⁺ to the thiazolium ion of B1⁺, also through the intermediate T° (eq. 53).



The plateau at pH 0-3 can be explained by the mechanism suggested above. At low pH, no catalysis is observed, since the necessary deprotonation of Es⁺ cancels with the proton catalysis of T° to give B1⁺, and hence, overall, the rate of the reaction appears to be pH independent. Above pH 3.5, the profile for process (c) rises and the reaction appears to be specific base-catalyzed. This arises because the conversion of T° to B1⁺ may be unassisted (k_o) at low [H⁺].

The overall expression derived for the mechanism shown in eq. 53 is:

$$k_{\text{obs}} = \frac{(k_{\text{o}} + k_{\text{H}}[\text{H}^+])K_{\text{Es}}}{K_{\text{Es}}[\text{H}^+]} \quad (54)$$

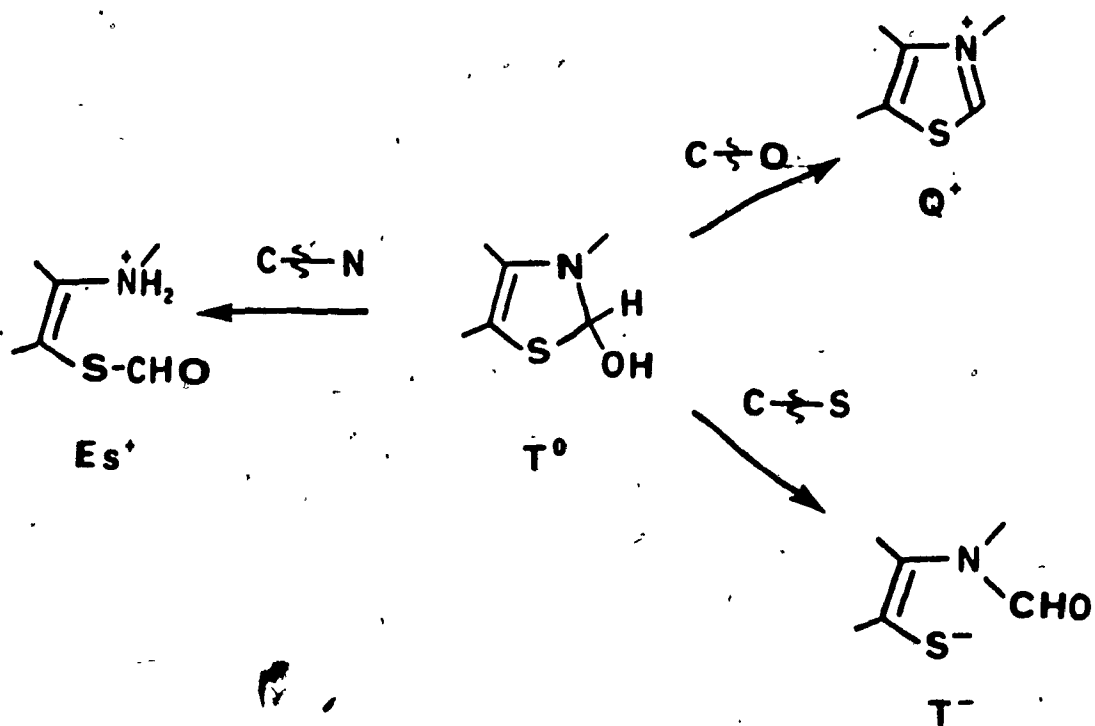
assuming that the amino group is protonated. At low pH, i.e. high [H⁺], below pH 3.5, the term k_H[H⁺] is dominant,

and so, eq. 54 simplifies to $k_{obs} = k_2 K_2 / K_1$ and a plateau is observed. Above pH 8.5, the reverse holds and $k_{obs} = k_2 K_2 / K_1 [H^+]$, which appears as specific base catalysis.

In general, all the processes described above in the ring-opening and ring-closing reaction can be understood in terms of the breakdown of the tetrahedral intermediate, T^* . This species may undergo C-O, C-N, or C-S bond cleavage (Scheme 16), depending upon the pH. In the ring opening direction, a C-S bond cleavage occurs, and the enethiolate T^- is formed. At acidic pHs, a C-N bond cleavage of T^* gives the amino enethiol ester, whereas the C-O bond cleavage results in the reconstitution of the thiazolium ring. Apparently, kinetic factors favour the former, whereas thermodynamic factors favour the thiazolium ring formation.

1'-Methylthiaminium Dication ($N_1 Me B_1^{2+}$). This ion, first prepared by Jordan and coworkers⁵⁶, serves as a model for thiamine protonated on the N_1 of its pyrimidine ring. Also, of course, it is a useful substituted analogue of thiamine.

In alkaline solution, $N_1 Me B_1^{2+}$ ring-opens in a similar manner to thiamine. The kinetics of equilibration of the cation and ring-opened thiolate were studied recently by Zoltewicz and Uray⁵⁷. They found that the pK_a was 8.56.



Scheme 16. Possible modes of cleavage of the tetrahedral intermediate T^0 .

(25.1 °C, $I = 0.2 \text{ M}$), about one unit lower than for thiamine, due to the positively-charged pyrimidine ring. The electron-withdrawing inductive effect of this group destabilizes the thiazolium ring and stabilizes the ring-opened thiolate anion. For similar reasons, the N_1MeB_1^+ ion is attacked 11 times more rapidly by the hydroxide ion, with $k_{\text{OH}} = 117 \text{ M}^{-1}\text{s}^{-1}$.

Ring-closing of N_1MeB_1^+

The ring-closing reaction of the thiol form of the 1'-methylthiaminium dication (11) was studied at the pH range 0-6.25, at 25 °C, and $I = 1.0 \text{ M}$ (NaCl). The pH rate profile for this thiazolium ion (Figure 19) is very similar to that of thiamine in this pH region, but only one process was observed. As with thiamine, the reaction is pH independent up to pH 3.5, forming a plateau, whereas an overall negative dependence on the pH is observed in the pH region 3.50 - 8.56.

A previous study on the ring-opening and ring-closing of the N_1MeB_1^+ ion by Zaltewicz and Uray^{3a} covered only pH region 7.5 - 10.0, around the pH of equilibration of the ring-opened form and the thiazolium ion. From their experiments, carried out at 25.1 °C, and $I = 0.2 \text{ M}$, they estimated the pK_a for the ring-opening process to be 8.56, and the second order rate constants k_{OH} and k_{H} for the ring-opening and ring-closing, equal to $117 \text{ M}^{-1}\text{s}^{-1}$ and

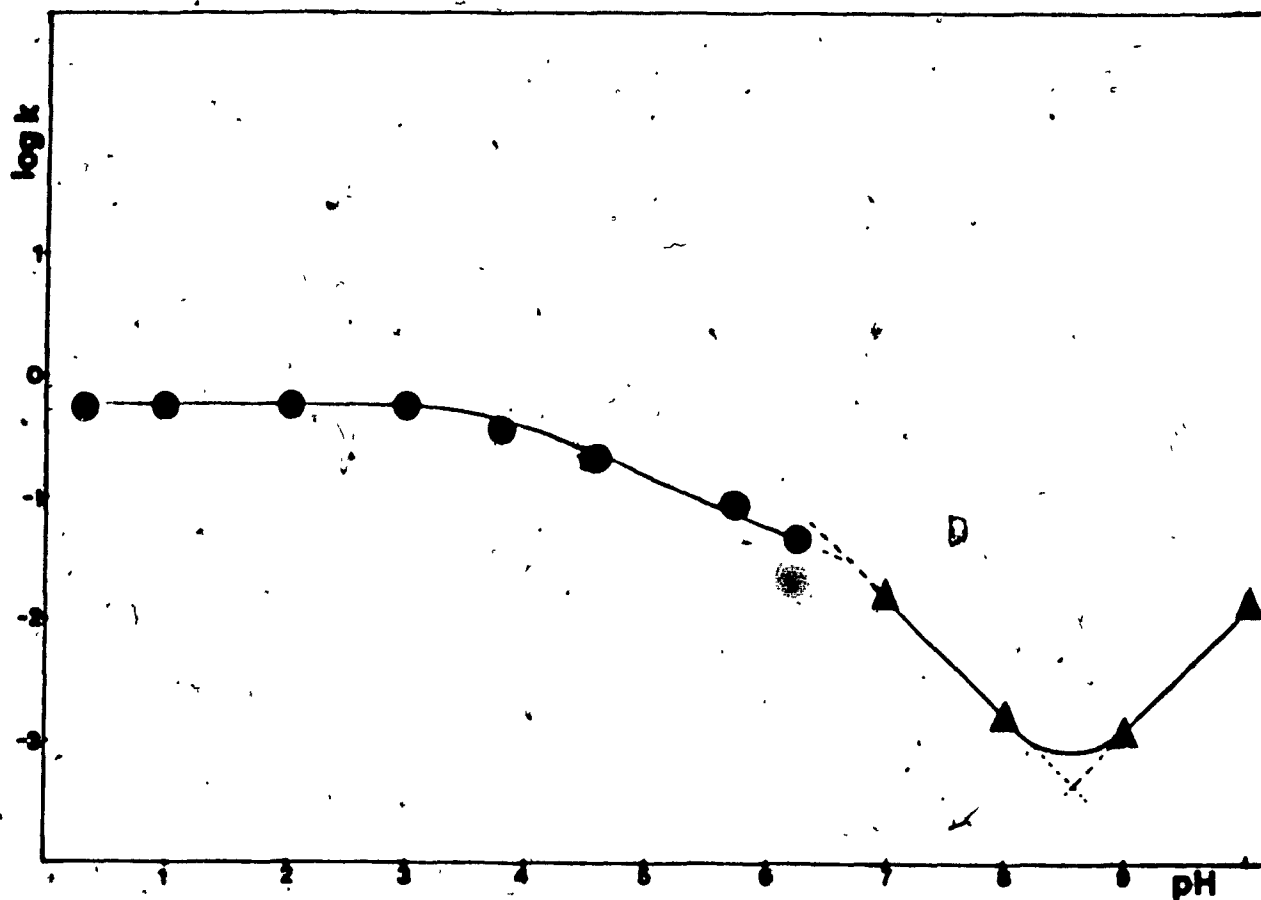


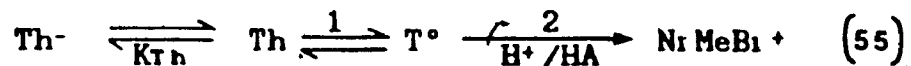
Figure 19. pH dependence of the first order rate constants for the ring closing of 1'-methylthiaminium ion (N^+MeB_4).

● data from this laboratory, given in Table 13 of the Appendix

▲ calculated data from Zoltewicz and Uray^{2a}

$1.55 \times 10^5 \text{ M}^{-1}\text{s}^{-1}$, respectively. Our data are in good agreement with their data, given the difference in the ionic strength.

As with other thiazolium ions studied, the plateau region (Figure 19), can be ascribed to rate-limiting formation of the tetrahedral intermediate from the undissociated thiol Th (eq. 55, Step 1). Again, the break in the rate profile at about pH 3.5 is due to change in the rate-limiting step, so that the general-acid catalyzed breakdown of T° becomes the rate-limiting step (eq. 55, Step 2).



Obviously, more experimental data are required in this pH region, so that a better mechanistic explanation of the pH-rate profile might be given, even though it looks very similar to that of thiamine, where a more extensive study has been done. For example, the pK_a of the thiol form Th is expected to be as for thiamine, i.e. about 6.7. Indeed, a discontinuity between our data and the literature data occurs there (Figure 19).

Surprisingly, no slow process has been observed for the reclosure of NlMeB_1^+ compound, which otherwise shows similar kinetic behaviour to that of thiamine. Of course, there is the possibility that, in this case, the slow process is too slow to be observed by stopped-flow.

Alternatively, the "slow" process may be faster than in the previous cases, so that, essentially, it overlaps with the fast phase. Also, for reasons which are not readily apparent, experimental difficulties were encountered during the study of the reclosure of N^+MeB^+ . The absorbance changes, though of reasonable size, gave noisy traces and the rate constants are less reliable than normal. It is conceivable that there is a "slow" process, involving a small absorbance change, which was not observed.

Clearly, further investigation of the kinetics of the ring-closing of this thiazolium ion is needed to elucidate the role of the positively charged pyrimidine ring as a substituent on the thiazolium ion and to clear up the uncertainty about the apparent absence of a "slow" process.

ACTIVATION PARAMETERS

To provide further insight and another way of comparing the different thiazolium ring systems, activation parameters have been measured. The measurements were carried out at pH 2, which is in the center of the plateau regions of both the fast and the slow processes, for three reasons. Firstly, these processes are the ones of most interest. Secondly, problems associated with the temperature dependence of pH should be minimal. Thirdly, no buffer catalysis was found in this region.

Table 4. Summary of results.

	pK_{av}	k_{OH} $M^{-1}S^{-1}$	$k_{plateau}$ S^{-1}	ΔH° Kcal/mole	ΔS° E.u.
BT+	6.5	8700			
fast			2.1	7.7	-31
slow			0.054	9.2	-34
HET+	10.3	1.3			
fast			0.68	7.5	-34
slow			0.016	10.0	-33
Bi+	9.6	10.6			
fast			0.57	6.3	-39
slow			0.029	9.7	-33

The activation entropy and enthalpy of the ring-closing of BT^+ , HET^+ , and B_1^+ thiazolium ions were obtained by carrying out experiments on the temperature dependence of k_{obs} . The values of ΔS^\ddagger and ΔH^\ddagger , given in Table 4, were obtained by the least square analysis of the plot of $\ln(k_{obs}/T)$ vs. $1/T$, for the temperature range 15-35 °C. As expected for a cyclization reaction, the activation entropies S^\ddagger have large negative values. Moreover, there are no major differences in the ΔH^\ddagger and ΔS^\ddagger values for the different thiazolium ring systems. Clearly, the principal factors involved in the fast and slow processes are the same for the various substrates.

CONCLUDING REMARKS

The analysis of the pH-rate profile of the reversible thiazolium ring cleavage of HET^+ , B_1^+ , and BT^+ (previously studied^{1,2}) have been investigated for the pH region 0-14. The ring-opening process shows a rate-limiting attack of hydroxide ion on the thiazolium ring to form the pseudobase T^+ which then undergoes, fast deprotonation and ring-opening to the enethiolate, T^- . The estimated pK_{av} of the equilibration of the thiazolium cations BT^+ , HET^+ , and B_1^+ to their ring-opened form, are 6.5, 10.3, and 9.6 (at 25 °C), respectively. A correlation of the structures of the thiazolium ion under study with their rate constants k_{obs} and pK_{av} (Table 4) leads to the conclusion that

electron withdrawing substituents, such as the aromatic ring in BT^+ and $-CH_2R$ (where R is the amino pyrimidine ring) in B_1^+ accelerates the attack of OH^- on the 2-position and

lowers the pK_a probably by destabilization of the thiazolium ring and stabilization of the thiolate.

Two kinetically distinguishable processes have been found, at low pH, for the ring-closing of the enethiolates T derived from B_1^+ , HET^+ , and BT^+ . According to proposed mechanism, the first (kinetic control) forms an amino enethiol ester, while the second (thermodynamic control) results in the reconstitution of the appropriate thiazolium ring. Comparison of the first-order rate constants (Table 4) of B_1^+ , HET^+ , and BT^+ , shows that acyl transfer takes place about 3 times faster in the thiol form of BT^+ than in HET^+ and B_1^+ . This can be explained by the lower pK_a value for BT^+ (5.6), compared to that of HET^+ (8.03) or B_1^+ (6.7), since the rate-limiting step for this process, from the proposed mechanism (eq. 52) is the formation of the tetrahedral intermediate T^* from the thiol form T.

No major differences have been found in the values of the activation parameters ΔH^\ddagger and ΔS^\ddagger (Table 4) between the fast and the slow phase of the ring-closing, which explains our mechanistic suggestion that both processes occur via the tetrahedral intermediate, T^* . Suggestions for further work include:

- More kinetic NMR studies for the fast process of the ring-closing, probably by a stopped-flow NMR spectrometer. This type of study should elucidate the product analysis of the fast process.
- Dynamic and static NMR experiments at room temperature, and at elevated temperature, will give information about the relative stability of the two observed rotamers of the thiol form. These studies, in connection with kinetics in stopped-flow at elevated temperature, may also indicate any possible connection between the two rotational isomers of the thiolate and the two processes observed on the reclosure.
- Finally, extended investigation in the kinetics of the N-methyl-thiaminium ion, as well as of other substituted thiamine derivatives, will help, so that the chemistry of thiamine, this so biologically important compound, be better understood.

R E F E R E N C E S

REFERENCES

1. "Thiamine. Twenty Years of Progress", H.Z. Sable and C.J. Gubler, Editors, New York Academy of Science, New York, 1982, (Annals New York Academy of Science, 378, 7-122 (1982)).
2. J.W. Bunting, Adv. Heterocycl. Chem., 25, 1 (1979) and references cited therein.
3. a) J.A. Zoltewicz and G.J. Uray, J. Org. Chem., 45, 2104 (1980).
b) R.F.W. Hopmann, Ann. New York Acad. Sci., 378, 32 (1982).
c) J.M. El Hage Chahine and J.E. Dubois, J. Am. Chem. Soc., 105, 2335 (1983).
4. a) P. Haake and J.M. Duclos, Tetrahedron Lett., 461 (1970).
b) J.M. Duclos and P. Haake, Biochemistry, 13, 5358 (1974).
c) J.M. Duclos, Ph.D. Thesis, Wesleyan University, Middletown, Connecticut (1972).
5. B.C.P. Jansen and W.F. Donath, Proc. Acad. Sci., Amsterdam, 29, 1390 (1982).
6. R.R. Williams, R.E. Waterman, and J.C. Keresztesy, J. Am. Chem. Soc., 56, 1187 (1934).
7. R.R. Williams, J. Am. Chem. Soc., 58, 1063, (1936).

8. R.R. Williams and J.K. Cline, J. Am. Chem. Soc., 58, 1504 (1936).
9. R. Breslow, J. Am. Chem. Soc., 80, 3719, (1958)
10. L.O. Krampitz, "Thiamin Diphosphate and its Catalytic Functions", Marcel Dekker, New York, 1970.
11. R. Kluger, J. Chin, and T. Smyth, J. Am. Chem. Soc., 103, 884 (1981).
12. H. Dugas and C. Penney, "Bioorganic Chemistry", Springer-Verlag (1981).
13. R.R. Williams and A.E. Ruehle, J. Am. Chem. Soc., 57, 1856 (1935).
14. a) A. Watanabe and Y. Asahi, J. Pharm. Soc. Japan, 75, 1046 (1955).
b) Y. Asahi and M. Nagoaka, Chem. Pharm. Bull. Japan, 19, 1017 (1971).
15. G.D. Maier and D.E. Metzler, J. Am. Chem. Soc., 79, 4386 (1957).
16. O. Zima and R.R. Williams, Ber., 73, 941 (1940).
17. R.F.W. Hopmann and G.P. Brugnani, Angew Chem. Int. Ed. Engl., 20, 961 (1981).
18. H. Vorsanger, Bull. Soc. Chim. Fr., 3118 (1964);
H. Vorsanger, Bull. Soc. Chim. Fr., 551, 556 (1967);
H. Vorsanger, Bull. Soc. Chim. Fr., 2124 (1967).
19. a) O.S. Tee and G.D. Spiropoulos, Concordia University, Unpublished results.

- b) O.S. Tee, G.D. Spiropoulos, R.J. McDonald, V.D. Geldard, and D. Moore, *J. Org. Chem.*, 51, 2150 (1986).
20. a) R.B. Martin, S. Lowry, E.L. Elson, and J.T. Edsall, *J. Am. Chem. Soc.*, 81, 5089 (1959).
b) R.B. Martin and R.I. Herdrick, *J. Am. Chem. Soc.*, 84, 106 (1962).
21. R. Barnett and W.P. Jencks, *J. Am. Chem. Soc.*, 90, 4199 (1968).
22. M.L. Bender, *Chem. Rev.*, 60, 53-113 (1960).
23. W.P. Jencks, "Catalysis in Chemistry and Enzymology", McGraw Hill, New York, 1968.
24. W.P. Jencks, *J. Am. Chem. Soc.*, 81, 475 (1959).
25. H. Decker, *J. Prakt. Chem. [N.S.]*, 47, 28 (1893).
26. a) A. Hantzsch, *Chem. Ber.*, 32, 575 (1899).
b) A. Hantzsch and M. Kalb, *Chem. Ber.*, 32, 3109 (1899).
27. D.R. Robinson and W.P. Jencks, *J. Am. Chem. Soc.*, 89, 7088 (1967).
28. B. Capon, A.K. Ghosh, and D.M.A. Grieve, *Acc. Chem. Res.*, 14, 306 (1981).
29. a) O.S. Tee, M. Trani, R.A. McClelland, and N.E. Seaman, *J. Am. Chem. Soc.*, 104, 7219 (1982).
b) M. Trani, Honours Research Project, Concordia University (1982).
30. O.S. Tee and M. Endo, *Can. J. Chem.*, 54, 2681 (1976).

31. D. Beke, *Adv. Heterocycl. Chem.*, 1, 167 (1983).
32. J.W. Bunting and W.G. Meathrel, *Can. J. Chem.*, 50, 917 (1972).
33. T.H. Lowry and K.S. Richardson, "Mechanism and Theory in Organic Chemistry", Harper & Row, New York (1981).
34. R.S. McDonald, P. Patterson, and A. Stevens-Whalley, *Can. J. Chem.*, 61, 1846 (1983).
35. T.H. Fife and N.W. Duddy, *J. Am. Chem. Soc.*, 105, 74 (1983).
36. J.A. Zoltewicz and T.D. Baugh, *Synthesis*, 217 (1980).
37. D.D. Perrin, *Austr. J. Chem.*, 16, 572 (1963).
38. D.D. Perrin and B. Dempsey, "Buffers for pH and Metal Ion Control", Chapman and Hall, London (1974).
39. a) L.H. Funderburk, L. Aldwin, and W.P. Jencks, *J. Am. Chem. Soc.*, 100, 5444 (1978).
b) H. Gilbert and W.P. Jencks, *J. Am. Chem. Soc.*, 99, 7391 (1977).
c) J. Sawyer and W.P. Jencks, *J. Am. Chem. Soc.*, 99, 464 (1977).
40. B. Chance, *J. Franklin Inst.*, 229, 455, 613, 737 (1940).
41. E.F. Caldin, "Fast Reactions in Solution", J. Wiley and Sons, Inc., New York (1964).

42. Q.H. Gibson, *J. Physiol.*, 117, 498 (1952);
Q.H. Gibson, *Faraday Soc.*, 17, 137 (1964);
Q.H. Gibson and C. Greenwood, *Biochem. J.*, 86, 541
(1963).
43. J.A. Sirs, *Trans. Faraday Soc.*, 54, 207 (1958).
44. J.A. Sirs, *Trans. Faraday Soc.*, 54, 201 (1958).
45. R.H. Prince, *Trans. Faraday Soc.*, 54, 838 (1958).
46. B. Venkataraman and G.K. Fraenkel, *J. Am. Chem. Soc.*,
77, 2707 (1955);
I. Yamazaki and H.S. Mason, *Biophys. Res. Comm.*, 1,
336 (1959).
47. F.J.W. Roughton, "Investigations of Rates and Mechanisms of Reactions. Part II", Interscience, New York (1963).
48. "Rapid Mixing and Sampling Techniques in Biochemistry", p. 109, B. Chance, R.H. Eisenhardt, A.H. Gibson, and K.K. Lonborg-Holm, Editors, Academic Press Inc., New York (1964).
49. "DW-2-Vis Spectrophotometer", Operator's Manual, American Instrument Company, Maryland (1973).
50. J.I. Morrow, *Chem. Instrumentation*, 2, (4), 375-387 (1970).
51. E.S. Swinbourne, "Analysis of Kinetic Data", pp. 78-84, T. Nelson and Sons, Limited, London (1971).
52. K.J. Laidler, "Chemical Kinetics", pp. 5-14, McGraw Hill, New York (1965).

53. G.J. Nesbitt, M.Sc. Thesis, Concordia University (1983).
54. L.M. Jackman, S. Sternhall, Appl. of NMR in Organic Chemistry, p. 191, Pergamon Press, 2nd Edition (1969).
55. L.M. Jackman, S. Sternhall, Appl. of NMR in Organic Chemistry, p. 361, Pergamon Press, 2nd Edition (1969).
56. F. Jordan and Y.H. Mariam, J. Am. Chem. Soc., 100, 25, 2534 (1978).
57. Y. Asahi and E. Mizuta, Talanta, 19, 567 (1972).
58. a) A. Pompon, J. Chim. Phys., 72, 505 (1975).
b) A. Pompon, E. Picquenard, C. Coupry, and P. Dizabo, J. Chim. Phys., 76, 351, (1979).
c) R. Stewart and R. Srinivasan, Acc. Chem. Res., 11, 271 (1978).
d) T.S. Batterham, D.J. Brown, and M.N. Paddon-Row, J. Chem. Soc. B, 171 (1967).
59. M.F. Aldersley, A.J. Kirby, P.W. Lancaster, R.S. McDonald, and C.R. Smith, J. Chem. Soc., Perkin Trans., 2, 1487 (1974).
60. A.J. Kirby and A.R. Fehrst, Prog Biorg Chem., 1, 1 (1971).
61. J. Suchy, J.J. Miezal, G. Bantle, and H.Z. Sable, J. Biol. Chem., 247, 5905 (1972).

APPENDIX

Table 5. Rate constants for ring-opening of HET⁺.

<u>pH</u>	<u>k_{obs}</u> s ⁻¹	<u>log k_{obs}</u>
13.52	0.657	-0.182
13.12	0.268	-0.572
12.82	0.131	-0.883
12.51	0.0736	-1.13
12.42	0.0582	-1.24
12.30	0.0456	-1.34
12.12	0.0313	-1.50
11.83	0.0151	-1.82
11.60	0.00900	-2.05
11.44	0.00658	-2.18
11.32	0.00525	-2.28
11.18	0.00410	-2.39
10.98	0.00325	-2.49
10.82	0.00148	-2.83
10.61	0.00135	-2.87
10.52	0.00114	-2.94
10.35	0.00111	-2.95
10.03	0.00120	-2.91

Table 6. Rate constants for ring-closing of HET⁺
(fast process).

pH	k_{obs} s ⁻¹	$\log k_{obs}$
0.44	0.610	-0.214
1.13	0.690	-0.161
2.13	0.688	-0.162
2.62	0.700	-0.155
3.20	0.696	-0.157
3.49	0.662	-0.179
3.94	0.641	-0.193
4.49	0.595	-0.225
4.56	0.589	-0.230
5.35	0.511	-0.292
5.75	0.476	-0.322
5.95	0.373	-0.428
6.31	0.330	-0.481
6.52	0.236	-0.627
6.57	0.244	-0.613
6.75	0.213	-0.672
7.06	0.149	-0.827
7.47	0.110	-0.958
7.80	0.082	-1.09
8.28	0.038	-1.42
8.59	0.0226	-1.65
8.70	0.0207	-1.68
8.83	0.0151	-1.82
8.90	0.0131	-1.89
8.95	0.0118	-1.93
9.01	0.0100	-2.00
9.13	0.00798	-2.10
9.21	0.00664	-2.18
9.25	0.00596	-2.22
9.31	0.00561	-2.25
9.53	0.00305	-2.52

Table 7. Rate constants for ring-closing of HET⁺
(slow process).

<u>pH</u>	<u>k_{obs}</u> s ⁻¹	<u>LOG k_{obs}</u>
0.38	0.0134	-1.87
0.52	0.0145	-1.84
0.90	0.0160	-1.79
1.13	0.0156	-1.81
1.40	0.0154	-1.81
1.79	0.0166	-1.78
2.09	0.0162	-1.79
2.10	0.0159	-1.80
2.47	0.0141	-1.85
2.66	0.0165	-1.78
2.81	0.0160	-1.80
3.16	0.0166	-1.78
3.41	0.0159	-1.80
3.73	0.0178	-1.75
4.05	0.0190	-1.72
4.11	0.0179	-1.75
4.50	0.0192	-1.72
4.52	0.0226	-1.64
5.06	0.0288	-1.54
5.14	0.0294	-1.53
5.35	0.0396	-1.40
5.38	0.0471	-1.33
5.53	0.0558	-1.25
5.59	0.0432	-1.36
5.79	0.0803	-1.10

Table 8. Buffer catalysis rate constants for process (b) of HET⁺. Phosphate buffers.

<u>pH</u>	<u>[buffer]</u> M	<u>k_{obs}</u> s ⁻¹
5.95	0.200	0.812
	0.150	0.754
	0.100	0.601
	0.050	0.478
	0.025	0.411
	0.010	0.336
6.31	0.200	0.517
	0.150	0.468
	0.100	0.390
	0.050	0.307
	0.025	0.256
	0.010	0.218
6.57	0.200	0.517
	0.150	0.468
	0.100	0.390
	0.050	0.307
	0.025	0.256
	0.010	0.218
6.75	0.200	0.408
	0.150	0.375
	0.100	0.319
	0.050	0.256
	0.025	0.215
	0.010	0.190
7.06	0.200	0.228
	0.150	0.221
	0.100	0.189
	0.050	0.168
	0.025	0.146
	0.010	0.132

Table 9. Rate constants for the formation of the "yellow form" of Bi^+ .

<u>pH</u>	<u>k_{obs}</u> <u>s^{-1}</u>	<u>$\log k_{\text{obs}}$</u>
13.7	21.1	1.32
13.4	8.94	0.951
13.0	3.96	0.598
12.5	1.33	0.126
12.0	0.607	-0.215
11.75	0.580	-0.236
11.50	0.668	-0.175
11.28	0.755	-0.122
10.88	1.68	0.226
10.50	1.71	0.233
10.05	4.04	0.606
9.65	4.78	0.679
9.42	8.42	0.925
9.10	10.9	1.04
9.01	12.6	1.10
8.54	17.0	1.23
8.22	30.1	1.48

Table 10. Rate constants for ring-opening of Bi^+ .

pH	k_{obs} s^{-1}	$\log k_{\text{obs}}$
13.4	0.00149	-2.83
13.0	0.00266	-2.57
12.5	0.00769	-2.11
12.0	0.0217	-1.66
11.53	0.0219	-1.66
11.16	0.0204	-1.69
10.87	0.0102	-1.99
10.72	0.00623	-2.21
10.57	0.00279	-2.56
10.17	0.00116	-2.94
9.67	0.00038	-3.42

Table 11. Rate constants for ring-closing of Bt
(fast process).

<u>pH</u>	<u>k_{obs}</u> s ⁻¹	<u>log k_{obs}</u>
0.33	0.549	-0.260
1.0	0.572	-0.243
1.5	0.569	-0.245
2.0	0.567	-0.247
2.55	0.555	-0.256
2.62	0.616	-0.210
2.87	0.537	-0.270
3.25	0.482	-0.317
3.36	0.429	-0.367
3.41	0.445	-0.351
3.60	0.439	-0.357
3.77	0.321	-0.493
4.12	0.252	-0.600
4.40	0.172	-0.763
4.51	0.167	-0.773
4.98	0.115	-0.938
5.06	0.107	-0.970
5.58	0.0820	-1.09
5.82	0.0686	-1.16
5.94	0.0704	-1.15
6.32	0.0554	-1.26
6.40	0.0608	-1.22
6.84	0.0408	-1.39
6.95	0.0373	-1.43
7.24	0.0240	-1.62
7.35	0.0220	-1.66
7.44	0.0162	-1.79
7.84	0.0098	-2.04
8.32	0.00393	-2.41
8.33	0.00378	-2.42
8.78	0.00155	-2.81
8.82	0.00124	-2.91
9.23	0.000670	-3.17
9.32	0.000660	-3.18

Table 12. Rate constants for ring-closing of B_1^+
(slow process).

<u>pH</u>	<u>k_{obs}</u> <u>s^{-1}</u>	<u>$\log k_{obs}$</u>
0.33	0.0253	-1.60
1.00	0.0253	-1.60
1.50	0.0269	-1.57
2.00	0.0273	-1.56
2.31	0.0293	-1.53
2.62	0.0350	-1.46
2.87	0.0316	-1.50
3.25	0.0342	-1.46
3.41	0.0465	-1.33
3.74	0.0771	-1.11
3.75	0.0696	-1.16
4.23	0.157	-0.804

Table 13. Rate constants for ring-closing of $N_1MeB_1^+$.

<u>pH</u>	<u>k_{obs}</u> s ⁻¹	<u>log k_{obs}</u>
0.33	0.522	-0.282
1.00	0.568	-0.246
2.00	0.589	-0.230
3.04	0.584	-0.234
3.80	0.460	-0.337
4.62	0.212	-0.674
5.75	0.0858	-1.07
6.25	0.0443	-1.35